UNIVERSITY OF CALIFORNIA, SAN DIEGO

Molecular Mechanisms of Atypical Protein Kinase C Regulation in Insulin Signaling

A dissertation submitted in partial satisfaction of the requirements for the degree

Doctor of Philosophy

in

Biomedical Sciences

by

Irene Sophie Tobias

Committee in charge:

Professor Alexandra Newton, Chair
Professor Jack Dixon
Professor Steve Dowdy
Professor Tracy Handel
Professor Joann Trejo

2016

The Dissertation of Irene Sophie Tobias is approved, and it is acceptable in quality and form for publication on microfilm and electronically:

_____

_____

_____

_____

_____

Chair

University of California, San Diego

2016

DEDICATION

For the Honor of Grayskull

EPIGRAPH

The ability to adapt to new information and hypotheses, to give up old dogmas, to admit that you are wrong, that is what separates the scientifically minded from the moronic masses of automatons.

Mat Lalonde, PhD

TABLE OF CONTENTS

LIST OF ABBREVIATIONS

WT: wild type

aPKC: atypical PKC

cPKC: conventional PKC

nPKC: novel PKC

mTORC2: mammalian target of rapamycin complex 2

PDK1: phosphoinositide-dependent kinase-1

PI3K, PI3-kinase: phosphoinositide 3-kinase

PIP_3: phosphatidylinositol-3,4,5-triphosphate

PH domain: pleckstrin homology domain

PB1 domain: Phox and Bem 1 domain

PS: pseudosubstrate

p62: sequestosome 1

Par6: partitioning-defective protein 6

MARK2: microtubule affinity regulating kinase 2

IRS-1: insulin receptor substrate 1

FRET: fluorescent resonance energy transfer

CKAR: C kinase activity reporter

CFP: cyan fluorescent protein

YFP: yellow fluorescent protein

PdS: phosphatidylserine

S6K: ribosomal protein S6 kinase

Sin1: stess-activated MAP kinase-interacting protein 1

PP1: protein phosphatase 1

GST: glutathione-S-transferase

HA: hemagglutinin

PM: plasma membrane

MBP: myelin basic protein

IEF: isoelectric focusing

WB: western blot

IP: immunoprecipitation

NT: no treatment

S.E.: standard error of mean

KD: kinase-dead

Vec: vector

PMSF: phenylmethylsulfonyl fluoride

DTT: dithiothreitol

LIST OF FIGURES

ACKNOWLEDGEMENTS

I would like to extend my deepest gratitude to Dr. Alexandra Newton for letting me explore the world of biochemistry and pharmacology in her lab. She has been a supportive and patient mentor whose excitement for science is infectious. Her advice has been invaluable in helping me approach science both during my time as a graduate student and on into the future. I will always appreciate the time and opportunity she has given me to grow as a researcher.

I would also like to thank my committee, Dr. Jack Dixon, Dr. Steve Dowdy, Dr. Tracy Handel, and Dr. JoAnn Trejo, for taking the time to provide me with feedback, help me grow as a researcher, and encourage my future pursuits in science. Thanks also to my collaborators, Estela Jacinto, Peter Kim, and Manuel Kaulich for all of your help in performing the experiments shown in Fig. 2.2c and 2.5 used in our *Biochemical Journal* publication.

Thank you also to everyone in the Newton lab: Dr. Maya Kunkel, Dr. CC King, Dr. Ksenya Cohen-Katsenelson, Tim Baffi, Julia Callendar, Agnes Grzechnik and Angela Van for sharing so many laughs and bringing such liveliness to the lab. You all have provided such help over the years. Thank you also to the undergraduates Nitya Simon and Emily Kang for your assistance provided in this project.

A thank you is also needed for my fellow BMS classmates, especially Chelsea Stewart, Sakina Palida, and Santiago Pineda. You have been an amazing support system and have helped me find a balance between life and lab. Thank you for joining me for regular Wednesday lunches, weightlifting sessions at RIMAC, Mixology

Mondays, adventure relay races, and drag queen convention excursions. Thank you also to the BMS staff, Leanne, Gina, Kathy and Pat. You all keep the program running so smoothly and always greet us with smiles, no matter the issue.

I would also like to thank my friends, coaches and training partners from my Crossfit gym and endurance club, Invictus, especially Kristine Grigsby, Eileen Donovan, Rachael Musser, Helen Szchorla, James Cekola, Christopher Walden, Ayo Anise, Melissa Hurley and Nuno Costa. Your support, inspiration and guidance over the past few years has helped me achieve the best state of physical fitness of my life in addition to mental release from work and the path towards achieving specific performance goals. Thanks also to Major Donovan and Lieutenant Commander Musser for their service to our country.

Finally, I would like to thank my parents for their love and support throughout my life in all that I have pursued. You managed to effectively instill a sense of self discipline and work ethic within me at a young age without ever making me feel pressured into achieving academic success. You have always encouraged me to pursue whatever I love to do most and to surround myself with like-minded people.

Chapter 2 in its entirety is published as "Protein kinase Cζ exhibits constitutive phosphorylation and phosphatidylinositol-3,4,5-triphosphate-independent regulation." Tobias IS, Kaulich M, Kim PK, Simon N, Jacinto E, Dowdy SF, King CC, Newton AC in *Biochem J*, 2016; 473: pg. 509-23. Chapter 3 in its entirety is published online as "Protein scaffolds control localized Protein Kinase Cζ activity," Tobias IS and Newton AC in *J Biol Chem* with expected print publication in July 2016. The dissertation author was the primary investigator and author of both these works.

VITA

Education

2016 Ph.D., Biomedical Sciences
University of California, San Diego

2008 M.Eng., Biomedical Engineering
Massachusetts Institute of Technology

2007 B.S., Materials Science and Engineering
Massachusetts Institute of Technology

Abstracts Presented at Meetings

2014: Experimental Biology/ASBMB- San Diego, CA

FASEB Lipid Regulated Kinases in Cancer- Steamboat Springs, CO

Molecular Mechanisms of Atypical Protein Kinase C Activation
Irene S. Tobias, Nitya Simon, Charles C. King and Alexandra C. Newton

2015: FASEB Protein Kinases and Protein Phosphorylation- Itasca, IL

Molecular Mechanisms of Atypical Protein Kinase C Activation
Irene S. Tobias, Manuel Kaulich, Peter K. Kim, Estela Jacinto, Steve Dowdy, Charles C. King and Alexandra C. Newton

2015: ASBMB Pseudokinases and Scaffolds- Coronado, CA

Atypical Protein Kinase C is regulated by scaffolding interactions that promote substrate localization and relief from autoinhibition
Irene S. Tobias and Alexandra C. Newton

Publications

Tobias IS and Newton AC. *Protein Scaffolds Control Localized Protein Kinase Cζ Activity.* J Biol Chem, 2016, in press.

Tobias IS, Kaulich M, Kim PK, Simon N, Jacinto E, Dowdy SF, King CC, Newton AC. *Protein Kinase Cζ exhibits constitutive phosphorylation and phosphatidylinositol-3,4,5-triphosphate-independent regulation*. Biochem J, 2016; 473: pg. 509-23.

Tobias IS, Lee H, Engelmayr GC, Macaya D, Bettinger CJ, Cima MJ. *Zero-order controlled release of ciprofloxacin-HCl from a reservoir-based, bioresorbable and elastomeric device.* J Controlled Release, 2010; 146 (3): pg. 356-62.

Thompson MT, Berg MC, **Tobias IS**, Lichter JA, Rubner MF, Van Vliet KJ. *Biochemical functionalization of polymeric cell substrata can alter mechanical compliance.* Biomacromolecules, 2006; 7 (6): pg. 1990-95

Thompson MT, Berg MC, **Tobias IS**, Rubner MF, Van Vliet KJ. *Tuning compliance of nanoscale polyelectrolyte multilayers to modulate cell adhesion.* Biomaterials, 2005; 26 (34): pg. 6836-45.

Patents

Tobias IS, Lee H, Cima MJ, Dimitrakov J. *Implantable Drug Delivery Device and Methods of Treating Male Genitourinary and Surrounding Tissues.*
US Patent Application #20100003297, licensed to Taris Biomedical and Astra Zeneca

ABSTRACT OF THE DISSERTATION

Molecular Mechanisms of Atypical Protein Kinase C Regulation in Insulin Signaling

by

Irene Sophie Tobias

Doctor of Philosophy in Biomedical Sciences

University of California, San Diego, 2016

Professor Alexandra Newton, Chair

Atypical protein kinase C (aPKC) isozymes are key modulators of insulin signaling, and their dysfunction correlates with insulin-resistant states in both mice and humans. Despite the engaged interest in the importance of aPKCs to type 2 diabetes, much less is known about the molecular mechanisms that govern their cellular functions than for the conventional and novel PKC isozymes and the functionally-related Akt family of kinases. Here we show that aPKC is constitutively phosphorylated and basally active in cells. Specifically, we show that phosphorylation

at two key regulatory sites, the activation loop and turn motif, of the aPKC PKCζ in multiple cultured cell types is constitutive and independently regulated by separate kinases: ribosome-associated mTORC2 mediates co-translational phosphorylation of the turn motif, followed by phosphorylation at the activation loop by PDK1. Live cell imaging reveals that global aPKC activity is constitutive and insulin-unresponsive. Thus, insulin stimulation does not activate PKCζ through the canonical phosphatidylinositol-3,4,5-triphosphate-mediated pathway that activates Akt, contrasting with previous literature on PKCζ activation.

We additionally show that protein scaffolds not only localize, but also differentially control the catalytic activity of PKCζ, thus promoting activity towards localized substrates and restricting activity towards global substrates. Using cellular substrate readouts and scaffolded activity reporters in live cell imaging, we show that PKCζ has highly localized and differentially-controlled activity on the scaffolds p62 and Par6. Both scaffolds tether aPKC in an active conformation as assessed through pharmacological inhibition of basal activity, monitored using a genetically-encoded reporter for PKC activity. However, binding to Par6 is of higher affinity and more effective in locking PKCζ in an active conformation. FRET-based translocation assays reveal that insulin promotes the association of both p62 and aPKC with the insulin-regulated scaffold IRS-1. Using the aPKC substrate MARK2 as another readout for activity, we show that overexpression of IRS-1 reduces the phosphorylation of MARK2 and enhances its plasma membrane localization, indicating sequestration of aPKC by IRS-1 away from MARK2. These results are

consistent with scaffolds serving as allosteric activators of aPKCs, tethering them in an active conformation near specific substrates. Thus, signaling of these intrinsically low activity kinases is kept at a minimum in the absence of scaffolding interactions, which position the enzymes for stoichiometric phosphorylation of substrates co-localized on the same protein scaffold.

Chapter 1:

Introduction

1.1 Structure of atypical PKC and its relation to the PKC family

Protein kinase C (PKC) is a family of Ser/Thr protein kinases consisting of 3 classes, conventional (α, γ and the alternatively spliced βI and βII), novel (δ, ε, η and θ), and atypical (ζ and ι/λ). PKC isozymes are primarily united by their catalytic and C-terminal regions: all family members share a conserved kinase core that is C-terminal to a series of N-terminal regulatory regions (**Fig 1.1**). The differential composition of the N-terminal regions is the principle divergence within the PKC family and produces alternate mechanisms of regulation. A key regulatory feature of conventional PKCs (cPKC) and novel PKCs (nPKC) is the presence of tandem diacylglycerol-sensing C1 domains which permit their binding to lipid second messenger agonists at cell membranes such as diacylglycerol and its analogues (1, 2).

Atypical PKCs (aPKC) have an atypical C1 domain that lacks determinants necessary for diacyleglycerol binding (3, 4), thus prohibiting this form of agonist response. aPKC isozymes also lack the Ca^{2+}-sensing C2 domain present in cPKCs that permits regulation by intracellular calcium levels. More important to aPKCs are their protein-binding domains, including a Phox and Bem1 (PB1) domain at their regulatory N-terminus (1, 2), and a C-terminal type III PDZ ligand (**Fig 1.1**). All PKC isozymes share the presence of an autoinhibitory pseudosubstrate that occupies the substrate-binding cavity in their inactive conformation. For cPKC and nPKC, the release of this pseudosubstrate is regulated through binding to diacylglycerol and is the principle mechanism of their agonist-induced activation. In contrast, the conformation of the pseudosubstrate found in aPKC is mediated through binding of aPKC to protein scaffolds. Additionally, the aPKC isozyme PKCζ has an alternate

transcript (PKMζ) preferentially expressed in brain tissue that contains the catalytic domain and lacks all N-terminal regulatory domains (PB1, pseudosubstrate, and atypical C1) thus existing in a constitutively non-autoinhibited state.

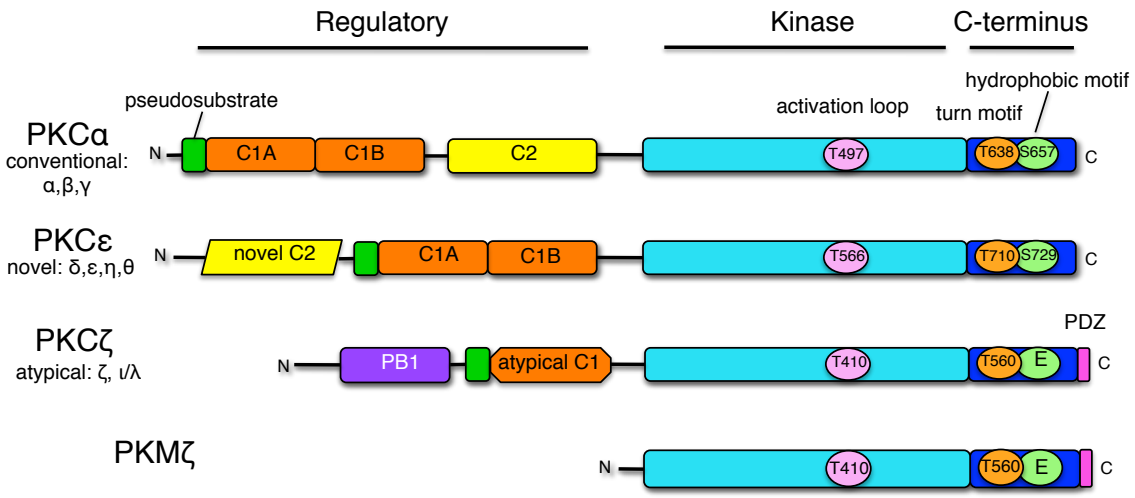

Figure 1.1: Protein domain composition of the PKC family. Regulatory and catalytic domains present in PKCα (representing conventional PKC isozymes), PKCε (novel PKC isozymes), PKCζ and its short transcript PKMζ (atypical PKC isozymes). Enzyme alignment is found principally in the kinase domain (cyan) and C-terminal region (blue) with the presence of 3 conserved phosphorylation sites: activation loop (pink circle), turn motif (orange circle) and hydrophobic motif (green circle, which is Glu for the atypical PKC isozymes). Regulatory domains shown include the autoinhibitory pseudosubstrate (green rectangle), the lipid-binding C1 domains (orange rectangle), the atypical C1 domain (orange hexagon), the conventional C2 domain (yellow rectangle), the novel C2 domain (yellow rhombus), and the protein-binding PB1 domain (purple rectangle).

Phosphorylation plays a key role in the regulation of PKC. cPKC and nPKC have 3 priming phosphorylation sites: the activation loop present near the ATP-binding site, and two sites present in the C-terminal tail, the turn motif, and the hydrophobic motif (1). These sites are also conserved among other AGC kinases present on the PKC branch of the kinome including Akt, p70 S6K, MSK and SGK

(**Fig 1.2**). aPKCs share the first two sites, but a phosphomimetic Glu occupies the phospho-acceptor position in the hydrophobic motif site, a feature shared by the nearby PKN family which has negatively-charged Asp at the hyrdrophobic motif (**Fig 1.2e**). The hydrophobic motif is an autophosphorylation site for cPKC and Akt kinases (5, 6), thus aPKC is lacking in this key regulatory feature exhibited by these enzymes. The absence of this phospho-site also renders aPKC insensitive to dephosphorylation by the phosphatase PHLPP that dephosphorylates this site on Akt (7) and on other PKCs leading to their degradation and downregulation (8-10).

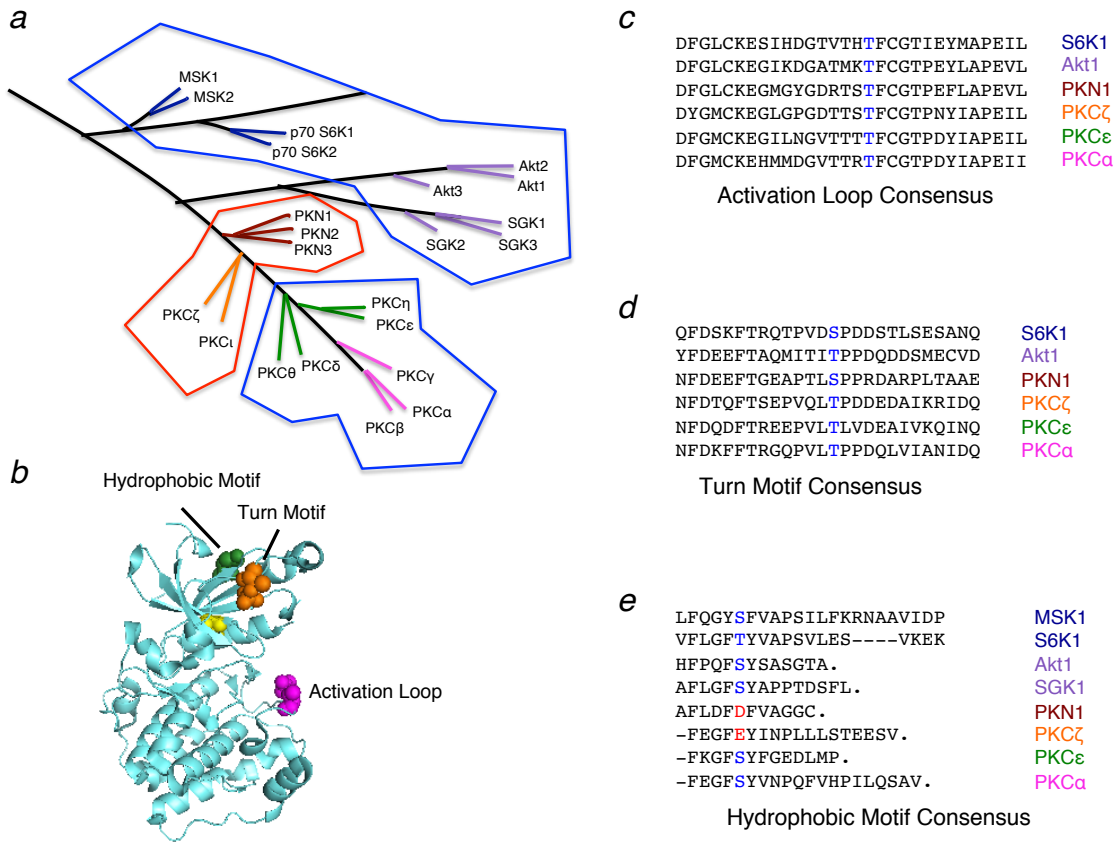

Figure 1.2: AGC branch of the kinome and consensus phosphorylation sites. (a) End of the AGC branch of the human kinome (11) including mitogen and stress-activated protein kinase (MSK) isozymes, ribosomal protein S6 kinase, 70kDa (p70 S6K) isozymes, Akt and Ser/Thr-protein kinase (SGK1) families, PKN family, aPKC isozymes, nPKC isozymes and the most divergent cPKC isozymes. The blue boxes contain isozymes that have Ser or Thr at the hydrophobic motif while the red boxes contain isozymes that have Glu or Asp at the hydrophobic motif. **(b)** Structure of an aPKC kinase domain (human PKCι, PDB: 3A8W) showing locations of analogous sites for PKCζ activation loop (pink), turn motif (orange) and hydrophobic motif (green). **(c,d,e)** Alignment of amino acid residues for the activation loop **(a)**, turn motif **(b)** and hydrophobic motif **(c)** sites shown in blue text for human PKC (conventional PKCα, novel PKCε and atypical PKCζ) and the other related AGC kinases MSK1, S6K1, SGK1, Akt1 and PKN1. The hydrophobic motif Glu and Asp residues of PKCζ and PKN1 are notated in red. Sequences for these kinases are listed in the order they appear on their branch of the kinome (11).

The activation loop of all PKCs and the related family of Akt kinases are phosphorylated by phosphoinositide-dependent kinase-1 (PDK1) (12-14). Phosphorylation at the activation loop is constitutive for cPKC and nPKC isozymes and is likely the first phosphorylation event in the maturation of PKC (2). However,

phosphate at the activation loop becomes dispensable for activity in cPKC isozymes once the kinases are fully phosphorylated (15). For Akt, phosphorylation at the PDK1 site is agonist-evoked through the PI3K pathway in which agonist-stimulated phosphatidylinositol-3,4,5-triphosphate (PIP_3) production by PI3-kinase evokes Akt translocation to the plasma membrane where its autoinhibitory PH domain binds to PIP_3 and permits activation loop phosphorylation and activation by PDK1 (16, 17). The regulation of activation loop in aPKCs is unclear. Many studies propose that activation loop phosphorylation by PDK1 on aPKC isozymes is agonist-evoked through PI3K and leads to increased activity (18-20), although other studies have shown that phosphorylation of the aPKC activation loop is unaffected by agonist stimulation (21-23). Thus, whether the activation loop phosphorylation of aPKCs is agonist-dependent, as it is for Akt, or constitutive, as it is for cPKCs remains to be resolved. aPKC's position on the kinome between the branch for Akt and the branch for cPKC (**Fig 1.2a**) places it at a crossroads of consensus and potentially regulation.

Phosphorylation at the turn motif site is necessary to stabilize cPKC in a catalytically-competent conformation (24); loss of phosphorylation at this site inactivates the enzyme (15, 25, 26). The mammalian target of rapamycin complex 2 (mTORC2) is required for the phosphorylation of the turn motif site in both PKC and Akt, however by different mechanisms (21, 27, 28). For Akt, mTORC2 directly phosphorylates the nascent Akt polypeptide as it emerges from the ribosome (29, 30). In contrast, cPKC isozymes are phosphorylated post-translationally, with a half-time on the order of 15 min, and at a membrane fraction (31, 32). Although mTORC2 is

required for PKC to become phosphorylated (28, 33), whether it directly phosphorylates the turn motif of cPKC or indirectly regulates the site by activation of another kinase or chaperoning remains to be established. The first phosphorylation of cPKCs is the PDK1-mediated phosphorylation on the activation loop, which is a prerequisite for phosphorylation of the turn motif (12, 15). The turn motif of aPKC has been proposed to be regulated by autophosphorylation subsequent to activation loop phosphorylation (19, 34), similar to the hydrophobic motif autophosphorylation of cPKC (5). However, evidence for this claim is also controversial, with recent studies identifying mTORC2 as responsible for phosphorylating the turn motif of aPKC (21).

The lack of second messenger-responsive regulatory moieties of aPKCs sets them apart from cPKC and nPKCs. Indeed their position on the kinome tree places them half way between Akt and the other PKCs, suggesting they should be considered as a separate family in the kinome.

1.2 Scaffold binding partners and substrates of atypical PKC

A key regulatory domain feature of aPKCs is the Phox and Bem 1 (PB1) domain present at the N-terminus. Both PKCζ and PKCι/λ direct their PB1 domains towards binding interactions with multiple partner proteins. Two key scaffolding proteins also containing PB1 domains that bind the aPKC PB1 domain and mediate its regulation are sequestosome 1 (p62) and partitioning-defective protein 6 (Par6) (35,

36). PB1 domains are conserved throughout multiple kingdoms, including animals, fungi, plants and amoebas, with at least 13 PB1 domain-containing proteins identified in humans (37). The PB1 structure exhibits the topology of ubiquitin-like β-grasp folds (38), and they are classified into 3 types. Type I PB1 domains contain 4 key acidic residues present in the β3 and β4 strands and α2 helix with the sequence Asp-X-(Asp/Glu)-Gly-Asp-X_8-(Glu/Asp) known as an OPCA motif (**Fig 1.3a**) (39-42). Type II PB1 domains have an invariant Lys present on the first β strand while Type I/II domains have both features present (**Fig 1.3a**) (39-42). Heterodimeric assembly of two PB1 domains requires the Type I acidic OPCA motif in one partner to bind with the Type II basic lysine in the other (37). aPKC belongs to the Type I/II class, as does p62, while Par6 has a Type II PB1, containing the invariant lysine in β1 but only 2 of the 4 residues of the OPCA motif (**Fig 1.3a**) which are incomplete for a binding interaction with other Type II PB1s (39, 40). aPKC functions as a Type I PB1 domain in its interactions with both p62 and Par6 which function as Type II PB1s (40). p62 also has the ability to homodimerize with itself in the absence of other PB1-containing partners by performing both interacting Type I and Type II roles, thus producing aggregates (39-41).

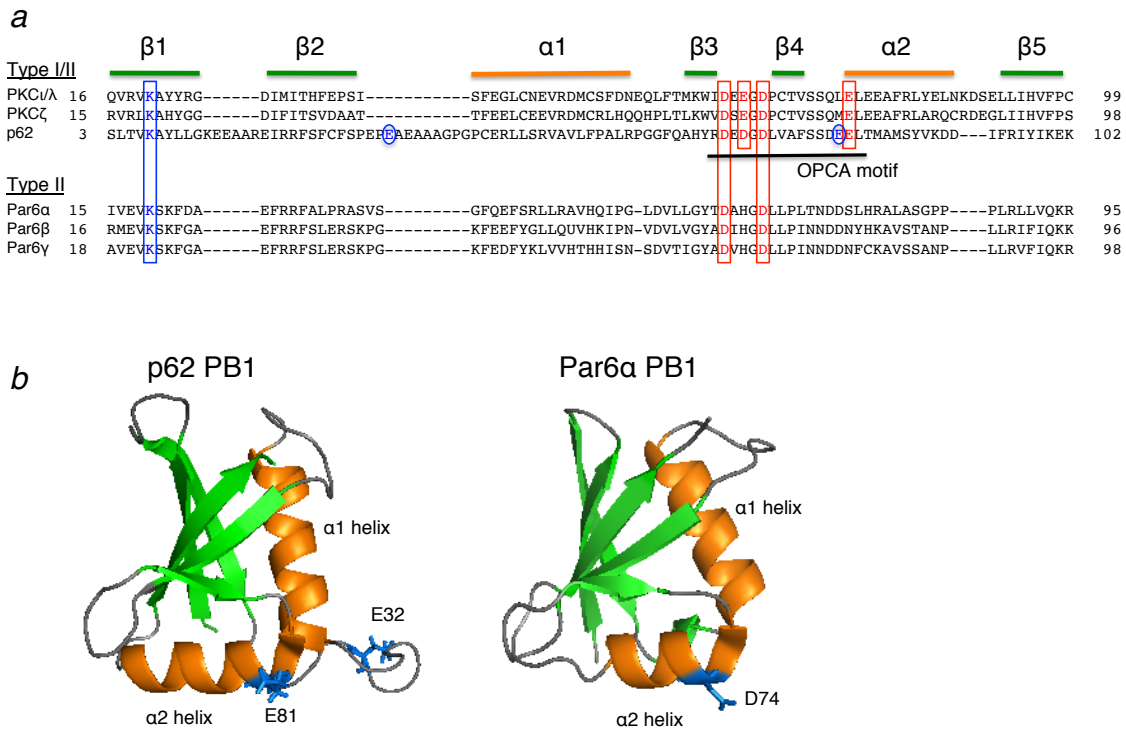

Figure 1.3: Alignment and structures of p62 and Par6α PB1 domains. (a) Alignment of human PKCι/λ, PKCζ, p62, Par6α, Par6β, and Par6γ PB1 domains separated into Type I/II and Type II classes showing locations of various alpha helices and beta strands. OPCA motif residues are highlighted in red boxes, the invariant lysine present in the β1 strand is highlighted in the blue box, and the acidic residues identified for aPKC pseudosubstrate binding to p62 (43) are circled in blue. **(b)** Structures of human p62 and Par6α PB1 domains with alpha helices colored in orange and beta strands colored in green. Position of the E81 and E82 acidic residues are indicated in blue sticks identified for aPKC pseudosubstrate binding to p62. The D74 residue on the alpha 2 helix of Par6α that best corresponds to E81 on p62 is also indicated in blue sticks.

Both p62 and Par6 have been shown to regulate bound aPKC activity through inducing pseudosubstrate displacement and relief from autoinhibition. In the case of p62, the pseudosubstrate of aPKC binds to an acidic surface present in the PB1 domain of p62, using two non-OPCA motif residues, E32 and E81 (**Fig 1.3**) (43). This tethering of the pseudosubstrate locks aPKC into an open active conformation when present on the p62 scaffold. The acidic surface for pseudosubstrate binding is not present in the PB1 domain of Par6 as it lacks the random coil region between the

β2 strand and the α1 helix present in p62 that contains the E32 residue (**Fig 1.3.b**). For Par6, the tethering of the aPKC PB1 domain to the Par6 PB1 domain opens the kinase into an active state by unraveling the autoinhibitory components of the N-terminus, the pseudosubstrate and the atypical C1 domain (44). The Par6 scaffolding platform is known to coordinate aPKC phosphorylation of cell polarity-regulating substrates Par3 and Lgl (45-50). Par3 and Lgl cannot simultaneously bind Par6 and are inferred to recognize overlapping epitopes on Par6 (48, 50, 51) (**Fig 1.4**). Ser827 was identified as the aPKC phosphorylation site on Par3 within a non-PDZ region found to bind with the aPKC kinase domain (47, 51, 52). The Par3/Par6 binding interaction requires the PDZ1 domain of Par3 along with the semi-CRIB and PDZ domains of Par6, thus forming a ternary complex along with the Par6/aPKC PB1 interaction (36, 51) (**Fig 1.4**). For Lgl, Ser653 was identified as the aPKC phosphorylation site promoted by association with the Par6 scaffolding platform (48). The identity of the substrate (Par3 vs Lgl) bound to the aPKC/Par6 complex is key to the regulation of epithelial cell polarity. The Par3/Par6/aPKC complex is known to promote the formation of epithelial junctions while requiring aPKC activity (46, 53, 54); the Lgl/Par6/aPKC complex is shown to suppress this formation (48, 55).

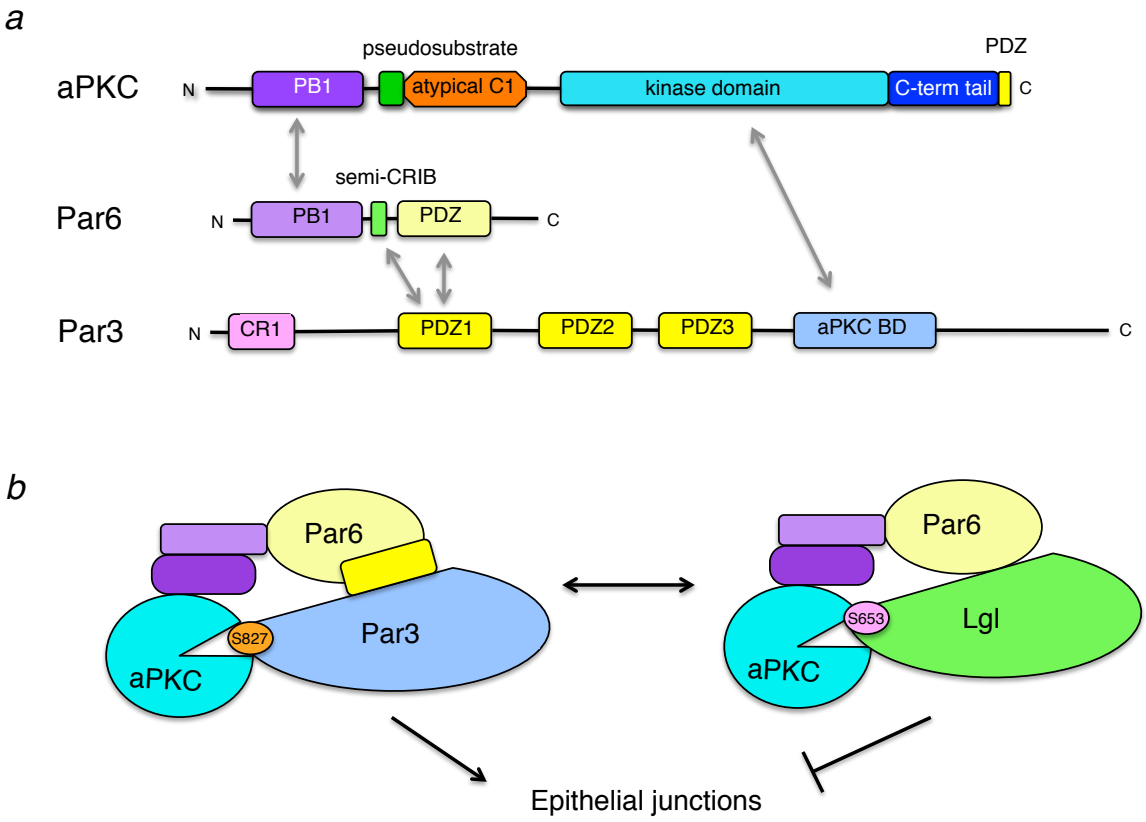

Figure 1.4: Composition of Par6 and Par3 and their interactions with aPKC. (a) Domains present in aPKC, Par6 and Par3 showing relevant binding interactions between the ternary complex. aPKC binds to the PB1 domain of Par6 through its PB1 domain (36). Par6 binds to the Par3 PDZ1 domain through its semi-CRIB and PDZ domains (36, 51). aPKC phosphorylates Ser827 and binds to a C-terminal region of Par3 through its kinase domain (47, 51, 52). **(b)** Complexes of aPKC/Par6 with either Par3 or Lgl which occupy the same binding epitope of Par6 and are phosphorylated by aPKC at Ser827 and Ser653, respectively. The Par3 complex is known to promote the formation of epithelial junctions (46, 53, 54) while the Lgl complex represses it (48, 55).

The scaffold protein p62 is a hub for many protein binding interactions and orchestrates multiple cellular functions besides signal transduction including cell proliferation, survival and death, inflammation, tumourigenesis and oxidative stress response (56, 57). Additionally, p62 plays important roles in metabolism. Mice that lack p62 exhibit obesity, insulin and leptin resistance as well as type 2 diabetes (58, 59). The mechanism for how p62 orchestrates insulin signaling remains unclear

though some key findings have recently been published. Insulin induces a dramatic binding interaction between p62 and the insulin receptor substrate 1 (IRS-1) which requires both the PB1 domain of p62 and the insulin-induced tyrosine phosphorylations on the YXXM motif of IRS-1 (60). More recently, PKCζ has been shown to increase its interaction with p62 through treatment with insulin-like growth factor 1 (IGF-1) and is shuttled to IRS-1 through its interaction with p62 (61). For aPKC, this agonist-induced translocation may be key to its role in insulin signaling. aPKCs are well known to be required for insulin-stimulated glucose transport yet the mechanisms for how they exert this function remain poorly understood. Insulin-induced localization of aPKC near IRS-1 may be critical for allowing it to access certain substrates. Vimentin, an intermediate filament protein that is a marker of mesenchymal cells, was also shown to be recruited to IRS-1 through IGF-1 and to be phosphorylated by localized PKCζ in an osteoblast precursor cell line (61). Additionally, PKCζ has been shown to phosphorylate IRS-1 itself both *in vitro* and in cells (62-65). However, the downstream effects of aPKC phosphorylation on IRS-1 and how they impact glucose transport remain unclear.

One of the best-validated substrates of aPKC is the microtubule affinity regulating kinase 2 (MARK2), a Ser/Thr protein kinase also known as Par-1b. Two independent groups published separately on its phosphorylation at Thr595 by aPKC in 2004, showing that p595 inactivates the kinase and induces a change in its localization away from the plasma membrane into the cytosol (66) or from the apical to the basolateral surface of polarized cells through interaction with 14-3-3, also known as

Par5 (67). MARK2 was also found to bind aPKC in co-immunoprecipitation studies (66), although the details of this interaction and whether it requires a scaffold platform such as Par6 remain unclear. Additional studies have identified the kinase associated-1 (KA1) domain present in MARK2 as the mechanism for which MARK2 binds to anionic phospholipids (68). One function of MARK2 is to phosphorylate microtubule-associated proteins, thus organizing microtubules at the basolateral domain to maintain cell polarity (69, 70). Indeed, mammalian MARK2 and its *Drosophil*a homologue Par-1b are required for maintenance of cell polarity in worms, flies and mammals (71-73). Another intriguing functional role for MARK2 has been identified in metabolism, the regulation of mitochondrial function in adipose tissue (74). Mice that lack MARK2 are resistant to weight gain when placed on a high fat diet due to an increased metabolic rate and insulin sensitivity (75). Thus, MARK2 presents another intriguing aPKC target yet unexplored avenue for the regulation of insulin-induced glucose transport.

1.3 Atypical PKC's role in insulin signaling and type 2 diabetes

Type 2 diabetes has become an alarmingly increasing worldwide epidemic over the past 30 years. In 1985, an estimated 30 million people had diabetes, which increased to 217 million in 2005 and is estimated to reach at least 366 million by 2030 as predicted by the WHO (76). The growing epidemic is largely a result of a worldwide trend towards unhealthy diets, obesity, and increasingly sedentary lifestyles. Diabetes is an extremely costly malady for both the effected individuals

and healthcare systems, accounting for 5-10% of total healthcare spending in several countries (76) and is expected to increase further over the next few decades. The majority of diabetes spending provides for the costs of managing the co-morbidities of the disease and the complications of chronic high glucose while overall drug therapy costs remain comparatively low. Thus, enhancing the efficacy of drugs that mediate insulin signaling and control glycemic levels presents a powerful solution to improve both the health and the economy of society at large. To develop better drug therapies, the mechanisms that regulate insulin signaling pathways must be better understood. Indeed, aPKC isozymes have been implicated as important modulators of insulin signaling for multiple decades (77-79), thus understanding the mechanisms of their regulation is key to the development of future improved therapies for type 2 diabetes.

aPKCs are required for insulin-stimulated glucose transport in skeletal muscle and adipose tissue through triggering translocation of GLUT4 transporters to the plasma membrane. Evidence for this functional role of aPKCs has been demonstrated predominantly through adenoviral expression of aPKC in multiple cell lines including 3T3-L1 adipocytes (80-82), L6 myotubes (83, 84), rat adipocytes (34) and human adipocytes (85) using [3H]2-deoxyglucose uptake assays and GLUT4 translocation assays. Additional supporting evidence has been shown through siRNA knockdown of aPKC in 3T3-L1 adipocytes and L6 myotubes (86) in addition to tissue-specific knock-out of aPKC in mouse muscle (87). The catalytic activity of aPKC is required for its effect on insulin-regulated biological functions as determined using either kinase-dead aPKC acting as a dominant negative (80, 81, 83-85, 88-90) or aPKC

inhibitors (80, 84, 85, 90, 91), both of which impair insulin-stimulated glucose transport. However, the precise molecular mechanisms by which aPKC acts to induce GLUT4 translocation remain largely unknown.

The aPKC isozymes, PKCζ and PKCι/λ function interchangeably to regulate GLUT4-mediated glucose transport (83, 88). Evidence for this phenomenon is primarily from studies expressing kinase-dead forms of either isozyme along with wild-type forms of the other enzyme which correspondingly rescue the inhibitory effects of glucose transport imposed by the kinase-dead form (79, 88). However, the isozymes exhibit species-specific and tissue-specific differential expression (79, 92). PKCλ is the predominant aPKC isozyme expressed in muscle and adiopocytes of mice (87) while PKCζ is the predominant isozyme expressed in these metabolic tissues of rats (83). Thus, 3T3-L1 adipocytes derived from mice primarily express PKCλ (81) while L6 myotubes derived from rats primarily express PKCζ (83, 86). However, in mouse liver both isozymes are substantially expressed (93, 94) while little is known about their relative expression in rats (92). For humans, mRNA levels of PKCι are higher than those of PKCζ in liver, muscle and adipocytes, though data for relative protein expression levels are still unclear (92).

While the total body knockout (KO) of PKCλ in mice is embryonic lethal, studies using Cre-loxP methods to obtain muscle-specific KO have indeed shown that depletion of this isozyme significantly impairs insulin-stimulated glucose uptake in the muscle of these animals (87, 92). Mice with muscle-specific KO of PKCλ exhibit metabolic syndromes that include insulin resistance, abdominal obesity,

hyperinsulinemia and glucose intolerance (87, 92). Mice with adipocyte-specific PKCλ KO have impaired glucose transport in adipocytes yet exhibit normal glucose tolerance, diminished adipocity, and do not develop the metabolic syndromes exhibited by the muscles-specific KO animals (95). Intriguingly, liver-specific KO of PKCλ diminishes generation of insulin-stimulated lipogenic and proinflammatory factors yielding mice that are insulin-sensitive and resistant to high-fat feeding (93, 96). This phenomenon is in concert with evidence that hepatic aPKC regulates the activation of sterol regulatory element binding-protein 1c (SREBP-1c) and nuclear factor kappa-light-chain-enhancer of activated B cells (NF-κB) (93, 94, 96, 97). SREBP-1c mediates several enzymes involved in lipid synthesis while NF-κB is a key regulator of inflammatory signaling and induces production of cytokines. Mice with either muscle-specific KO of PKCλ or that are fed high fat diets both exhibit chronic increased activation of SREBP-1c and NF-κB along with insulin resistance and hyperlipidemia, effects that were reversed with adenoviral expression of kinase-dead aPKC (94).

Evidence for aPKC's important role in metabolic disease has also been supported by data from human studies. Levels of aPKC are diminished in the muscle of humans with type 2 diabetes (98-100) while the residual activity of aPKC in these patients as well as obese humans is defective (99-101). Furthermore, aPKC is hyperactive in the hepatic tissues of diabetic humans (102), stimulating the hepatic production of lipids and cytokines that perpetuate the disease state. The reason for this paradoxical pathology resulting in dysfunction of aPKC in muscle combined with

hyperactivation of aPKC in liver remains unknown. However, specific pharmacological inhibition of hepatic aPKC has indeed been proposed as treatment for type 2 diabetes and metabolic syndrome (78, 92).

1.4 Tools used to study atypical PKC

As with many kinases, activity assays to study the biochemistry of aPKC were primarily performed *in vitro* for multiple decades using purified protein and multiple substrates such as myelin basic protein, histones and PKC-specific substrate peptides (103, 104). While *in vitro* assays can elucidate several important mechanisms of kinase regulation, knowledge inferred from them cannot always translate to the more complex regulation of kinase signaling in live cells and *in vivo* settings. Efforts to establish a live cell activity assay for multiple kinases lead to the development of kinase activity reporters (or "KARs") for tyrosine kinases (105) and Ser/Thr kinases such as AKAR for PKA (106), BKAR for Akt (aka PKB, (107)), DKAR for PKD (108) and indeed CKAR for PKC (109) based on fluorescent protein technology discovered and spearheaded by the Tsien Lab (105, 106). Within these reporters, a substrate sequence specific for the kinase of interest is inserted between a donor-acceptor fluorescence resonance energy transfer (FRET) pair of cyan fluorescent protein (CFP) and yellow fluorescent protein (YFP). Also contained within the construct is a phospho-peptide-binding module (forkhead-associated 2 domain, FHA2 in the case of CKAR) capable of binding to the phosphorylated target within the substrate sequence, thus changing the intramolecular conformation of the reporter and

repositioning the distance between the FRET pair (**Fig 1.5a**). This disturbance produces a measurable change in FRET capable of detection by fluorescence microscopy and effectively corresponds to the activity of the specific kinase. Advantages of these assays over conventional immunoblotting methods of cellular substrates include a high sensitivity for detecting minute spatiotemporal changes in activity and a capacity for monitoring direct agonist-activation and inhibition of specific kinases in real time (110).

As commonly used for the pharmacological study of protein kinases, effective and selective inhibitors are valuable tools to elucidate the regulatory mechanisms, specific substrates and downstream effectors of aPKC. However, the toolbox of inhibitors that selectively inhibit atypical PKCs is scant compared to the collection of compounds that can effectively inhibit conventional and novel PKCs in pharmacological manipulation (111). Additionally, there is a history of compounds published in the literature that were shown to effectively inhibit aPKC *in vitro* yet have presented incompetency when directed towards inhibition of aPKC in cells (111-113). Zeta inhibitory peptide (ZIP) is a myristoylated peptide designed to mimic the autoinhibitory pseudosubstrate of PKCζ to inhibit its active site. ZIP demonstrated effective inhibition of aPKC when tested *in vitro* (108, 112) and was inferred to inhibit PKMζ *in vivo* when it produced striking long term memory loss in rats (114) under the controversial hypothesis that PKMζ is necessary for long term memory formation (108, 114-116). However, when tested in live cell assays on CKAR, ZIP failed to inhibit basal activity of overexpressed PKMζ whereas the general kinase inhibitor

staurosporine successfully inhibited PKMζ basal activity on CKAR as compared to a vector transfected control (112). ZIP was also ineffective at inhibiting PKMζ activity on other cellular substrate readouts such as MARK2 and PKC-serine substrate as detected by immunoblotting. Chelerythrine, another controversial inhibitor previously proposed and marketed to inhibit PKCs (105, 117) also failed to inhibit PKMζ in the same assays (112). Recent studies have since identified a specific region in the PB1 binding surface of p62 as the molecular target of ZIP (43). ZIP can indirectly inhibit full-length aPKCs by displacing the binding of the autoinhibitory aPKC pseudosubstrate from an acidic surface on the PB1 domain of p62. This displacement permits the pseudosubstrate to re-enter the active site of aPKC and autoinhibit the kinase (43).

Other inhibitors of aPKC have also been published in recent studies yet have experienced minimal usage within the field. An extensive investigation conducted in 2007 comparing the efficacy for a plethora of inhibitors on a wide panel of kinases including PKCζ found almost none that effectively inhibited aPKC *in vitro* (118). One exception was the bisindolylmaleimide active site inhibitor Ro-31-8220 (structure shown in **Fig 1.5b**) that inhibited PKCζ by 75% yet was far more effective at inhibiting PKCα (97%), thus not exhibiting specific inhibition of aPKC and only demonstrated *in vitro* (118). In 2009, a 2-(6-phenyl-1H indazol-3-yl)-1H-benzo[d]imidazole named PZ09 (**Fig 1.5b**) was designed as a selective active site inhibitor of PKCζ (119). *In vitro* studies demonstrated PZ09's potent inhibition and selectivity of aPKC over cPKC and nPKC, with reported IC-50s of 5.18 nM for PKCζ,

10-fold higher for PKCι and over 500-fold higher for other PKCs (119). The compound was further used for *in vivo* studies of aPKC function (120), yet was dosed at a higher concentration of 10 μM that was shown to have off-target effects on PDK1 and other non-PKC kinases in the initial *in vitro* publication (119). PZ09 has not yet been thoroughly validated for selective inhibition of aPKC in cellular assays on specific aPKC substrates. Other compounds published to inhibit aPKC *in vitro* include myricetin (**Fig 1.5b**), a flavonoid inhibitor developed for the proto-oncogene Ser/Thr-protein kinase PIM1, which inhibited the PKCζ active site with an *in vitro* IC-50 of 1.7 μM (121). An allosterically-acting small molecule, PS315 (**Fig 1.5b**) was shown in 2014 to disrupt the salt bridges between the PIF-pocket and the ATP-binding site of PKCζ (122), demonstrating selective inhibition of PKCζ and PKCι over PDK1 through *in vitro* assays. However, PS315 was used at 100 μM in these studies, a substantially high concentration for a kinase inhibitor to be used *in vitro*. The general kinase inhibitor staurosporine (**Fig 1.5b**) has indeed been used to successfully inhibit PKMζ basal activity on CKAR in cells (112), but is a particularly promiscuous non-selective inhibitor and mainly acts on aPKC indirectly through its potent inhibition of PDK1, thus reducing phosphorylation at the aPKC activation loop necessary for activity (112).

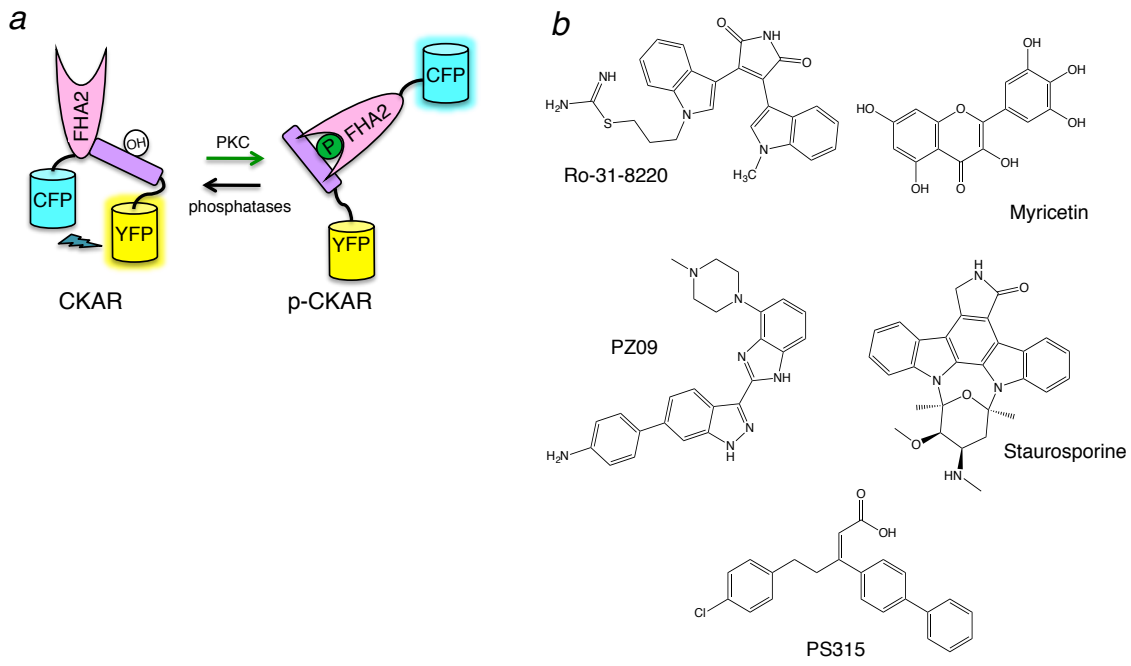

Figure 1.5: Tools used to study aPKC. (a) Schematic of C kinase activity reporter (CKAR) conformation between its dephosphorylated and phosphorylated states. In the dephosphorylated state, the CFP and YFP fluorophores are in proximity to transmit fluorescent resonance energy. In the phosphorylated state, the FHA2 domain binds to the phosphorylated Thr residue in the PKC substrate sequence, causing a conformational change that separates the CFP and the YFP, reducing FRET. **(b)** Chemical structures of compounds used to inhibit aPKC including Ro-31-8220 (bisindolylmaleimide), myricetin (flavonoid), PZ09 (benzoimidazole), staurosporine and PS315.

Agonist compounds are another valuable tool key to studying the regulatory mechanisms of kinases, particularly in real time. As with the inhibitors, a collection of agonists capable of potently activating cPKCs and nPKCs exists that dwarfs the resources available to the study of aPKC (111). Indeed, many of these activating mechanisms rely on the presence of diacyglycerol-binding tandem C1 domains that translocate PKC to membranes, a domain feature that is absent in aPKC. A functionally-related kinase of aPKC, Akt, that sits near the PKC family on the AGC branch of the kinome (11) also has a multitude of activators capable of directly stimulating Akt activity on BKAR and several endogenous substrates. Many of these

agonists are growth factors such as insulin, insulin-like growth factor (IGF-1) and epidermal growth factor (EGF) that regulate Akt activation through the PI3-kinase pathway (16). Some of these agonists have also been proposed to activate aPKC through similar mechanisms, yet have lacked convincing demonstration of aPKC intramolecular activation in cells or effects on downstream substrates compared to their robust modulation of Akt and its effectors published prolifically throughout the field. Additionally, no published study has yet shown aPKC activation by an agonist through real-time FRET readout in cells in the manner demonstrated profusely for other PKCs and Akt.

1.5 Research Goals

The work presented here investigates the regulation of the atypical PKC, PKCζ by phosphorylation, lipids, scaffolds and insulin. Chapter 2 examines the role and processing of phosphorylation at the activation loop, T410, and the turn motif, T560, in the regulation of PKCζ activity, in addition to effects of lipids and the agonist insulin. It demonstrates that phosphorylations at T410 and T560 are required for enzyme activity, are constitutive in nature, and regulated by the kinases PDK1 and mTORC2, respectively. Additionally, phosphorylation at T560 occurs first during translation, with phosphorylation at T410 following translation. The membrane lipid phosphatidylserine affects both the susceptibility of PKCζ to dephosphorylation at the activation loop, T410 and the activity of PKCζ *in vitro*. However, the agonist-produced lipid PIP_3 does not affect that activity of PKCζ *in vitro* nor does it stimulate

PKCζ translocation to plasma membrane as it does for Akt. The growth factor insulin that stimulates PI3K and Akt activity does not affect phosphorylation of PKCζ, nor does it change its innate activity. Chapter 2 challenges the accepted literature model for the mechanism of activation for aPKC, previously thought to be analogous to that of Akt in which agonist stimulated production of PIP_3 recruits the kinase to the plasma membrane where it is released from autoinhibition and inducibly phosphorylated at its activation loop by PDK1 with subsequent autophosphorylation at its hydrophobic motif. The data within Chapter 2 reveal how multiple features of this model are incorrect for aPKC regulation.

Chapter 3 examines the effects of scaffolds in the regulation of aPKC and how their role in mediating its activity may be more important to understanding its mechanism of activation than the role of phosphorylation or lipids. It focuses on the PB1 domain-containing scaffolds, p62 and Par6, well-known binders of aPKC, in addition to the insulin-regulated scaffold IRS-1 and the aPKC substrate MARK2. It identifies key differences in the binding and regulation of p62 vs Par6 with respect to PKCζ and its basal activity. Chapter 3 also examines the role of PKCζ autoinhibition with respect to scaffolds using the short transcript PKMζ and domain deletion mutants of PKCζ. PKMζ is found to exhibit a liberated nature that allows it to phosphorylate global substrates that PKCζ does not due to its lack of scaffold sequestration. Additionally, Chapter 3 demonstrates that different scaffolds (p62, Par6 and IRS-1) have different effects on aPKC phosphorylation of MARK2 and its cellular localization. Furthermore, it identifies an agonist-induced effect on PKCζ, namely its insulin-

stimulated translocation to IRS-1 provided by scaffolding to p62. Thus, Chapter 3 presents a model of aPKC regulation where agonists such as insulin can change the localization and activity of aPKC through scaffolds, either placing the kinase near or sequestering it away from different substrates.

Chapter 2:

Protein kinase Cζ Exhibits Constitutive Phosphorylation and Phosphatidylinositol-3,4,5-triphosphate-independent Regulation

2.1 Introduction

Atypical protein kinase C (aPKC) isozymes have been implicated as key modulators of insulin signaling and type 2 diabetes (77-79). aPKCs are required for insulin-stimulated glucose transport in skeletal muscle and adipocytes (34, 80, 84, 85). The aPKC isozymes, PKCζ and PKCι/λ (PKCι is the human ortholog of mouse PKCλ) can function interchangeably to regulate glucose transport (88), although they exhibit species-specific differential expression (79). Knockout of PKCλ (the predominant aPKC isozyme expressed in mice (83)) in embryonic stem cells and adipocytes impairs insulin-stimulated glucose transport (123). Mice with muscle-specific knockout of PKCλ also exhinbit metabolic and diabetic syndromes (87). Furthermore, the activity of aPKC immunoprecipitated from skeletal muscle or adipocyte tissues of obese humans or patients with type 2 diabetes is non-responsive to prior treatment of the tissue with insulin (99, 100, 124), yet aPKC is hyperactive in liver tissue of rodents and humans with type 2 diabetes (102, 125). Hepatic aPKC is known to activate lipogenic and pro-inflammatory pathways (93, 96), further exacerbating disease. Indeed, pharmacological inhibition of aPKC in the liver has been proposed as a treatment for type 2 diabetes and metabolic syndrome (78). Despite the heightened interest in the role and drugability of aPKC in metabolic disease, much less is understood about the molecular mechanisms that drive the cellular functions of aPKCs compared to other PKCs.

aPKCs are classified as one of the three subfamilies of the PKC Ser/Thr protein kinases. However, unlike the other two classes (conventional and novel),

aPKCs are not regulated by diacylglycerol. Conventional PKC (cPKC) and novel PKC (nPKC) isozymes sense diacyglycerol via a C1 domain, and although atypical PKCs have a C1 domain, it lacks determinants that allow the binding of diacylglycerol (3, 4). Nor are they regulated by Ca^{2+}, a defining feature of conventional PKCs that is mediated by a Ca^{2+}-sensing C2 domain. In place of second messenger-sensing modules, atypical PKCs have a protein-binding PB1 domain at their regulatory N-terminus and a PDZ ligand at the C-terminus (1, 2). They also have an autoinhibitory pseudosubstrate segment shared by all PKCs. In order for aPKCs to be active, this pseudosubstrate must be removed from the substrate binding cavity, an event that can occur upon binding to protein scaffolds such as Par6 (44) and p62 (43). The aPKC isozyme PKCζ has an alternate transcript (PKMζ) preferentially expressed in brain tissue that contains the cataylic domain and lacks all N-terminal regulatory domains (PB1, pseudosubstrate, and atypical C1). The lack of second messenger-responsive regulatory moieties of aPKCs sets them apart from cPKCs and nPKCs. Indeed, their position on the kinome tree places them halfway between Akt and the other PKCs (11), suggesting they should be considered as a separate family in the kinome.

Phosphorylation plays a key role in regulating all PKCs. cPKC and nPKC isozymes have 3 priming phosphorylation sites: the activation loop present near the ATP-binding site, and two sites present in the C-terminal tail, the turn motif, and the hydrophobic motif (1). aPKCs share the first two sites, but a phosphomimetic Glu occupies the phospho-acceptor position in the hydrophobic motif site; this unique feature of aPKC renders them insensitive to dephosphorylation by the phosphatase

PHLPP which dephosphorylates this site on Akt (7) and on other PKCs leading to their inactivation and downregulation, repsectively (8-10). The activation loop of all PKCs and the related family of Akt kinases are phosphorylated by phosphoinositide-dependent kinase-1 (PDK1) (12-14). Phosphorylation at the activation loop is constitutive for cPKC and nPKC isozymes and is likely the first phosphorylation event in the maturation of these PKCs (2). However, phosphate at the activation loop becomes dispensable for activity in cPKC isozymes once the kinases are fully phosphorylated (15). For Akt, phosphorylation at the PDK1 site is agonist evoked.

The regulation of activation loop phosphorylation in aPKCs is unclear. Previous studies proposed that activation loop phosphorylation by PDK1 on aPKC isozymes is agonist-evoked and leads to increased activity upon insulin stimulation (18-20). Indeed, the literature commonly cites the activation of aPKC to be analogous to the mechanism of Akt activation in which agonist-stimulated phosphatidylinositol-3,4,5-triphosphate (PIP_3) production by PI3-kinase evokes Akt translocation to the plasma membrane where its autoinhibitory PH domain binds to PIP_3 and permits activation loop phosphorylation by PDK1 (16, 17). However, multiple studies also report data showing that insulin stimulation does not affect activation loop phosphorylation on aPKC in immortalized cell lines (21), primary rat hepatocytes (22), and even in biopsied human muscle tissue following insulin injection *in vivo* (23). Thus, whether the activation loop phosphorylation of aPKCs is agonist-dependent, as it is for Akt, or constitutive, as it is for cPKCs, remains to be resolved.

The role and mechanism of phosphorylation for the turn motif of aPKCs are unclear. For cPKCs, phosphorylation at this site is necessary to stabilize the enzyme in a catalytically-competent conformation (24); loss of phosphorylation at this site inactivates the enzyme (15, 25, 26). The mammalian target of rapamycin complex 2 (mTORC2) is required for the phosphorylation of the turn motif site in both PKC and Akt, however by different mechanisms (21, 27, 28). For Akt, mTORC2 directly phosphorylates the nascent Akt polypeptide as it emerges from the ribosome (29, 30). In contrast, cPKC isozymes are phosphorylated post-translationally, with a half-time on the order of 15 min, and at a membrane fraction (31, 32). Although mTORC2 is required for PKC to become phosphorylated (28, 33), whether it directly phosphorylates the turn motif of cPKC or indirectly regulates the site by activation of another kinase or chaperoning remains to be established. The first phosphorylation of cPKCs is the PDK1-mediated phosphorylation on the activation loop, which is a prerequisite for phosphorylation of the turn motif (12, 15). The turn motif of aPKC has been proposed to be regulated by autophosphorylation subsequent to activation loop phosphorylation (19, 34), similar to the hydrophobic motif autophosphorylation of cPKC (5). However, evidence for this claim is also controversial, with recent studies identifying mTORC2 as responsible for phosphorylating the turn motif of aPKC (21).

Given the incomplete understanding of how aPKC isozymes are regulated, we set out to examine the regulation of PKCζ by phosphorylation, insulin, and lipids. Our data reveal that PKCζ is processed by two ordered phosphorylations: the nascent

enzyme is co-translationally phosphorylated by ribosome-localized mTORC2 followed by PDK1-catalyzed phosphorylation at the activation loop to yield a constitutively-phosphorylated and catalytically-competent enzyme. The phosphorylations are stable and insensitive to both insulin and PIP_3. Live cell imaging using a genetically-encoded reporter to measure cellular PKC activity reveals no detectable basal or insulin-stimulated activity on a cytosolic substrate. Based on the exceptionally low turn-over of PKCζ (on the order of 5 reactions per minute), our data support a model in which a mechanism other than phosphorylation is responsible for activating PKCζ, likely involving conformational changes and opportunistic localization towards substrates via protein scaffolds.

2.2 Materials and Methods

Materials

Calyculin A, staurosporine, and LY294002 were purchased from Calbiochem. OSU-03012 was acquired from Cayman Chemical Co. Torin 1 was purchased from Tocris, and GDC-0068 was acquired from Selleckchem. Insulin and cyclohexamide were purchased from Sigma. PZ09 was a kind gift from Dr. Sourav Ghosh and Dr. Christopher Hulme. The following antibodies were purchased from Santa Cruz Biotechnology: anti-p410 PKCζ (sc-12894-R), anti-total PKCζ (sc-216), anti-rpL23a (sc-130252), and anti-GST (sc-138). Antibodies for p308 Akt (9275), p450 Akt (9267), p473 Akt (4060), total Akt (9272), PDK1 (3062), GAPDH (2118), mTOR (2983), rpS6 (2317) p389 S6K (9205), total S6K (9202) and GFP (2555) were

purchased from Cell Signaling Technology. The anti-p560 PKCζ antibody was purchased from AbCam (ab62372), the anti-HA antibody was from Covance (MMS-101P), and the anti-actin antibody was from Sigma (A2228). HRP-conjugated goat anti-mouse IgG and goat anti-rabbit IgG were from Calbiochem (401215 and 401315). AlexaFluor 488-conjugated goat anti-rabbit IgG was from Invitrogen (A110034). Phosphatidylserine (PdS), phosphatidylinositol (3,4,5)-triphosphate (PIP_3) and phosphatidylinositol (4,5)-biphosphate (PIP_2) were purchased from Avanti Polar Lipids (840034, 850457, 850156, and 850155, respectively). Phosphatidic acid (PA) was purchased from Santa Cruz Biotechnology (201059).

Cell Lines and Plasmid Constructs

The PDK1-/- and +/+ MEFs were generously provided by Dr. Wataru Ogawa, Dr. Feng Liu, and Dr. Kun-Liang Guan. The Sin1 -/- and +/+ MEFs were also a gift from Dr. Kun-Liang Guan. The Hep1C1C7 mouse liver cells were a gift from Dr. Jerry Olefsky. Human PKCζ cDNA was a gift from Dr. Tony Hunter while human Akt2 cDNA was a gift from Dr. Alex Toker. The C-kinase activity reporter (CKAR), B-kinase activity reporter (BKAR) and plasma membrane-targeted CFP (PM-CFP) constructs were described previously (107, 109). The pFastBac HT/B vector (Invitrogen) was modified in-house to insert a GST tag for purification in place of the His tag preceding the TEV cleavage site. The first 151 amino acids of human Akt2 were fused to human PKMζ (residues 184 to 592 of PKCζ) to construct the Akt2R-PKMζ chimeric kinase. Human PKCζ, Akt2, and Akt2R-PKMζ constructs were

cloned into the pDONR221 vector and subsequently recombined with various pDEST vectors constructed in-house to make fusion proteins with HA, mCherry, or YFP tags at the N-terminus in pcDNA3 vectors for mammalian cell expression or N-terminal GST-tagged constructs in pFastBac vector for insect cell expression using the Gateway cloning system (Invitrogen). Point mutations were made using Quikchange site-directed mutagenesis (Stratagene).

Baculovirus Construction and Purification of PKCζ

Baculoviruses were made in Sf-9 insect cells from pFastBac plasmids using the Bac-to-Bac expression system (Invitrogen). Batch purification using glutathione sepharose beads was used to purify the GST-tagged proteins from infected Sf-9 insect cell cultures. Briefly, cells were rinsed with PBS and lysed in 50 mM HEPES pH 7.5, 100 mM NaCl (Buffer A) with 0.1% Triton X-100, 100 μM PMSF, 1 mM DTT, 2 mM benzamidine, and 50 μg/ml leupeptin. The soluble lysate was incubated with glutathione resin beads for 30 min at 4°C. Protein-bound beads were washed 3 times in Buffer A and then eluted 3 times in Buffer A with 10 mM glutathione. Eluent was loaded in a 30 kDa Amicon centrifugal filter unit (EMD Millipore) and washed/concentrated 3 times with Buffer B (20 mM HEPES, pH 7.4, 0.1 mg/ml BSA, 2 mM DTT). Glycerol was added to 50% volume before measurement of PKCζ concentration using BSA standards on a Coomassie brilliant blue stained gel and storage of enzyme stocks at -20°C. We note that absolute PKCζ concentrations may not be accurate using BSA as standards.

Lipid Stock Preparation

PIP_3 and PIP_2 were dissolved in 80% chloroform and 20% methanol, wheras all other lipids were dissolved in 100% chloroform. Lipid mixtures were dried under nitrogen gas and then rehydrated in 20 mM Tris, pH 7.4 (for PdS, PC and PA) or water (for PIP_3 and PIP_2) and sonicated to form 10x stocks. For Triton X-100 micelle systems, dried lipids were dissolved in 1% protein-grade Triton X-100 (Calbiochem) and diluted to form different 10x mole % lipid formulations.

In vitro Kinase Activity Assay

Purified or immunoprecipitated proteins were diluted in Buffer B. Kinase activity was measured in 80 μL reactions supplemented with 140 μM PdS for standard multilammellar assay or 10x lipid/Triton X-100 formulation for mixed micelle assays. aPKC reactions were initiated by addition of 100 μM ATP, 100 μg/ml myelin basic protein (MBP, Sigma), 5 mM $MgCl_2$ and 10 μCi/ml [γ-^{32}P]ATP (Perkin Elmer). Reactions were conducted for 15-30 min at 30°C with 20-25 nM enzyme for purified proteins, stopped by addition of 25 mM ATP, 25 mM EDTA, pH 8.0, and spotted onto P81 Whatman filters. Filters were washed 4x with 0.4% phosphoric acid before measurement using a Beckman scintillation counter.

In vitro Phosphatase Assay

25 nM purified GST-PKCζ was incubated in Buffer B with 140 μM PdS, 200 μM $MnCl_2$, 500 μM $CaCl_2$, 400 μM EDTA, and 100 units/ml protein phosphatase 1

(PP1, New England Biolabs) for 0-60 min at 30°C in 40 µl reactions. Reactions were stopped at various time points with Buffer C (62.5 mM Tris, 2% SDS, 10% glycerol, 20 µg/ml bromophenol blue, 2.86 M 2-mercaptoethanol) with 5 mM EDTA then run on immunoblots to quantify dephosphorylation of GST-PKCζ over time.

Cell Culture and Transfection

Sf-9 cells were grown in Sf-900 II SFM media (Gibco) in shaking cultures at 27°C. All mammalian cells were maintained at 37°C in 5% CO_2. CHO-IR cells were grown in DMEM/F-12 50/50, 1X (Cellgro) supplemented with 5% dialyzed fetal bovine serum (FBS, Atlanta Biologics), 100 units/ml penicillin, 100 µg/ml streptomycin and 50 µg/ml geneticin (Gibco). Hep1C1C7 cells were grown in MEM Alpha 1X (Gibco) supplemented with 10% FBS, 100 units/ml penicillin and 100 µg/ml streptomycin. COS-7, 293T, and all MEFs were grown in DMEM 1X supplemented with 10% FBS, 100 units/ml penicillin and 100 µg/ml streptomycin. 3 µg/ml puromycin (Sigma) was added to the media for PDK1+/+ and -/- MEFs. Mammalian cells were transiently transfected using jetPrime (Polyplus Transfection).

Immunoprecipitation and Immunoblotting

Cells transfected with HA-tagged kinases to be immunoprecipitated were serum starved overnight and treated with or without 100 nM insulin (Sigma) for 10 min before rinsing in PBS and lysing in Buffer D (100 mM KCl, 50 mM Tris, 3 mM

NaCl, 3.5 mM $MgCl_2$, pH 7.3) with 1% protein-grade Triton X-100 (Calbiochem), 100 μM PMSF, 1 mM DTT, 2 mM benzamidine, 50 μM PMSF, 50 μg/ml leupeptin, 1 μM microcystin-LR (Calbiochem) for activity assays or Buffer E (150 mM NaCl, 50 mM Tris, 100 mM NaF, 100 mM β-glycerophosphate, 1% IGEPAL pH 7.8) with 20 μg/ml RNaseA, 20 μg/ml DNaseI, phosphatase inhibitor cocktails #2 and #3 diluted 1:100 (Sigma, P5726 and P0044) and protease inhibitor cocktail diluted 1:200 (Sigma, P8340) for immunoprecipitation prior to isoelectric focusing (IEF). Soluble lysates were incubated with anti-HA antibody (Covance) for 1-2 hrs followed by incubation with Protein A/G resin beads (Thermo Scientific) for 1-2 hrs. Protein-bound beads were washed 3 times with Buffer D and diluted in Buffer B before assaying activity or were washed 3 times with Buffer E, PBS, and 1 mM EGTA, 75 mM KCl, 50 mM Tris pH 8.5 prior to elution for IEF. For experiments with immunoblotting only, cells were lysed in Buffer F (100 mM NaCl, 50 mM Tris, 10 mM $Na_4P_2O_7$, 50 mM NaF, 1% Triton X-100, pH 7.2) with 100 μM PMSF, 1 mM DTT, 2 mM benzamidine, 50 μM PMSF, 50 μg/ml leupeptin, 1 μM microcystin-LR, and whole cell lysates were sonicated prior to adding Buffer C, boiling at 100°C and performing SDS-PAGE. Gels were transferred to PVDF membrane and blocked with 5% milk before incubating with antibodies and imaging via chemiluminescence on a FluorChemQ imaging system (Protein Simple).

Isoelectric Focusing (IEF)

2D-IEF was performed as described (126) by immunoprecipitating HA-PKCζ and eluting in 7 M urea, 2 M thiourea, 2% CHAPS (pH 8.4), then loading onto the acidic end of 3–10 immobiline strips (GE Healthcare) with the current ramped up from 200 V for 2 hr, 500 V for 1 hr, 800 V for 1 hr, 1000 V for 0.5 hr, 1200 V for 0.5 hr, 1400 V for 0.5 hr, 1600 V for 0.5 hr, 1800 V for 2.5 hr, and 2000 V for 2.5 hr. Second dimension was performed by soaking IEF strip in 2% SDS, 6 M urea, 75 mM Tris (pH 8.8), 29% (wt/vol) glycerol, 10 mg/ml DTT, and 25 mg/ml iodoacetamide (Sigma Aldrich), and placing the strip on top of a 10% SDS-PAGE containing a single large well to accommodate the IEF strip with molecular weight marker side wells.

Cell Fractionation and Polysome Analysis

Cells were grown, serum starved overnight, re-stimulated with 10% serum for 1 hour, treated with 100 mg/ml cyclohexamide for 15 min, then harvested, lysed and processed for fractionation as previously described (29) with the following modification: lysates were layered on a 10 mL 7-47% (wt/vol) sucrose gradient (5 layers: 7, 17, 27, 37, 47%). Fractions were concentrated to a final volume of 100 μL with Amicon Ultra-4 centrifugal filter unit (EMD Millipore). Proteins were separated by SDS-PAGE and detected by immunoblotting.

Live Cell Fluorescence Imaging

COS-7 cells were plated onto sterilized glass coverslips in 35 mm dishes, co-transfected with the indicated constructs, and imaged in Hanks' balanced salt solution supplemented with 1 mM $CaCl_2$ approximately 24 hours post-transfection. For experiments with insulin stimulation, cells were serum starved for 4-6 hours or overnight prior to imaging via a 40X objective. Kinase activity was monitored via intramolecular FRET of the activity reporters (CKAR or BKAR) while kinase translocation was monitored via intermolecular FRET between the YFP-tagged kinase and the plasma membrane targeted CFP using methods previously described (127).

Immunofluorescence

COS-7 cells were seeded onto 22 mm poly-D-lysine-treated glass coverslips in a 6-well plate, grown for approximately 20 hours, serum starved for 4 hours, and treated with or without 100 nM insulin for 10 min. Cells were rinsed briefly in PBS and fixed with 4% paraformaldehyde for 15 min at room temperature followed by incubation with 100% methanol for 3 min at -20°C. Cells were rinsed again in PBS 3 times followed by permeabilization and blocking in PBS containing 0.25% Triton X-100, 5% BSA and 5% goat serum for 15 min at room temperature. Cells were incubated in a humidified chamber for 1 hour at room temperature with either a PKCζ-specific antibody (Santa Cruz Biotechnology sc-216 diluted 1:40, also detects PKCλ) or a pan-Akt antibody (Cell Signaling 9272, diluted 1:200). Cells were then rinsed 3

times in PBST and incubated in a humidified chamber protected from light for 30 min at room temperature with an AlexaFluor 488-conjugated secondary antibody (Invitrogen A110034, diluted 1:500). Cells were rinsed a final 3 times in PBST prior to mounting the coverslips on glass slides and imaging via a 40X objective on a Zeiss Axiovert fluorescent microscope (Carl Zeiss Microimaging, In.) using a MicroMax digital camera (Roper-Princeton Instruments) controlled by MetaFluor software version 3.0 (Universal Imaging Corp.).

Statistical Analysis

All statistical analyses were performed using GraphPad Prism 6.0 (GraphPad Software, Inc).

2.3 Results

Phosphorylation at the activation loop and turn motif of PKCζ is each independently required but not sufficient for activity

Similar to conventional and novel PKC isoyzmes and to Akt, the atypical PKCζ has a Thr residue at the phospho-acceptor site of the conserved activation loop and turn motif. However, contrasting with these closely-related enzymes, it contains a phosphomimetic Glu at the hydrophobic motif, a property shared by PKN family members, which have an Asp at this position (**Fig 2.1a**). To validate the requirement of phosphorylation at the key conserved Thr residues for enzyme activity using

purified protein, rather than immunoprecipitated protein (19), we constructed phospho-resistant Ala mutants at both the activation loop (T410) and the turn motif (T560) of human PKCζ (analogous site locations shown on structure of PKCι in **Fig 2.1b**). We purified an N-terminally tagged GST fusion construct of PKC from Sf-9 insect cells. Protein purity of > 90% was achieved, with yields on the order of 50 μg protein from 5 x 10^7 cells for wild-type (wt) enzyme and corresponding mutants (**Fig 2.1c**). Wild-type enzyme had a specific activity of 5 ± 1 mol phosphate per min per mol PKC with lipid present (**Fig 2.1d**), over an order of magnitude lower than that of conventional PKCs, which catalyze approximately 200 reactions per min with lipid present (128). Both the T410A and T560A mutants had significantly reduced activity compared to the wild-type enzyme, with the T560A mutation being even more detrimental to catalytic competency (**Fig 2.1d**), in agreement with previous studies conducted on immunoprecipitated versions of these mutants (19). Consistent with the lack of T410A and T560A mutants' activity, *in vitro* dephosphorylation of wild-type enzyme with protein phosphatase 1 (PP1) decreased its activity (data not shown). Mutation of either site to negatively charged phospho-mimetic Glu (T410E or T560E) resulted in a slightly reduced specific activity that was more comparable to that of wild-type enzyme. The Glu residue present at the hydropohic motif (E579) was also mutated to Ala to assess the requirement of negative charge at the hydrophobic motif on activity. The E579A mutant had similar activity to wild-type protein (**Fig 2.1d**).

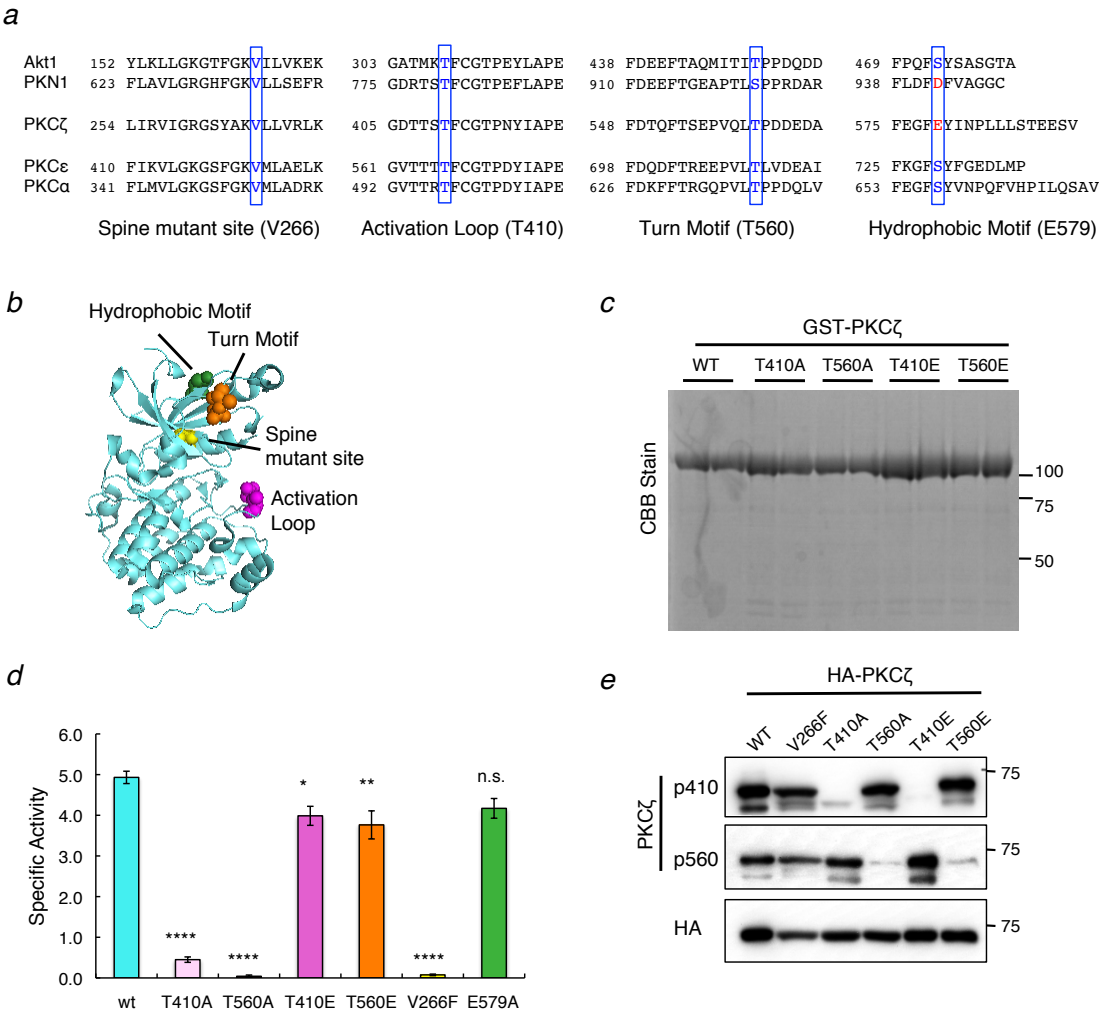

Figure 2.1: Phosphorylation at the activation loop and turn motif of PKCζ is each independently required but not sufficient for activity. (a) Alignment of amino acid residues at the spine mutant, activation loop, turn motif and hydrophobic motif sites shown in blue text for human PKC (conventional PKCα, novel PKCε and atypical PKCζ) and the other related AGC kinases Akt1 and PKN1. The hydrophobic motif Glu and Asp residues of PKCζ and PKN1 are notated in red. Sequences for these kinases are listed in the order they appear on their branch of the kinome (11). Specific residue numbers for human PKCζ are indicated. **(b)** Structure of an aPKC kinase domain (human PKCι, PDB: 3A8W) showing locations of analogous sites for PKCζ. **(c)** Coomassie brilliant blue (CBB) stain of GST-PKCζ expressed and harvested from baculoviral-infected Sf-9 cells, isolated to >90% purity. **(d)** Specific activity, measured in mol of phosphate (P)*min^{-1}*mol $PKC\zeta^{-1}$, of wild-type (wt) and various mutants of purified GST-PKCζ incubated *in vitro* with myelin basic protein (MBP) as substrate. Error bars represent standard error of mean (± S.E.) for n=3 reaction experiments. Statistical analysis was performed using ordinary one-way ANOVA followed by Dunnett's multiple comparison test with wild-type as control. Significance notated as * ($p < 0.05$), ** ($p < 0.01$), **** ($p < 0.0001$), or n.s. (not significant). **(e)** Immunoblots showing activation loop and turn motif phosphorylationstatus of HA-PKCζ and mutants expressed in mammalian CHO-IR cells.

The turn motif (T560) of PKCζ is not regulated by autophosphorylation

To address whether T560 is an autophosphorylation site as previously proposed (19, 34), we constructed a catalytically-inactive "spine mutant" V266F in the kinase domain of PKCζ (conserved alignment with other AGC kinases showin in **Fig 2.1a**, structural location in relation to other key sites shown in **Fig 2.1b**). This Val residue was mutated to a Phe capable of inserting into the ATP-binding pocket of the enzyme and blocking ATP binding, a method for inactivating a kinase without compromising its structural integrity, recently developed by Taylor et al. (129). Indeed, the V266F mutant was catalytically dead (**Fig 2.1d**) yet was fully phosphorylated at T560 as demonstrated by Western blot analysis of mammalian CHO-IR lysates expressing this construct (**Fig 2.1e**). The specificity of the phospho-specific antibodies was confirmed and validated by the lack of significant labeling of the T410A or T410E constructs by the p410 antibody and the T560A or T560E constructs by the p560 antibody (**Fig 2.1e**). Note that replacement of the activation loop with Ala did not affect phosphorylation of the turn motif nor did replacement of the turn motif site with Ala affect phosphorylation of the activation loop. The phosphorylation of the V266F mutant at the turn motif reveals that the intrinsic catalytic activity of PKCζ is not required for phosphorylation of the turn motif.

Phosphorylation at the activation loop (T410) and turn motif (T560) of PKCζ is basal and insensitive to phosphatase inhibition

To assess whether the key phospho-sites of PKCζ are phosphorylated under basal conditions, COS-7 cells were treated with the phosphatase inhibitor calyculin A (50 nM) and phosphorylation was monitored via immunoblotting for a time course up to 10 min after treatment. As a control for phosphatase inhibition, phosphorylation at the hydrophobic motif of S6 kinase (S6K, T389, an agonist-induced phosphorylation site) was monitored and steadily increased over the time period (**Fig 2.2a, 2.2b**). Quantification of data from 4 separate experiments revealed no change in the phosphorylation state of T410 or T560 following treatment with calyculin (**Fig 2.2b**). These data reveal that phosphorylation of PKCζ at the activation loop and turn motif is insensitive to calyculin, reflecting either stoichiometric phosphorylation under basal conditions or regulation by calyculin-insensitive phosphatases. To further investigate the basal phosphorylation state at T410 and T560, two dimensional isoeletric focusing (2D IEF) was performed on wild-type HA-PKCζ, single phosphorylation site mutants T410A, T560A and double phosphorylation site mutant T410A T560A immunoprecipitated from CHO-IR cells (**Fig 2.2c**). Phosphorylation is a highly acidic modification that is readily resolved by 2D IEF. Wild-type HA-PKCζ enzyme migrated predominantly as two acidic species. Quantitation of the data from 3 independent experiments revealed that the most acidic species comprised 41 ± 2% of the signal. This species likely represents enzyme phosphorylated at both T410 and T560. An intermediate species resolved at the same isoelectic point as each of the single mutants (T410A and T560A) and likely represents a mono-phosphorylated species. A few times, we observed the intermediate species of the wild-type enzyme separate into a third species (data not shown) that resolved at the same isoelectric

point as the T410A T560A double mutant. This spot likely represents enzyme that was dephosphorylated during the immunoprecipitation process. These data reveal that doubly phosphorylated PKCζ is a significant species in cells.

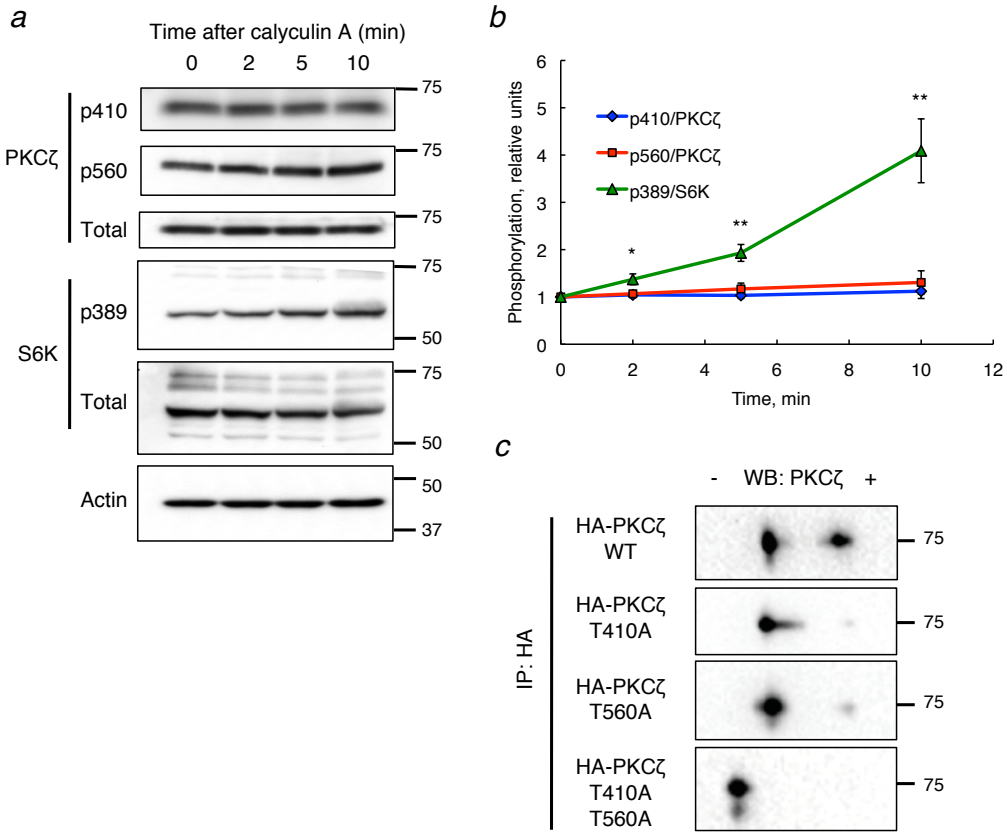

Figure 2.2: PKCζ is basally phosphorylated and insensitive to phosphatase inhbition. (a) Immunoblots of lysates from COS-7 cells treated with 50 nM calyculin A (phosphatase inhibitor) for a time course of 0-10 min showing degree of T410 and T560 phosphorylation on PKCζ over time in comparison to T389 phosphorylation on S6K. **(b)** Quantification of blots from (a) using n=4 separate experiments shown as phosphorylated protein over total protein normalized to t=0 min baseline, plotted as mean ± S.E. Statistical analysis was performed using ordinary one-way ANOVA at each time point followed by Dunnett's multiple comparison test with p389/S6K as control. Significance notated as * ($p < 0.05$) or ** ($p < 0.005$). **(c)** Immunoblots of 2D-IEF run on immunoprecipitated HA-PKCζ wild-type and phosphorylation site mutants.

Phosphatidylserine promotes the open conformation of PKCζ, as evidenced by increased rate of dephosphorylation at T410 on PKCζ, and increases specific activity of purified PKCζ; low concentrations of phosphoinositides do not activate PKCζ

For conventional PKC isozymes, binding to activating lipids promotes an open conformation that results in a two-orders of magnitude increase in phosphatase sensitivity at their priming sites (15). To investigate whether binding to phosphatidylserine (PdS), which binds the C1 domain of all PKCs (130) also induces an open conformation of PKCζ, we examined the effect of PdS on the rate of dephosphorylation of PKCζ. Purified GST-PKCζ was incubated *in vitro* with protein phosphatase 1 (PP1), a phosphatase known to dephosphorylate both the activation loop and turn motif of PKC isozymes (15). The rate of dephosphorylation at T410 was measured through quantitative immunoblots and was significantly increased in the presence of PdS lipid (**Fig 2.3a, 2.3b**). To assess the effect of lipids on the specific activity of PKCζ, we employed 2 different *in vitro* lipid systems: multilamellar structures and Triton X-mixed micelles, used previously to examine the effects of lipids on the activity of conventional PKC (128, 131, 132). The abundant lipids PdS and phosphatidic acid (PA) were prepared as multilamellar structures whereas the rare lipids PIP_3 (phosphatidylinositol (3,4,5)-triphosphate) and its PI3-kinase-targeted precursor PIP_2 (phosphatidylinositol (4,5,)-biphosphate) were solubilized with Triton X-100 to form mixed micelles with varying mole percent lipid, illustrated by cartoons in **Fig 2.3c**. The latter system is particularly useful in examining lipid specificity and stoichiometry for activation of monomeric PKC (133-135). The specific activity of

GST-PKCζ was increased nearly 3-fold with increasing PdS multilamellar concentrations up to 140 μM; PA multilamellae activated PKCζ to a more modest extent (**Fig 2.3d**). Neither PIP_3 nor PIP_2 activated PKCζ at concentrations up to 2.5 mole % (corresponding to 3-4 molecules of the lipid per micelle) in the mixed micelle system (**Fig 2.3e**) revealing these lipids are not acting as specific agonists for PKCζ. Higher concentrations were not tested given the low abundance of these lipids in membranes. These data support previous findings that the activity of PKCζ is stimulated by cellular phosphatidylserine but suggest that phosphoinositides and most notably PIP_3 do not stimulate the activity of PKCζ in cells given the low abundance of these lipids

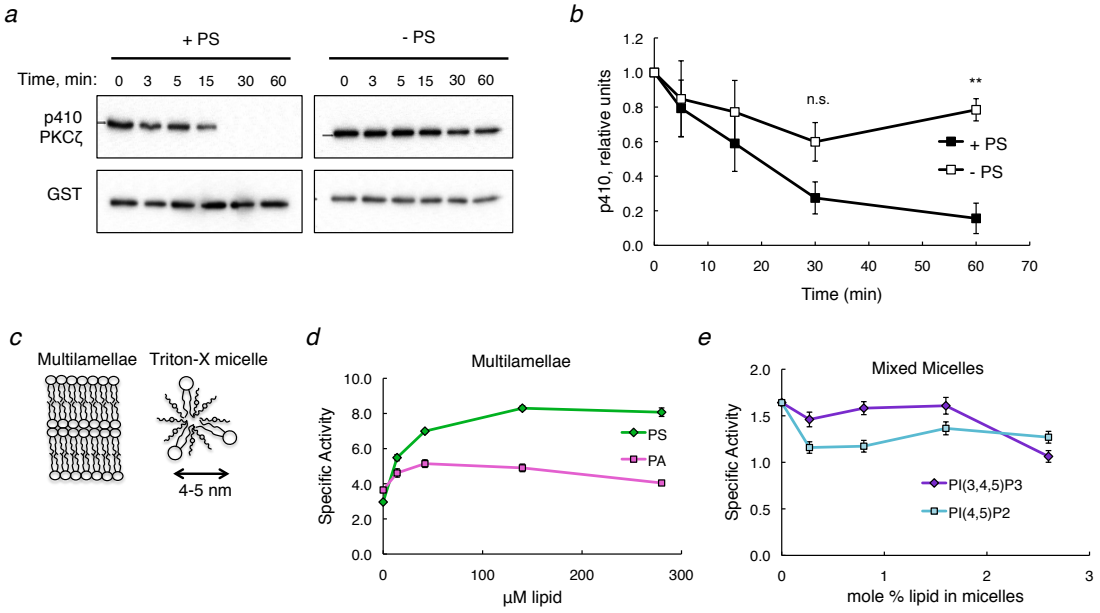

Figure 2.3: Phosphatidylserine promotes the open conformation of PKCζ and increases specific activity of purified PKCζ; low concentrations of phosphoinositides do not activate PKCζ. (a) Time course of purified GST-PKCζ and pure PP1 incubated with or without phosphatidylserine (PS) lipid. Immunoblots show degree of T410 dephosphorylation over time, with corresponding GST signal representing total GST-PKCζ present. Experiements performed by Nitya Simon. **(b)** Quantification of blots from (A) using n=4 separate experiments shown as p410 signal over GST signal normalized to t=0 min baseline, plotted as mean ± S.E. Statistical analysis was performed using unpaired t-tests for t=30 min and t=60 min time points. Significance notated as ** ($p < 0.005$) or n.s. (not significant). **(c)** Diagram depicting structural presentation of lipids in multilamellar systems and Triton X-100 detergent soluble micelles. **(d)** Specific activity, measured in mol(P)*min^{-1}*mol PKCζ of purified GST-PKCζ incubated with either PS or phosphatidic acid (PA) multilamellae of variable lipid concentrations. **(e)** Specific activity of purified GST-PKCζ incubated with Triton X-100 mixed micelles of varying mole % lipid present for PI(3,4,5)P_3 and PI(4,5)P_2**.**

PDK1 is required for constitutive phosphorylation of the PKCζ activation loop but not the turn motif

PDK1 phosphorylates the activation loop of PKCζ (12-14), but whether this event is required for phosphorylation of the turn motif is unclear. We examined lysates from PDK1 knockout MEFs (PDK1-/-) vs their wild-type (PDK1+/+) counterparts (**Fig 2.4a**). As expected, PKCζ from the PDK1 knockout MEFs had significantly reduced T410 phosphorylation compared to the PKCζ in the wild-type

MEFs. In contrast, phosphorylation at T560 was not decreased in the PDK1 -/- MEFs, quantification shown in **Fig 2.4b**. We also examined the insulin sensitivity of PKCζ phosphorylation. Treatment of either wild-type or PDK1-/- MEFs with insulin had no effect on the phosphorylation of either the PDK1 site, T410, or the turn motif, T560 (**Fig 2.4a**). As a control, we examined Akt, whose activation loop (T308) phosphorylation is insulin dependent and regulated by PDK1, and was indeed ablated in the PDK1-/- MEFs. Treatment of the PDK1+/+ MEFs with insulin produced a significant increase in T308 Akt phosphorylation, which was blocked by pre-treatment with the general kinase inhibitor staurosporine and reduced by pre-treatment with PDK1-specific inhibitor OSU03012 (**Fig 2.4c**). Thus, under conditions where insulin regulates the phosphorylation of the activation loop of Akt, the phosphorylation of the PKCζ activation loop was insensitive to insulin. This result was also observed in the insulin-sensitive CHO-IR cell line (**Fig 2.4d**). Taken together, these data reveal that the activation loop of PKCζ is constitutively phosphorylated by PDK1 and that this reaction is not necessary for turn motif phosphorylation.

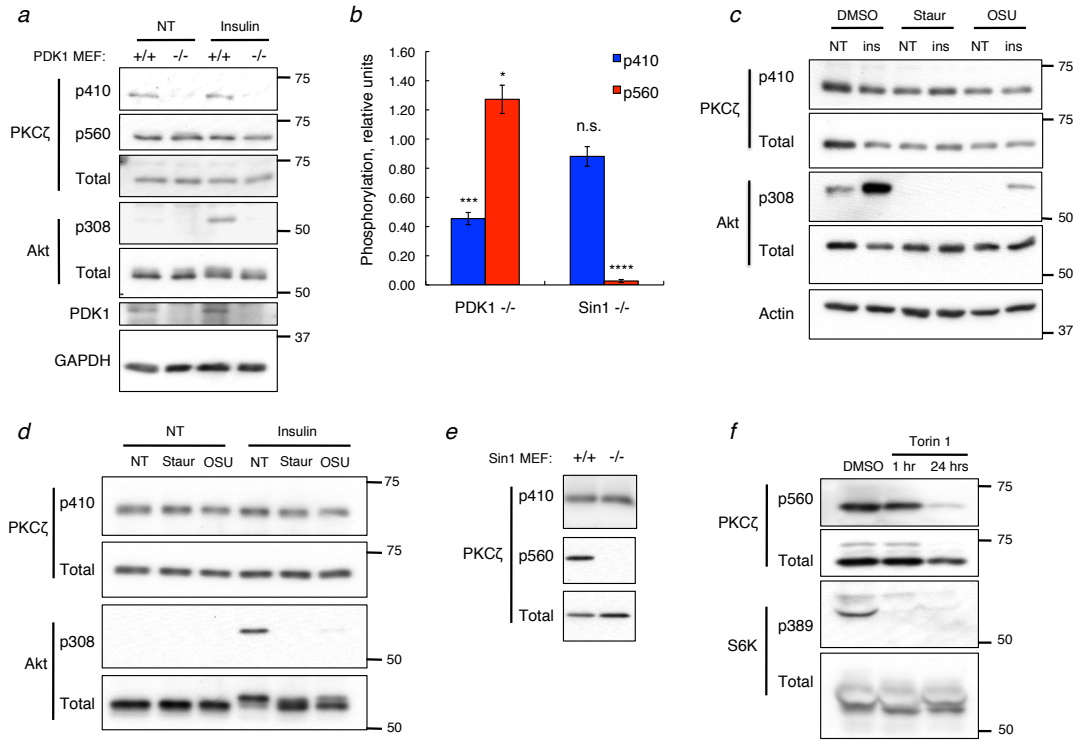

Figure 2.4: PDK1 and mTORC2 are required for constitutive phosphorylation of T410 and T560 sites on PKCζ, respectively. (a) Immunoblots of PDK1+/+ and PDK1-/- lysates comparing phosphorylation at the activation loop (p410) and turn motif (p560) sites of PKCζ along with activation loop phosphorylation of Akt (p308) with or without 100 nM insulin treatment for 10 min. **(b)** Quantification of blots from (A) and (E) using n=3-4 separate experiments shown as phosphorylated protein over total protein normalized to corresponding +/+ MEFs, plotted as mean ± S.E. Statistical analysis was performed using ordinary one-way ANOVA followed by Dunnett's multiple comparison test with wild-type baseline as control. Significance notated as * ($p < 0.05$), *** ($p < 0.001$), **** ($p < 0.0001$), or n.s. (not significant). PDK1+/+ MEFs **(c)** and CHO-IR **(d)** were serum starved overnight and treated with DMSO, 1 μM staurosporine (Staur) or 10 μM OSU03012 (OSU) for 30 min prior to treatment with or without 100 nM insulin for 10 min. Lysates were immunoblotted for activation loop phosphorylation status of PKCζ and Akt. **(e)** Immunoblots of Sin1+/+ and Sin1-/- MEFs showing phosphorylation at the activation loop and turn motif sites of PKCζ. **(f)** Immunoblots of Sin1+/+ MEFs treated with DMSO or 100 nM Torin 1 (mTOR inhibitor) for 1 hour or 24 hours prior to lysis showing phosphorylation of T560 on PKCζ. Phosphorylation of S6K at T389 is shown as validation of mTOR inhibition.

mTORC2 is required for constitutive phosphorylation of the PKCζ turn motif but not the activation loop

mTORC2 has previously been shown to be required for phosphorylation at the turn motif sites on both conventional PKC and Akt (28), with a recent study also

supporting its phosphorylation of the turn motif of PKCζ (21). To address whether this phosphorylation is necessary for phosphorylation of the PDK1 site, we examined lysates from MEFs that are deficient in Sin1, a necessary component for mTORC2 formation (136). Phosphorylation at T560 was ablated in Sin1-/- MEFs (**Fig 2.4e**) while phosphorylation of T410 was comparable between Sin1+/+ MEFs and Sin1-/- MEFs, as quantified in **Fig 2.4b**. Phosphorylation of T560 was unaffected by a 1 hour treatment with an mTOR inhibitor, Torin 1, in Sin1+/+ MEFs (**Fig 2.4f**) yet was significantly reduced by Torin 1 treatment after 24 hours, in agreement with previous studies using long term mTOR inhibition (21). In contrast, the phosphorylation at T389 on S6K, the agonist-evoked site of mTORC1 phosphorylation (137), was blocked within 1 hour, thus validating mTOR inhibition (**Fig 2.4f**). These data reveal that phosphorylation at the turn motif is also constitutive and not necessary for phosphorylation at the PDK1 site.

The phosphorylation of PKCζ at the turn motif but not the activation loop occurs during translation

Previous studies have established that the turn motif of Akt (T450) is phosphorylated during translation, an event that precedes subsequent agonist-evoked phosphorylation of the activation loop (T308) and hydrophobic motif (S473) (29). These results were acquired by immunoblot analysis of polysomes obtained by fractionation of serum-starved and re-stimulated cells treated with cyclohexamide to preserve intact polysomes. Similar fractionations (**Fig. 2.5a**) revealed that the PKCζ

associated with polysomes is phosphorylated at the turn motif (p560) but not the PDK1 site (p410) (**Fig. 2.5b**, polysome fractions 7-9). Polysome fractions were devoid of significant PDK1 but had readily detectable levels of mTOR. These data reveal that similar to Akt, the turn motif of PKCζ is co-translationally phosphorylated by mTORC2 at polysomes.

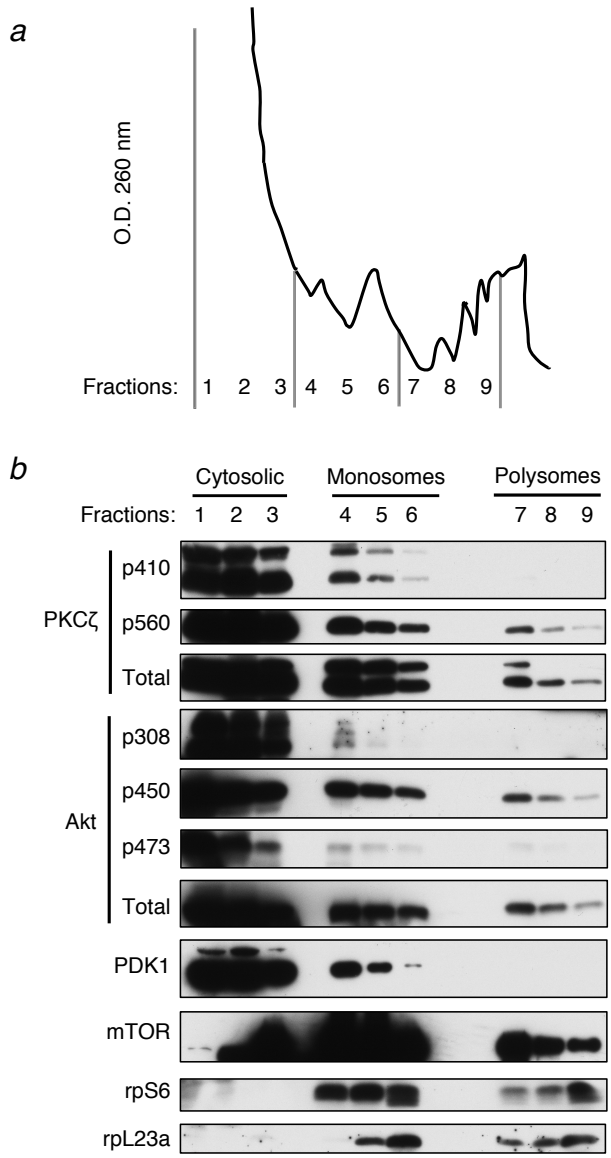

Figure 2.5: The turn motif site of PKCζ is phosphorylated during translation. Wild type murine embryonic fibroblasts (MEFs) were starved starved overnight and re-stimulated with serum for 1 hour, then treated with cycloheximide for 15 minutes. **(a)** Absorbance (A260; y axis) versus increasing density (x axis) of sucrose fractions from cell lysates was monitored. **(b)** Aliquots of each fraction were separated by SDS-PAGE followed by immunoblotting for analysis of protein expression and phosphorylation state of PKCζ and Akt. Ribosomal marker proteins rpS6 and rpL23A are shown for validation of fractionation process. Experiments were performed by Peter Kim.

The catalytic activity of PKCζ does not increase following insulin stimulation

We employed both *in vitro* and live cell methods to investigate whether insulin stimulates the intrinsic catalytic activity of PKCζ. Using the *in vitro* assay with MBP as a substrate that we previously validated with pure GST-PKCζ (**Fig 2.1d**), we measured the relative catalytic activity of over-expressed HA-PKCζ immunoprecipitated from Hep1C1C7 liver cells treated with or without 100 nM insulin for 10 min. The T560A catalytically-inactive mutant was employed as a control for background kinase activity from the immunoprecipitate. **Fig 2.6a** shows that wild-type HA-PKCζ had significantly higher activity than the T560A mutant yet there was no significant difference in activity of enzyme immunoprecipitated from cells treated with or without insulin. We also examined the phosphorylation state of the immunoprecipitated protein and observed no changes in the phosphorylation of the activation loop of PKCζ (p410, **Fig. 2.6b**). Under the conditions of these assays, insulin caused a robust increase in the activation loop phosphorylation of endogenous Akt (p308). Similar results were also observed in insulin-sensitive CHO-IR cells (data not shown). Using a genetically-encoded FRET reporter, C Kinase Activity Reporter (CKAR, (109)) previously validated for examining activity of the PKCζ catalytic moiety, PKMζ in real time in live cells (112), we measured the activity of N-terminally tagged mCherry-PKCζ in live COS-7 cells. Insulin treatment did not stimulate PKCζ activity as assessed using CKAR. Under comparable conditions, insulin effectively stimulated Akt activity in cells expressing mCherry-Akt2 as assessed using the Akt reporter B Kinase Activity Reporter (BKAR, (107)); this

activity was reversed with the Akt active site inhibitor GDC-0068 (**Fig 2.6c**). Endogenous Akt activity was also stimulated by insulin in cells expressing mCherry vector with BKAR and inhibited by treatment with GDC-0068. Similar results were obtained using a C-terminally tagged PKCζ-RFP construct, examining either cytosolic CKAR or plasma membrane-targeted CKAR, in both COS-7 and CHO-IR cells (data not shown).

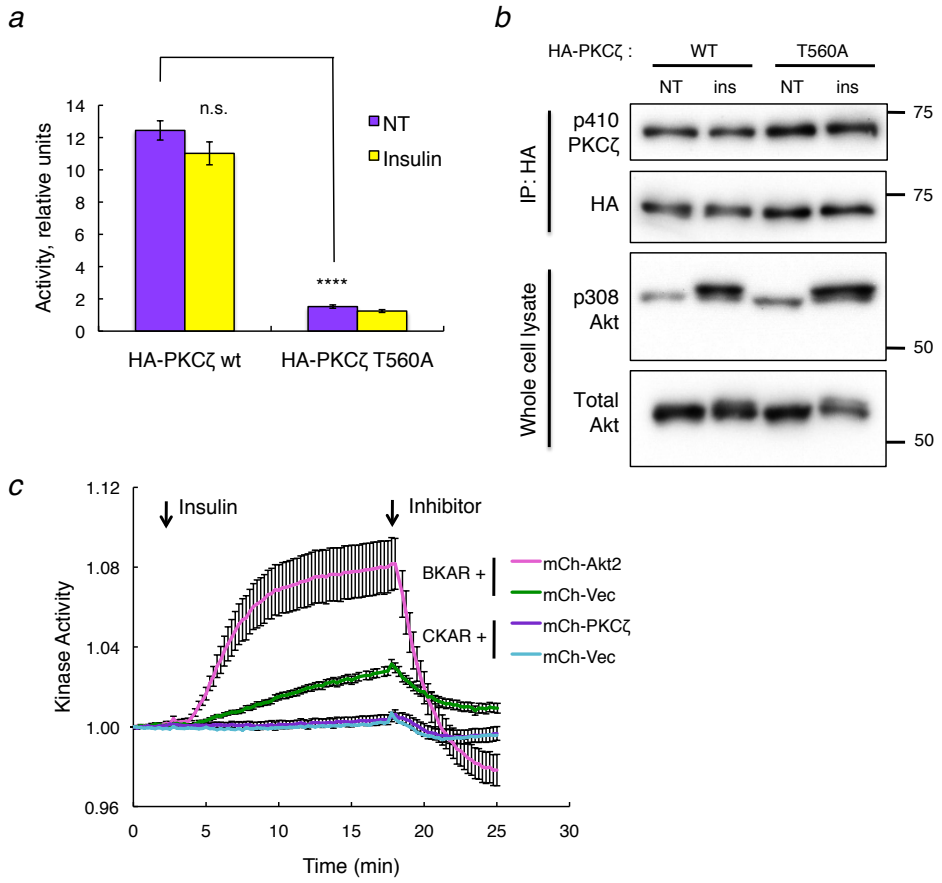

Figure 2.6: The catalytic activity of PKCζ does not increase due to insulin stimulation. (a) Activity of wild-type (wt) and kinase-dead (T560A) HA-PKCζ immunoprecipitated from Hep1C1C7 serum starved overnight and treated with (Insulin) or without (NT, no treatment) 100 nM insulin for 10 min prior to lysis. Kinase-bound beads were incubated *in vitro* with MBP substrate and [γ-^{32}P]ATP. Activity was measured as CPM normalized by total HA signal from immunoblot and plotted as mean ± S.E. for n=3 reaction experiments. Statistical analysis was performed using ordinary two-way ANOVA followed by Dunnett's multiple comparison test with non-treated wild-type (wt NT) as control. Significance notated as **** ($p < 0.0001$) or n.s. (not significant). **(b)** Immunoblots of activation loop phosphorylation for immunoprecipitated HA-PKCζ from (a) along with total HA signal and activation loop phosphorylation of Akt from whole cell lysate. **(c)** Global cytosolic kinase activity measured via changes in CFP over FRET ratio using Akt-specific reporter BKAR and mCherry-tagged Akt2 or vector (Vec) or PKC-specific reporter CKAR and mCherry-tagged PKCζ or vector in live COS-7 cells serum starved for 4-6 hours prior to imaging and treatment with 100 nM insulin then inhibitors (20 μM GDC-0068 for BKAR assays or 1 μM staurosporine for CKAR assays). The trace for each cell imaged was normalized to its t=0 min base-line value, and normalized FRET ratios were combined from three independent experiments and plotted as mean ± S.E.

The phosphorylation of PKCζ is neither agonist-evoked nor regulated by PI3-kinase through translocation to the plasma membrane in response to insulin

Previous studies have suggested that PI3-kinase mediates agonist-evoked phosphorylation of aPKCs by recruiting the enzymes to the membrane through production of PIP_3 in a similar fashion to the activation of Akt (14, 19, 138, 139). To address this claim, we treated Hep1C1C7 cells with 20 μM of the PI3-kinase inhibitor LY294002 (LY) prior to insulin stimulation (**Fig 2.7a**). No change in T410 or T560 PKCζ phosphorylation was observed with either insulin or LY treatment for either cell line quantified over 8 separate experiments (**Fig 2.7b**). Similar results were seen with CHO-IR cells under the same conditions (data not shown). As a control, immunoblot analysis revealed that LY abolished the robust insulin-dependent phosphoryation of T308 on Akt. To directly assess whether PKCζ was recruited to the plasma membrane in response to insulin treatment, we monitored changes in intermolecular FRET between N-terminally-tagged YFP-PKCζ or YFP-Akt2 and plasma membrane-targeted CFP (PM-CFP) in live COS-7 cells during treatment with 100 nM insulin. YFP-Akt2 exhibited a translocation response that was evident through the steady increase in FRET ratio following treatment with insulin (**Fig 2.7c**). However, the traces for YFP-PKCζ remained flat after insulin stimulation, indicating that no translocation to the plasma membrane had occurred for PKCζ. To corroborate that endogenous PKCζ and Akt displayed the same translocation results as their over-expressed counterparts imaged in **Fig 2.7c**, we performed immunofluorescence imaging of COS-7 cells treated with or without insulin, fixed and stained with

antibodies against PKCζ or Akt. The representative images shown in **Fig 2.7d** reveal a classic plasma membrane translocation of Akt in response to insulin, evident through the ruffled appearance of stained Akt in comparison to the untreated control, similar to translocation images from COS7 shown previously (140). However, no change in the localization of endogenous PKCζ was observed in any of the images taken.

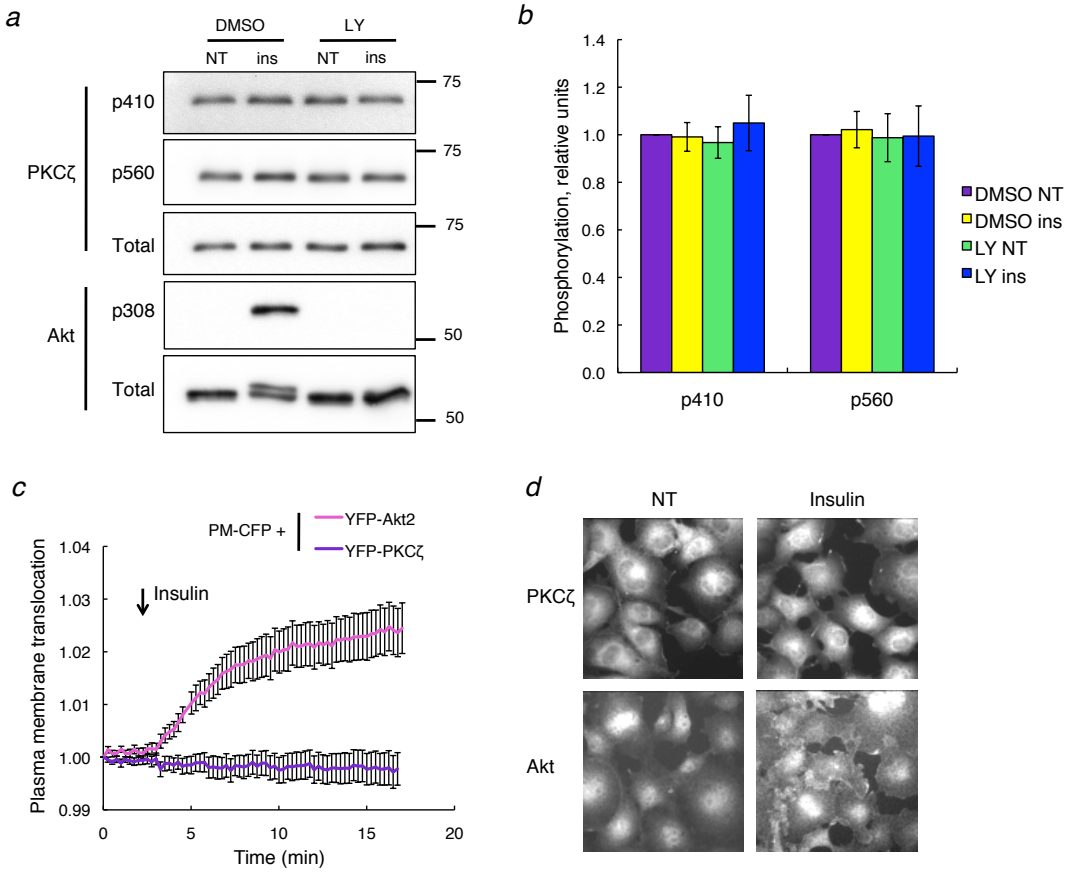

Figure 2.7: The phosphorylation of PKCζ is not agonist-evoked nor regulated by PI3-kinase through translocation to the plasma membrane in response to insulin. **(a)** Hep1C1C7 cells were serum starved for 4 hours then treated with DMSO or 20 μM LY294002 (LY) for 20 min prior to treatment with or without 100 nM insulin for 10 min. Immunoblots showing phosphorylation status of PKCζ at the activation loop (p410), turn motif (p560) and Akt at the activation loop (p308). **(b)** Quantification of blots from (A) using n=8 separate experiments shown as p410 or p560 over total PKCζ normalized to "DMSO NT" control, plotted as mean ± S.E. **(c)** Translocation assay of YFP-tagged Akt2 or PKCζ to plasma membrane (PM-CFP) in live COS-7 cells serum starved for 4-6 hours prior to imaging, measured as change in FRET over CFP ratio in response to 100 nM insulin. The trace for each cell imaged was normalized to its t=0 min base-line value, and normalized FRET ratios were combined from three independent experiments and plotted as mean ± S.E. **(d)** Representative images of COS-7 cells treated with or without 100 nM insulin for 10 min prior to fixation and staining with antibodies for PKCζ or Akt as described in Materials and Methods.

A fusion construct of the Akt2 PH domain with PKMζ translocates to the plasma membrane in response to insulin yet does not exhibit agonist-evoked activity nor phosphorylation at the activation loop

The pleckstrin homology (PH) domain of Akt is a well characterized binder of activated PIP_3 lipid at the plasma membrane (141, 142). To investigate whether this domain was also capable of generating aPKC agonist-induced translocation, we fused the regulatory portion of Akt2 that contains the PH domain to the catalytic portion of PKCζ (PKMζ, thus lacking the N-terminal regulatory domains of PKCζ), constructing the chimeric kinase Akt2R-PKMζ (**Fig 2.8a)**. Using the plasma membrane translocation assay from **Fig 2.7c**, we monitored translocation of YFP-tagged Akt2R-PKMζ to PM-CFP in live COS-7 cells during treatment with 100 nM insulin compared to YFP-Akt2 and YFP-PKCζ controls. YFP-Akt2R-PKMζ translocated to plasma membrane in response to insulin slightly slower than YFP-Akt2 (half-times of 3.01 ± 0.05 min and 2.7 ± 0.1 min, respectively). Note a greater level of steady-state binding was achieved by the chimera, likely because intramolecular interactions of the PH domain with its native partner Akt kinase domain, but not the foreign aPKC kinase domain, restrain accessibility of the Akt PH domain (**Fig 2.8b**); consistent with this, the isolated PH domain translocated to a similar extent as that of the chimeric kinase (data not shown). We next examined insulin-induced activity of Akt2R-PKMζ on CKAR, using the activity assay from **Fig 2.6c**. mCherry-tagged Akt2R-PKMζ did not exhibit increased activity on cytosolic CKAR following insulin treatment but was basally active on CKAR as shown by the decrease in FRET ratio following inhibition

with the aPKC active site inhibitor PZ09, previously characterized to selectively inhibit aPKC over other PKCs *in vitro* (119) (**Fig 2.8c**). The control of mCherry-Akt2 showed insulin-induced activity on BKAR while the control for background CKAR activity (mCherry-Vec) was minimally responsive to treatment with 5 μM PZ09. Finally, given that the translocation of Akt2R-PKMζ to plasma membrane in response to PIP_3 production could potentially localize the kinase domain of PKCζ to be more opportunistically phosphorylated at its activation loop by PDK1, we examined T410 phosphorylation on Akt2R-PKMζ following insulin treatment. The data in **Fig 2.8d** show no change in p410 levels of transfected YFP-Akt2R-PKMζ in response to insulin (within a detection limit of ± 20% S.E. for immunoblotting quantified after 4 independent experiments) yet dramatic increases in p308 levels of transfected YFP-Akt2. These results reveal that the catalytic domain of PKCζ does not exhibit agonist-induced activity nor agonist-induced phosphorylation at the activation loop even if dragged to a location that causes Akt to be activated and phosphorylated at its activation loop.

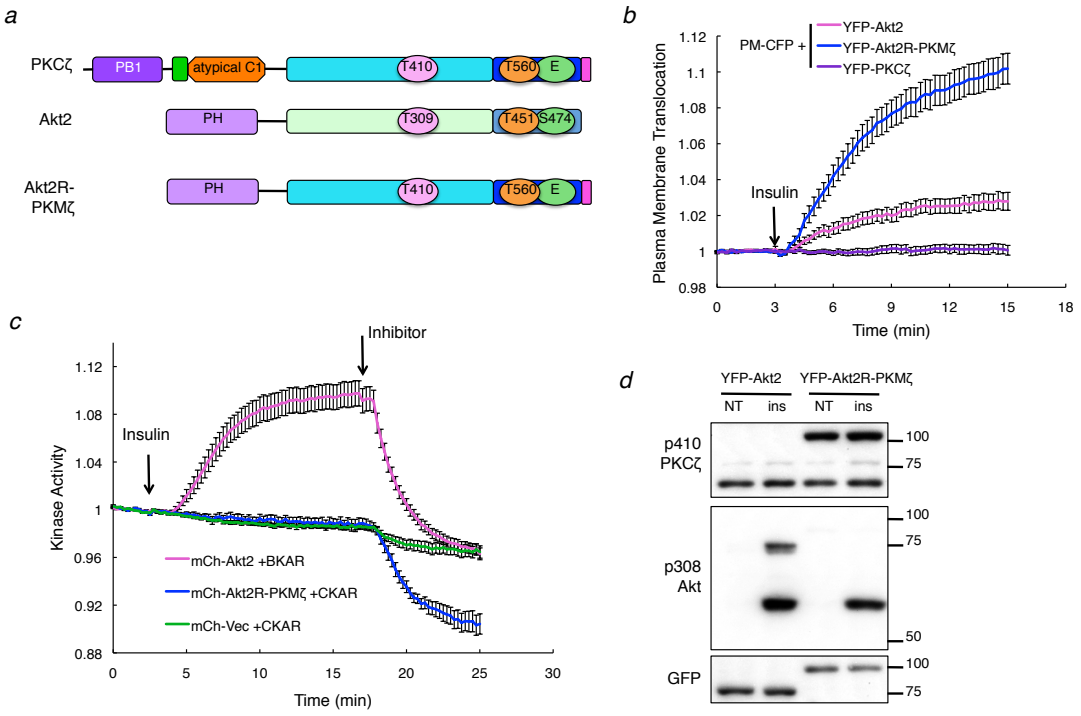

Figure 2.8: A fusion construct of the Akt2 PH domain with PKMζ translocates to the plasma membrane in response to insulin yet does not exhibit agonist-evoked activity or phosphorylation at the activation loop. (a) Schematic of the domains and phosphorylation sites present in PKCζ, Akt2, and the chimeric kinase Akt2R-PKMζ, consisting of the PH domain of Akt2 with the catalytic moiety of PKCζ (PKMζ). **(b)** Translocation assay of YFP-tagged Akt2, Akt2R-PKMζ or PKCζ to plasma membrane (PM-CFP) in live COS-7 cells serum starved prior to imaging, measured as change in FRET over CFP ratio in response to 100 nM insulin. The trace for each cell imaged was normalized to its t=0 min base-line value, and normalized FRET ratios were combined from three independent experiments and plotted as mean ± S.E. **(c)** Global cytosolic kinase activity measured via changes in CFP over FRET ratio using Akt-specific reporter BKAR and mCherry-tagged Akt2 or PKC-specific reporter CKAR and mCherry-tagged Akt2R-PKMζ or vector in live COS-7 cells serum starved prior to imaging and treatment with 100 nM insulin then inhibitors (20 μM GDC-0068 for BKAR assays or 5 μM PZ09 for CKAR assays). The trace for each cell imaged was normalized to its t=0 min base-line value, and normalized FRET ratios were combined from three independent experiments and plotted as mean ± S.E. **(d)** CHO-IR cells were transfected with either YFP-Akt2 or YFP-Akt2R-PKMζ, serum starved overnight then treated with or without 100 nM insulin for 10 min. Immunoblots showing phosphorylation status of Akt2R-PKMζ and Akt2 at their respective activation loops (p410 and p308). Upper bands on p410 and p308 blots indicate overexpressed YFP-tagged constructs while lower bands are indicative of endogenous PKCζ or Akt.

2.4 Discussion

On the kinome tree, atypical PKCs occupy a position on the AGC branch that lies between Akt and conventional PKCs (11). Here we show that the atypical PKCζ

maintains some properties unique to Akt and other properties unique to conventional PKCs, placing aPKCs at the cross-roads of regulatory mechanisms for these two different families of lipid second messenger-regulated kinases. Notably, regulation of the turn motif follows the same mechanism as that for Akt: co-translational phosphorylation by ribosome-associated mTORC2. In contrast, activation loop phosphorylation at T410 follows the same mechanism as that for conventional PKCs: post-translational, constitutive phosphorylation by PDK1, concurring with previous studies that have shown constitutive phosphorylation at T410 for the short transcript PKMζ (143), and no change in p410 on purified PKCζ when treated *in vitro* with recombinant PDK1 (144). Thus, unlike Akt but like conventional PKC, aPKCs are constitutively phosphorylated, but differ in that the first phosphorylation occurs co-translationally at the ribosome rather than post-translationally on a membrane compartment. Coupled with their lack of regulation by diacylglycerol, these results suggest that aPKCs should be considered as a separate family of kinases from the cPKCs and nPKCs.

Previous reports have suggested that aPKC autophosphorylates at the turn motif (19, 145). More recently, this site has been shown to be phosphorylated by mTORC2 *in vitro* and that phosphorylation of this site in cells depends on the integrity of mTORC2 with dephosphorylation occurring within 24 hours of mTOR inhibition via Torin 1 treatment (21). Here we show that a construct of aPKC (V266F) that maintains a native kinase domain fold but is incapable of binding ATP (129) is phosphorylated to the same level as the wild-type protein. These data reveal that the

turn motif is not regulated by autophosphorylation on aPKCs; rather, the site is modified as newly-synthesized polypeptide emerges from the ribosome by ribosome-associated mTORC2. This co-translational phosphorylation by mTORC2 likely accounts for why acute treatment with Torin 1 does not affect the steady-state phosphorylation at the turn motif (because the bulk PKC was previously co-translationally processed by phosphorylation) and why prolonged treatment does (because loss of p560 immunoreactivity reflects turn-over of the protein). Our data also reveal that phosphorylation of the turn motif precedes that of the activation loop, similar to the order for Akt and contrasting with the order for conventional PKCs. Also contrasting with conventional PKCs, phosphorylation of the turn motif is not required for subsequent phosphorylation of the activation loop as the T560A mutant is fully phosphorylated at the activation loop. Conversely, phosphorylation of the activation loop is not required for phosphorylation of the turn motif.

Several recent studies reveal that aPKCs are regulated by autoinhibition through their pseudosubstrate segment (44, 146) as are cPKCs and nPKCs. For conventional and novel PKCs, binding of diacylglycerol and its analogues to their C1 domains releases the pseudosubstrate from the substrate-binding cavity. Although aPKCs have diacylglycerol-insensitive C1 domains, recent evidence suggests that their C1 domains contribute to autoinhibition (44, 146). In support of this, our data show that PS and PA, lipids that bind the C1 domain (130), increase the catalytic activity of PKCζ, consistent with previous studies showing activation of PKCζ by these anionic membrane lipids (103, 147). Supporting conformational changes upon anionic lipid

binding, *in vitro* assays reveal that the rate of dephosphorylation of PKCζ by PP1 is increased in the presence of PS, a result observed for conventional PKCs (15). Thus, the enhanced activity and phosphatase sensitivity of aPKC by anionic lipids likely reflects engagement of the C1 domain on membranes promoting the open conformation of aPKCs, as it does for other PKCs. Because there is no high affinity ligand of the aPKC C1 domain, this interaction with anionic lipids is unlikely to provide any regulation beyond possibly stabilizing the open conformation of any aPKC scaffolded near membranes.

Akt and aPKC both exhibit overlapping functions in insulin signaling, most prominently being their requirement for insulin-stimulated glucose transport as shown through knockout models (123, 148). As for Akt, the catalytic activity of aPKC is required for its effect on insulin-regulated biological functions as determined using either kinase-dead aPKC acting as a dominant negative (80, 81, 83-85, 88-90) or aPKC inhibitors (80, 84, 85, 90, 91), both of which impair insulin-stimulated glucose transport. However, the pathophysiological modulation of Akt vs aPKC displays tissue-dependent differences, suggesting that the regulation of these enzymes is divergent even if they exhibit similar functions. Akt is defective in the livers of diabetic mice and humans yet aPKC is hyperactive in these hepatic tissues (102, 125) while remaining dysfunctional in diabetic skeletal muscle (99, 100). Our data show that the canonical mechanism of activation for Akt involving agonist-evoked phosphorylation facilitated by PIP_3 production by PI3-K in response to growth factors is not the mechanism of activation for aPKC. In all of the cell types studied, no

significant increase in activation loop phosphorylation at T410 on PKCζ was ever observed following insulin treatment as assessed using a phospho-specific antibody that does not detect a T410A mutant. Yet under the same conditions and in the same cells, dramatic increases in activation loop phosphorylation at T308 on Akt were observed. Most strikingly, forced insulin-dependent recruitment of PKCζ by replacement of its regulatory moiety with the PH domain of Akt did not cause any change in the T410 phosphorylation or catalytic activity. Concurrently, addition of the phosphatase inhibitor calyculin did not result in increased phosphorylation at either of the two priming sites, but did cause an increase in the activation loop phosphorylation of S6K. Although it is possible the T410 site is dephosphorylated by calyculin-insensitive phosphatases, 2D gel analysis reveals that a substantial amount of PKCζ is modified by phosphorylation at two sites. Additionally, treatment of cells with the PI3-K inhibitor LY294002 (LY) had no effect on the phosphorylation of T410 when treated within a time frame (20 min) that effectively blocked the insulin-induced phosphorylation of Akt at T308. A recent study reported a moderate reduction in basal phosphorylation of T410 with no change in phosphorylation of T560 following 60 min treatment with an increased dosage of LY (30 μM, (21)). This could reflect off-target effects of more prolonged LY treatment that are potentially affecting T410 phosphorylation through an indirect route not involving the canonical PI3-K/Akt pathway. Thus, insulin acutely regulates the location, phosphorylation, and global activity of Akt but has no detectable effect on any of these parameters for aPKC.

Live cell imaging studies also revealed no insulin-stimulated activity of aPKC. In contrast, insulin stimulated robust activation of Akt as assessed using the Akt activity reporter, BKAR. Correspondingly, we did not observe insulin-dependent translocation of PKCζ to the plasma membrane under conditions that caused readily detectable plasma membrane translocation of Akt and the chimeric kinase Akt2R-PKMζ that contains the PIP_3-binding PH domain. These data indicate that the production of PIP_3 by agonist-evoked PI3-K activity does not affect PKCζ to change its proximity relative to membrane-bound PIP_3. By not reaching PIP_3 or the plasma membrane where other growth factor-stimulated lipids may be present, PKCζ cannot undergo the conformational change to relieve autoinhibition that occurs for Akt to yield activity as suggested recently (145). We also show that no increase in the specific activity measured *in vitro* occurs for PKCζ immunoprecipitated from cells treated with insulin compared to no insulin. This observation contrasts with early studies reporting insulin-dependent increases in PKCζ activity (19, 34) and supports other studies showing no increases in activity of PKCζ immunoprecipitated from insulin-treated cells (21, 149) along with no increases in the phosphorylation of T410 for either tagged or endogenous PKCζ (21-23).

The lack of insulin-induced changes in aPKC location, phosphorylation, or activity begs the question of how aPKCs transduce the insulin signal. We have recently shown that an acidic surface on the PB1 domain of the scaffold p62 tethers the basic pseudosubstrate of bound aPKCs to maintain the enzyme in an open and active conformation (43). Similarly, another scaffold, PAR6 has been shown to lock

aPKC in an open and active conformation (44) and to facilitate its phosphorylation of localized substrates such as PAR3 and Lgl1 (36, 48, 50, 52, 150). Given the exceptionally low catalytic rate of PKCζ (5 mol phosphate per min per mol PKC), in our study and 42 mol phosphate per min per mol PKC with MBP substrate reported previously (103), compared with cPKCs (200 mol phosphate per min per mol PKC) (128), it is likely that coordination of the enzyme next to substrates on protein scaffolds drives its signaling. By this mechanism, the constitutive presence of aPKC on scaffolds allows it to phosphorylate substrates that may be recruited to these scaffolds in an insulin-dependent manner, thus mediating the biological functions of insulin signaling such as induced glucose transport. Thus, the aPKC-regulating mechanism may derive from the insulin dependence of substrate recruitment or substrate conformation. This model is analogous to the regulation of PDK1 signaling: the enzyme is constitutively active but substrate phosphorylation is dictated by substrate conformation or accessibility (151).

The foregoing data reveal that PKCζ is primed by phosphorylation to yield a constitutively-phosphorylated, catalytically-active enzyme. First, the enzyme is co-translationally phosphorylated at the ribosome by mTORC2, followed by phosphorylation at the activation loop by PDK1. Phosphorylation at both sites is required for catalytic activity. Phosphorylations are relatively stable and insensitive to agonists such as insulin or levels of PIP_3. Although the activity of kinase moiety PKMζ is readily detectable using the genetically-encoded activity reporter CKAR, insulin-stimulated global PKCζ activity on this cytosolic substrate reporter cannot be

detected. Our data support a model in which the coordination of aPKCs next to substrates on protein scaffolds drives the biological function for this class of PKC enzymes.

Chapter 2 in its entirety is published as "Protein kinase Cζ exhibits constitutive phosphorylation and phosphatidylinositol-3,4,5-triphosphate-independent regulation." Tobias IS, Kaulich M, Kim PK, Simon N, Jacinto E, Dowdy SF, King CC, Newton AC in *Biochem J*, 2016; 473: pg. 509-23. The dissertation author was the primary investigator and author of this work.

Chapter 3:

Protein Scaffolds Control Localized Protein Kinase Cζ Activity

3.1 Introduction

The coordination of signal transduction by protein scaffolds controls downstream signaling for a multitude of protein kinases (115). Protein scaffolds locally enrich the kinase, positioning it near, or sequestering it away, from substrates to allow specificity and fidelity in cell signaling. In addition, binding to scaffold proteins can impact the conformation of kinases, tuning their signaling output. The atypical PKC isozymes (aPKC) are an example of a kinase whose interaction with a scaffold tethers them in a signaling-competent conformation.

aPKCs comprise one of three classes of the PKC family of enzymes. These classes are the canonical diacylglycerol-regulated conventional (Ca^{2+}-dependent; α, β, γ) and novel (Ca^{2+}-independent but also diacylglycerol-regulated; δ, ε, η, θ) PKCs, and the aPKCs (ζ, ι/λ), which are regulated by neither diacylglycerol nor Ca^{2+} (1, 2, 116). aPKCs share the same general architecture of other family members, with a C-terminal kinase domain whose function is controlled by determinants in the N-terminal regulatory moiety. Specifically, all PKCs have an autoinhibitory pseudosubstrate segment immediately preceding a C1 domain that masks the kinase domain to maintain the enzyme in an autoinhibited conformation. In addition, all PKCs are constitutively phosphorylated following their biosynthesis (2, 106). aPKCs differ from the diacylglycerol-regulated PKCs in that 1] they are not regulated by second messengers, 2] their catalytic activity is an order of magnitude lower than the diacylglycerol PKCs (106), and 3] they have a protein:protein interacting Phox and Bem1 (PB1) domain at their N-terminus. Additionally, they have a Type III PDZ ligand at the end of their C-terminus (2). For the diacylglycerol-regulated PKCs,

binding of second messengers results in release of the pseudosubstrate. In the case of aPKCs, binding to protein scaffolds promotes the release of the atypical pseudosubstrate.

Two scaffolds that regulate the activity of aPKCs are p62 (also known as sequestosome 1, SQSTM1) (43) and partitioning-defective protein 6 (Par6), a cell polarity regulator (44). Binding to these scaffolds promotes the open and active conformation of the aPKCs. In the case of p62, an acidic surface unique to its PB1 domain binds the basic pseudosubstrate of aPKCs, tethering it away from the substrate binding cavity to engage aPKC in an active conformation (43). Binding of aPKC to Par6 also displaces the pseudosubstrate to tether aPKC in an open and signaling-competent conformation (44). Par6 is well characterized as a signaling platform to localize aPKC near substrates such as the cell polarity regulators Par3 and Lgl (47, 86, 95, 97, 148, 152). As a signaling hub with multiple interacting domains and partners (57, 98), p62 may also function to localize aPKC near its targets, though specific substrates on this platform remain to be identified.

A key function of aPKC is the regulation of insulin-stimulated glucose transport (80-83, 85, 87), yet the mechanism for how it transduces this signal is poorly understood. We have recently shown that PKCζ is not regulated by the insulin-induced PI3-kinase pathway that activates Akt (106), a mechanism previously proposed to regulate aPKC activity (18-20). Rather, scaffold interactions may be the critical regulator of aPKC function in insulin signaling. In this regard, insulin promotes a multitude of phosphorylation-dependent protein interactions, many

centralized around the insulin receptor substrate (IRS-1/2) (153). The p62 scaffold has recently been shown to interact with IRS-1 in an insulin-dependent manner (60, 61) and is also known to have functions in metabolism as p62-deficient mice exhibit an insulin-resistant, obese and diabetic phenotype (58, 101). A metabolic phenotype is also observed in mice lacking microtubule affinity regulating kinase 2 (MARK2), an aPKC substrate (66, 67). These animals are insulin-hypersensitive and resistant to weight gain when placed on a high fat diet (74, 75). MARK2 has a well-characterized role in mediating cell polarity, but the mechanism by which it regulates insulin signaling is less understood. How aPKCs control substrate phosphorylation and downstream signaling in response to insulin remains to be elucidated.

Here we address the role of protein scaffolds in controlling the activity of aPKCs. Specifically, we examine the scaffold-associated activity of full-length PKCζ or constructs lacking the pseudosubstrate, PB1, or entire N-terminal regulatory moiety using the C Kinase Activity Reporter (CKAR, (109)) fused to the PB1 domain of p62 or Par6. Basal activity at each scaffold is assessed by monitoring the drop in activity following addition of a validated aPKC active site inhibitor, PZ09. Our data reveal that aPKC is differentially bound and activated on the two PB1 scaffolds: it binds with higher affinity to Par6, which tethers it in a fully active conformation, compared with binding to p62 which is of lower affinity and which tethers a partially active enzyme. Furthermore, we demonstrate the ability of IRS-1 to regulate the phosphorylation and localization of the aPKC substrate MARK2. Lastly, a fluorescent resonance energy transfer (FRET) assay reveals that insulin promotes the association of PKCζ with p62

in addition to p62 and PKCζ with IRS-1. Our data support a model in which scaffolds regulate aPKC signaling by not only providing a signaling platform, but by differentially tuning activity.

3.2 Materials and Methods

Materials

Staurosporine, forskolin and Gö6983 were purchased from Calbiochem. PZ09 was a kind gift from Dr. Christopher Hulme and Dr. Sourav Ghosh. Insulin was purchased from Sigma. The following antibodies were purchased from Santa Cruz Biotechnology: anti-p410 PKCζ (sc-12894-R), anti-total PKCζ (sc-216), and anti-MARK2 (sc-98800). Antibodies for p308 Akt (9275), total Akt (9272), PKC serine substrate (2261 Lot #18), and GAPDH (2118) were purchased from Cell Signaling Technology. The anti-HA (MMS-101P) antibody was from Biolegend. The anti-p595 MARK2 antibody was from AbCam (ab34751). The anti-GFP antibody was from Clontech (#632376). The pSer24 p62 antibody was a kind gift from Dr. George Baillie. HRP-conjugated goat anti-mouse IgG and goat anti-rabbit IgG were from Calbiochem (#401215 and #401315).

Cell Lines and Plasmid Constructs

Human PKCζ and PKCα cDNA were gifts from Dr. Tony Hunter. Human p62 was a gift from Dr. Jorge Moscat. Human MARK2 and human IRS-1 were purchased

from Addgene (plasmid #66706 and plasmid #11025, respectively) while human Par6α was a gift from Dr. Sourav Ghosh, originally from Addgene (plasmid #15474). The C-kinase activity reporter (CKAR) construct was described previously (107, 109). Human PKCζ, PKCα, MARK2, Par6α, IRS-1 and p62 constructs were cloned into the pDONR vector and subsequently recombined with various pDEST vectors constructed in-house to make fusion proteins with HA, mCherry, CKAR, CFP or YFP tags at the N-terminus in pCDNA3 vectors for mammalian cell expression using the Gateway cloning system (Invitrogen). Human PKMζ (residues 183 through 592) of PKCζ was inserted into pDONR for Gateway recombination. The PB1 domains of both human p62 (residues 3 through 102) and human Par6α (residues 1 through 101) were cloned into pDONR and inserted into a Gateway expression vector for expression with CFP and CKAR N-terminal tags. Domain deletion mutations were constructed in PKCζ as follows: ΔPS (deleted pseudosubstrate, residues 113-130) and ΔPB1 (deleted aPKC PB1 domain, residues 25-106). Point and domain mutations were made using Quikchange site-directed mutagenesis (Stratagene). The catalytically-inactive spine mutant (V266F, (106)) was used for the kinase-dead controls of PKCζ and PKMζ.

Cell Culture and Transfection

Mammalian cells were maintained at 37°C in 5% CO_2. CHO-IR cells were grown in DMEM/F-12 50/50, 1X (Cellgro) supplemented with 5% dialyzed fetal bovine serum (FBS, Atlanta Biologics), 1% penicillin/streptomycin (P/S) and 50 μg/ml geneticin (Gibco). COS7 cells were grown in DMEM 1X supplemented with

10% FBS and 1% P/S. Mammalian cells were transiently transfected using jetPrime (Polyplus Transfection).

Immunoprecipitation and Immunoblotting

Cells transfected with HA-tagged kinases were rinsed in PBS and lysed in Buffer A (100 mM KCl, 50 mM Tris, 3 mM NaCl, 3.5 mM $MgCl_2$, pH 7.3) with freshly added 1% protein-grade Triton-X (Calbiochem), 100 μM PMSF, 1 mM DTT, 2 mM benzamidine, 50 μg/ml leupeptin, 1 μM microcystin-LR and 1 mM sodium orthovanadate. Soluble lysates were incubated with anti-HA antibody (Biolegend) for 1-2 hrs followed by incubation with Protein A/G resin beads (Thermo Scientific) for 1-2 hrs at 4°C. Protein-bound beads were washed 3 times with Buffer A prior to adding 25% sample buffer (62.5 mM Tris, 2% SDS, 10% glycerol, 20 μg/ml bromophenol blue, 2.86 M 2-mercaptoethanol), boiling at 100°C and performing SDS-PAGE. For experiments with immunoblotting only, cells were lysed in Buffer B (100 mM NaCl, 50 mM Tris, 10 mM $Na_4P_2O_7$, 50 mM NaF, 1% Triton-X, pH 7.2 plus inhibitors) and whole cell lysates were sonicated prior to adding 25% sample buffer, boiling at 100°C and performing SDS-PAGE. Gels were transferred to PVDF membrane and blocked with 5% BSA before incubating in antibodies.

Live Cell Fluorescence Imaging

COS-7 cells were plated onto sterilized glass coverslips in 35 mm imaging dishes, co-transfected with the indicated constructs, and imaged in Hanks' balanced salt solution supplemented with 1 mM $CaCl_2$ approximately 24 hours post-transfection. For experiments with insulin stimulation, cells were serum-starved overnight prior to imaging via a 40X objective. For experiments with forskolin treatment, cells were treated approximately 24 hrs prior to imaging and transfected the day before. Kinase activity was monitored via intramolecular FRET of the activity reporters (CKAR or CKAR-PB1) while protein translocation was monitored via intermolecular FRET between the YFP-tagged protein and the CFP-tagged target using methods previously described (43, 127).

Statistical Analysis

All statistical analyses were performed using GraphPad Prism software.

3.3 Results

PZ09 inhibits atypical PKCs but not conventional PKCs in cells

The toolbox of inhibitors that selectively inhibit atypical PKCs is scant compared to the collection of compounds that can effectively inhibit conventional and novel PKCs for pharmacological studies (111). Additionally, certain compounds

previously claimed to be inhibitors of aPKC from *in vitro* studies (ZIP and chelerytherine (105, 108)) have been shown to be ineffective at inhibiting aPKC in cells (112). Given the need for an effective aPKC modulator to investigate its biochemical regulation, and the history within the field of *in vitro* efficacy not concurring with efficacy in cells, we set out to validate an active site inhibitor of aPKC, PZ09 (**Fig 3.1a**), previously shown to inhibit aPKC *in vitro* (119) and already used for studies *in vivo* (120) for selective modulation of aPKC substrate readouts in cells. Using a genetically-encoded FRET reporter, C Kinase Activity Reporter (CKAR,(109)) previously validated for measurement of basal aPKC activity in real time in live cells (43, 106, 112), we examined inhibition of mCherry-tagged PKMζ basal activity by increasing PZ09 concentrations (**Fig 3.1b**). PKMζ, an alternate transcript of PKCζ preferentially expressed in brain tissue that contains the kinase domain, was effectively inhibited by PZ09, with an IC50 of approximately 3 μM. The addition of inhibitor caused a small drop in FRET readout in mCherry-Vector (Vec)-transfected control cells, reflecting inhibition of endogenous aPKCs and background activity on CKAR by other kinases sensitive to PZ09. (**Fig 3.1b**). As an additional control, a kinase-dead version of mCherry-PKMζ with a catalytically-inactive spine mutation V266F (106) was tested on CKAR and displayed the same response as the mCherry-Vec control (data not shown). To examine the selectivity of PZ09 in cells for aPKC vs conventional PKCs, cells expressing CKAR and mCherry-PKCα were treated with 200 nM phorbol dibutyrate (PdBu) to stimulate cPKC activity then treated with either 5 μM PZ09 or 250 nM Gö6983, a potent inhibitor of cPKCs and nPKCs (**Fig 3.1c**). Gö6983 reversed stimulated PKCα activity (blue trace); in contrast 5 μM

PZ09 had no effect on PKCα activity in cells (red trace), confirming previous selectivity results performed *in vitro* (119). Thus, monitoring PZ09-sensitive phosphorylation of CKAR is an effective tool to measure aPKC activity in cells.

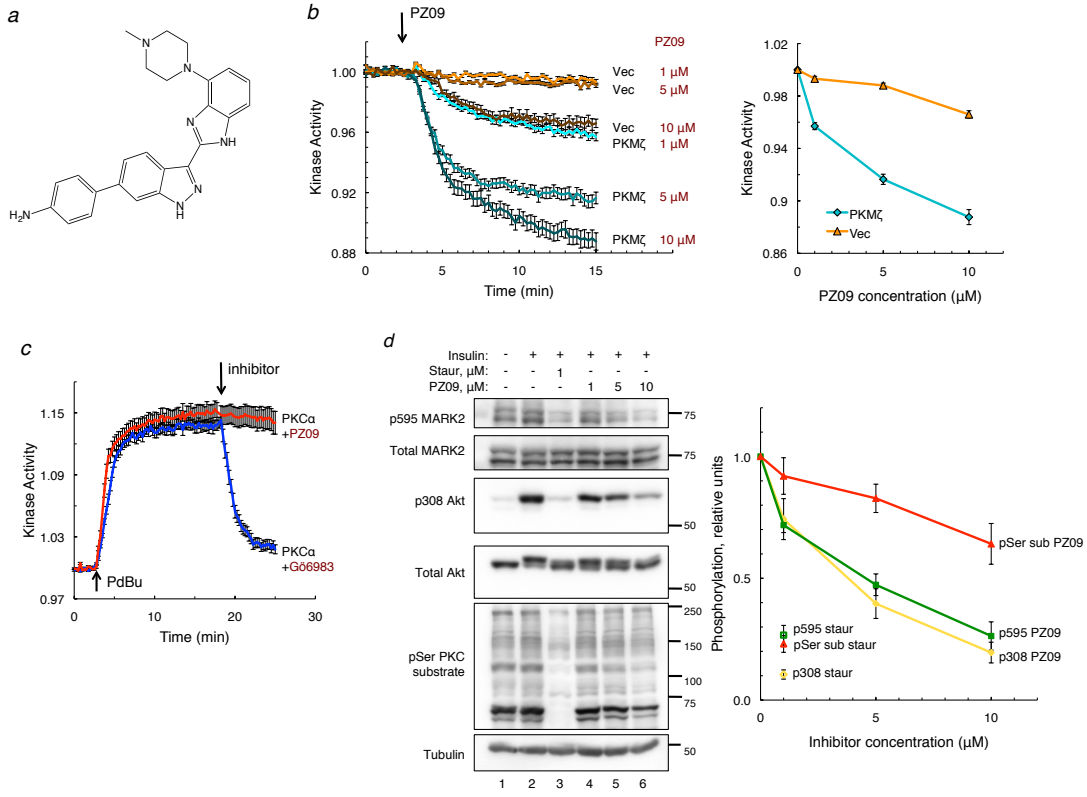

Figure 3.1: PZ09 inhibits atypical PKCs but not conventional PKCs in cells. (a) Chemical structure of PZ09. **(b)** Basal kinase activity measured via changes in CFP over FRET ratio using PKC-specific substrate reporter CKAR and mCherry-tagged PKMζ vs mCherry-Vector (Vec) control in live COS-7 cells treated with increasing concentrations of aPKC inhibitor PZ09. The trace for each cell imaged was normalized to its t=0 min baseline value, and normalized FRET ratios were combined from 3-5 independent experiments and plotted as mean ± S.E. Dose response curve is plotted as amplitude of drop from baseline activity at 15-minute time point vs PZ09 concentration. **(c)** Stimulated kinase activity on CKAR of mCherry-PKCα after treatment with 200 nM PdBu followed by treatment with either cPKC/nPKC specific inhibitor Gö6983 (250 nM) or PZ09 (5 μM). The trace for each cell imaged was normalized to its t=0 min baseline value, and normalized FRET ratios were combined from 3 independent experiments and plotted as mean ± S.E. **(d)** COS-7 cells were serum-starved overnight and treated with either DMSO, staurosporine (1 μM) or increasing concentrations of PZ09 for 30 minutes prior to stimulation with 100 nM insulin for 10 minutes before lysis. Immunoblots show endogenous substrate phosphorylation representing aPKC inhibition (p595 MARK2), PDK1 inhibition (insulin-stimulated p308 Akt) and cPKC inhibition (pSer sub, using an antibody for a PKC-specific serine substrate sequence). Quantification of phosphorylated protein substrate over total protein normalized to DMSO +insulin control using n=5 separate experiments plotted as mean ± S.E. vs inhibitor concentration (PZ09 or staurosporine). Phosphorylated PKC serine substrate was quantified as the intensity of the total band ensemble detected between 50 and 250 kDa divided by tubulin signal and normalized to DMSO +insulin control.

Higher concentrations of PZ09 have off-target effects on endogenous PDK1 in cells

While *in vitro* inhibition studies of PZ09 have demonstrated its selectivity for aPKC over other PKCs (119), PZ09 also inhibited several other non-PKC kinases including PDK1, PKA and p70 S6K when used at 10 μM concentration. To examine the effects of increasing concentrations of PZ09 on endogenous readouts of aPKC, PDK1 and cPKC, we pre-treated cells with PZ09 followed by stimulation with insulin prior to lysis to achieve optimal readout of PDK1 activity on the agonist-induced site p308 Akt (lane 2 vs lane 1, **Fig 3.1d**). We then blotted for p595 MARK2 (aPKC substrate, (66, 67)), p308 Akt (PDK1 substrate, (38)) or phosphorylated PKC serine substrate using an antibody specific for the PKC substrate recognition sequence and quantified each phosphorylation relative to total protein. As a control for general kinase inhibition, we also treated cells with 1 μM staurosporine (lane 3), an inhibitor we have previously used to examine aPKC activity in cells (112). Both aPKC and PDK1 were inhibited to the same extent by increasing concentrations of PZ09 up to 10 μM (lanes 4-6 compared to lane 2 control, p595 and p308 readouts, respectively) while cPKC experienced significantly less inhibition by PZ09 (pSer PKC substrate readout). However, off-target effects of PZ09 on PDK1 and cPKC were considerably less than those of the general kinase inhibitor staurosporine used at 1 μM concentration (quantification, **Fig 3.1d**).

PKCζ is constitutively active on CKAR substrate reporter tethered to interacting PB1 domains of scaffold proteins p62 and Par6

To investigate the role of scaffolds in regulating the localized activity of PKCζ, we fused CKAR to either the PB1 domain of p62 or the PB1 domain of Par6α (**Fig 3.2a**). We have previously used a fusion construct of CKAR tethered to full-length p62 to measure aPKC activity (43). Because this reporter had a tendency to form large clusters of aggregated p62 within the cells, we fused CKAR to just the PB1 domain of p62 or the PB1 of Par6α (which also forms aggregates when expressed in full length form (44)), as the PB1 domain of each scaffold is the principle surface for aPKC binding (35, 36). Untethered CKAR was expressed throughout the cell; the CKAR-PB1^{p62} reporter became excluded from the nucleus, localizing within the cytosol in the same regions as PKCζ, with minimally visible puncta (**Fig 3.2a**). The CKAR-PB1^{Par6} construct was only partially excluded from the nucleus. We next examined the PZ09-sensitive activity globally or on the p62 or Par6 scaffolds (**Fig 3.2b**) in cells expressing either mCherry-Vec (panel i) or full-length mCherry-PKCζ (panel ii). Cells chosen for analysis had the same range of expression for the reporter and mCherry. PZ09 caused a small drop in the activity of endogenous global PKC activity (CKAR, panel i) and activity on the p62 scaffold (CKAR-PB1^{p62}, panel i), and a more significant drop in the activity measured on the Par6 scaffold (CKAR-PB1^{Par6}, panel i). In cells overexpressing PKCζ, the greatest inhibitor-sensitive activity was observed on the Par6 scaffold (CKAR-PB1^{Par6}, panel ii). Curiously, lower basal activity was detected on the CKAR-PB1^{p62} reporter compared to CKAR alone,

although there was a pronounced drop in activity compared to its vector-transfected control (panel ii vs panel i). The pronounced difference in basal activity readout by the two PB1 domain-tagged reporters prompted us to investigate whether the PB1 domain of Par6 was binding more tightly to PKCζ, thus recruiting more of the overexpressed enzyme to phosphorylate CKAR. Co-immunoprecipitation (co-IP) experiments shown in **Fig 3.2c** revealed that PKCζ pulled down significantly more CKAR-PB1^{Par6} (lane 3) than CKAR-PB1^{p62} (lane 2) (2.5 ± 0.5 fold, p=0.0187) as determined through quantification of anti-GFP signal (detecting CKAR) over anti-PKCζ signal from four independent experiments. PKCζ did not pull down the CKAR reporter alone (lane 1), confirming its non-interaction with the untethered substrate and reliance on the PB1 domain for scaffolding. These results reveal that aPKC is basally active at both the Par6 and p62 scaffolds, with significantly more effective binding and thus activity at the Par6 scaffold.

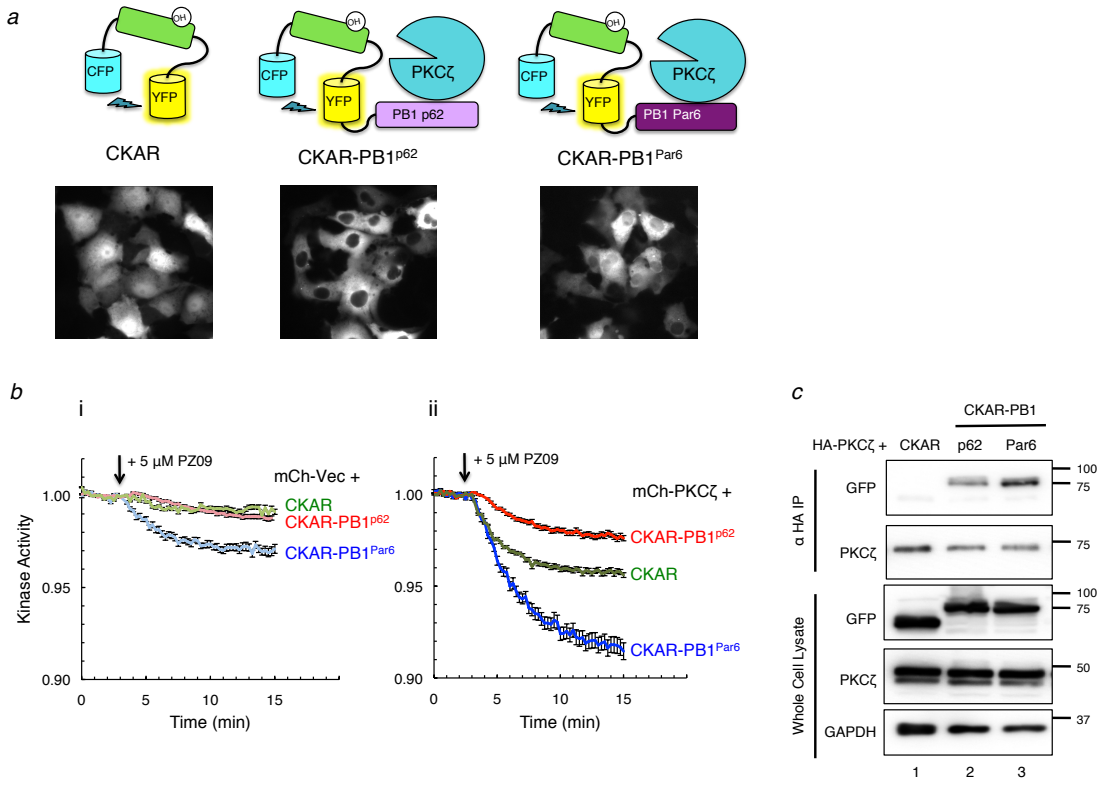

Figure 3.2: PKCζ is constitutively active on CKAR substrate reporter tethered to interacting PB1 domains of scaffold proteins p62 and Par6. (a) Cartoon diagram of reporters constructed to measure aPKC activity: CKAR, CKAR-PB1^{p62} and CKAR-PB1^{Par6}, with corresponding images of COS-7 cells transfected with each reporter showing its localization. **(b)** Basal kinase activity of mCh-Vec (panel i) and mCh-PKCζ (panel ii) on each reporter shown in **(a)** after treatment with 5 μM PZ09 in live COS-7 cells. The trace for each cell imaged was normalized to its t=0 min baseline value, and normalized FRET ratios were combined from 3-5 independent experiments and plotted as mean ± S.E. **(c)** HA-PKCζ was co-expressed with CKAR, CKAR-PB1^{p62} or CKAR-PB1^{Par6} in COS-7 cells, immunoprecipitated (IP) from soluble lysates using anti-HA antibody and blotted for co-IP of CKAR tag using anti-GFP antibody, whole cell lysate loaded at 10% input.

Negative charge at S24/A30 in the PB1 domains of p62 and Par6α impairs binding of PKCζ and activity on CKAR-PB1^{Par6}

A protein kinase A (PKA)-mediated phosphorylation site present in the PB1 domain of p62, residue S24, has recently been identified (154). Phosphorylation at this site is proposed to regulate aPKC binding to the PB1 domain of p62: co-IP studies comparing S24A and S24D mutants showed that negative charge at this site

dismantled the ability of aPKC to bind the p62 scaffold (154). Intriguingly, the sequence surrounding the S24 site of p62 is present in the PB1 domain of the Par6 isoforms, except that an Ala occupies the position of the Ser for Par6α (residue A30) but not for Par6β and Par6γ (**Fig 3.3a**). To address whether negative charge at this position in the PB1 domain of Par6α would dismantle capacity to bind PKCζ, we constructed an A30D mutant in our CKAR-PB1^{Par6} reporter. Indeed, co-IP studies revealed that PKCζ binding to the A30D mutant was dramatically reduced compared with binding to wild-type Par6α PB1 (**Fig 3.3b**; 95 ±1 % reduction, $p< 0.0001$ from 3 independent experiments). Subsequently, we compared the activity of full-length mCherry-PKCζ on CKAR-PB1^{Par6} in which the PB1 domain was wild-type or had the A30D mutation (**Fig 3.3c**). In accordance with the co-IP results, the basal activity of PKCζ was significantly reduced on the A30D mutant compared to the wild-type (WT) version of the Par6α PB1 reporter and comparable to its vector-transfected control. We also examined whether mutating the Ser24 site on the PB1 domain of p62 affected PKCζ binding and activity. Activity readout by the S24A CKAR-PB1^{p62} reporter demonstrated no difference in overexpressed or endogenous PKCζ basal activity compared to the wild-type version (**Fig 3.3d**) and did not differ in its ability to bind PKCζ in co-IP (data not shown). The S24D CKAR-PB1^{p62} also did not change the basal activity response of PKCζ though was previously shown to displace binding of aPKC in co-IP (154). To examine the effect of S24 phosphorylation on PKCζ binding to p62, cells were treated with forskolin (24 hrs at 50 μM) prior to lysis, previously shown to induce PKA-mediated phosphorylation of S24 (154). Treatment with forskolin increased pSer24 on CFP- PB1^{p62} and diminished binding to PKCζ (40 ± 8%

reduction, p = 0.005) as demonstrated through co-IP from six independent experiments (**Fig 3.3e**).

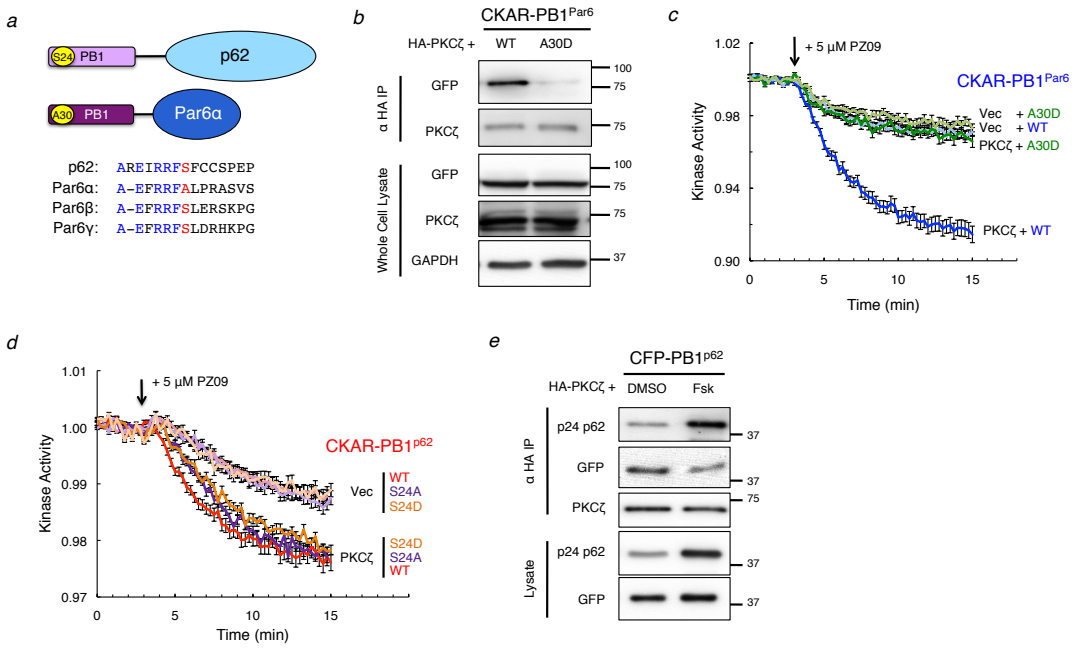

Figure 3.3: Negative charge at S24/A30 in the PB1 domains of p62 and Par6α impairs binding of PKCζ and activity on CKAR-PB1^{Par6}. (a) Cartoon diagram showing consensus within the PB1 domain for the S24 site of p62 vs the A30 site of Par6α and corresponding Ser sites in Par6β and Par6γ. **(b)** HA-PKCζ was co-expressed with either wild-type (WT) or A30D mutation of CKAR-PB1^{Par6} in COS-7, IPd from soluble lysates using anti-HA antibody and blotted for co-IP of CKAR tag using anti-GFP antibody, whole cell lysate loaded at 10% input. **(c,d)** Basal kinase activity of mCherry-PKCζ vs mCherry-Vec on either WT or A30D CKAR-PB1^{Par6} **(c)** or WT, S24A or S24D CKAR-PB1^{p62} **(d)** after treatment with 5 μM PZ09 in live COS-7 cells. The trace for each cell imaged was normalized to its t=0 min baseline value, and normalized FRET ratios were combined from 4-6 independent experiments and plotted as mean ± S.E. **(e)** HA-PKCζ was co-expressed with WT CFP-PB1^{p62}, treated for 24 hours prior to lysis with either DMSO or 50 μM forskolin (Fsk) in COS-7, immunopricipitated from soluble lysates using anti-HA antibody and blotted for co-IP of CKAR tag using anti-GFP antibody along with a phosphospecific antibody for pSer24, whole cell lysate loaded at 10% input.

The basal activity of PKCζ is regulated by a combination of autoinhibition and scaffold-regulated localization or sequestration

We next investigated the role of the N-terminal regulatory domains, namely the PB1 domain and the pseudosubstrate (PS), in regulating the scaffolded activity of PKCζ on the various CKAR reporters examined in **Fig 3.2**. The alternate transcript PKMζ lacks the N-terminal regulatory domains (PB1, pseudosubstrate and atypical C1 regions) and consists of the kinase domain, the C-terminal region, and the PDZ ligand (**Fig 3.4a**). In addition to PKMζ, we constructed two deletion mutants, PKCζ ΔPS (deleted pseudosubstrate) and PKCζ ΔPB1 (deleted PB1 domain) to investigate the role of these domains in regulating the activity of PKCζ on scaffolds (**Fig 3.4a**). Co-expressing these constructs first with non-tethered CKAR and measuring basal activity after treatment with PZ09 (**Fig 3.4b**), PKMζ demonstrated the most pronounced basal activity on CKAR. The ΔPS and ΔPB1 constructs displayed equal basal activity to full length PKCζ, which was significantly increased from the vector-transfected control. Next, we examined the basal activity of the PKCζ constructs on the CKAR-PB1^{p62} reporter, this time showing equal activity between PKCζ ΔPS and PKMζ that was more pronounced than full length PKCζ and PKCζ ΔPB1 (**Fig 3.4c**). On CKAR-PB1^{Par6}, PKCζ ΔPS and PKMζ once again displayed equal basal activity but were slightly less active than full length PKCζ and more active than PKCζ ΔPB1 (**Fig 3.4d**). To compare the binding of PKCζ vs PKMζ on the reporters, we immunoprecipitated HA-PKCζ or HA-PKMζ co-expressed with CKAR-PB1 or CKAR and examined co-IP of the reporters using the αGFP antibody for detection

(**Fig 3.4e**). Intriguingly, PKMζ was capable of binding the untethered version of CKAR while PKCζ did not (lane 4 vs lane 3, note identities of bands in αGFP blot of the immunoprecipitate indicated in red arrows as the αGFP antibody also recognized HA-aPKC signal), in addition to binding CKAR-PB1^{Par6} (lane2). This binding interaction was confirmed to be between PKMζ and the CFP/YFP fluorophores present in CKAR, as PKMζ also co-IPd CFP alone but not Myc-PB1^{Par6} (data not shown), thus confirming the expected non-interaction between PKMζ and PB1.

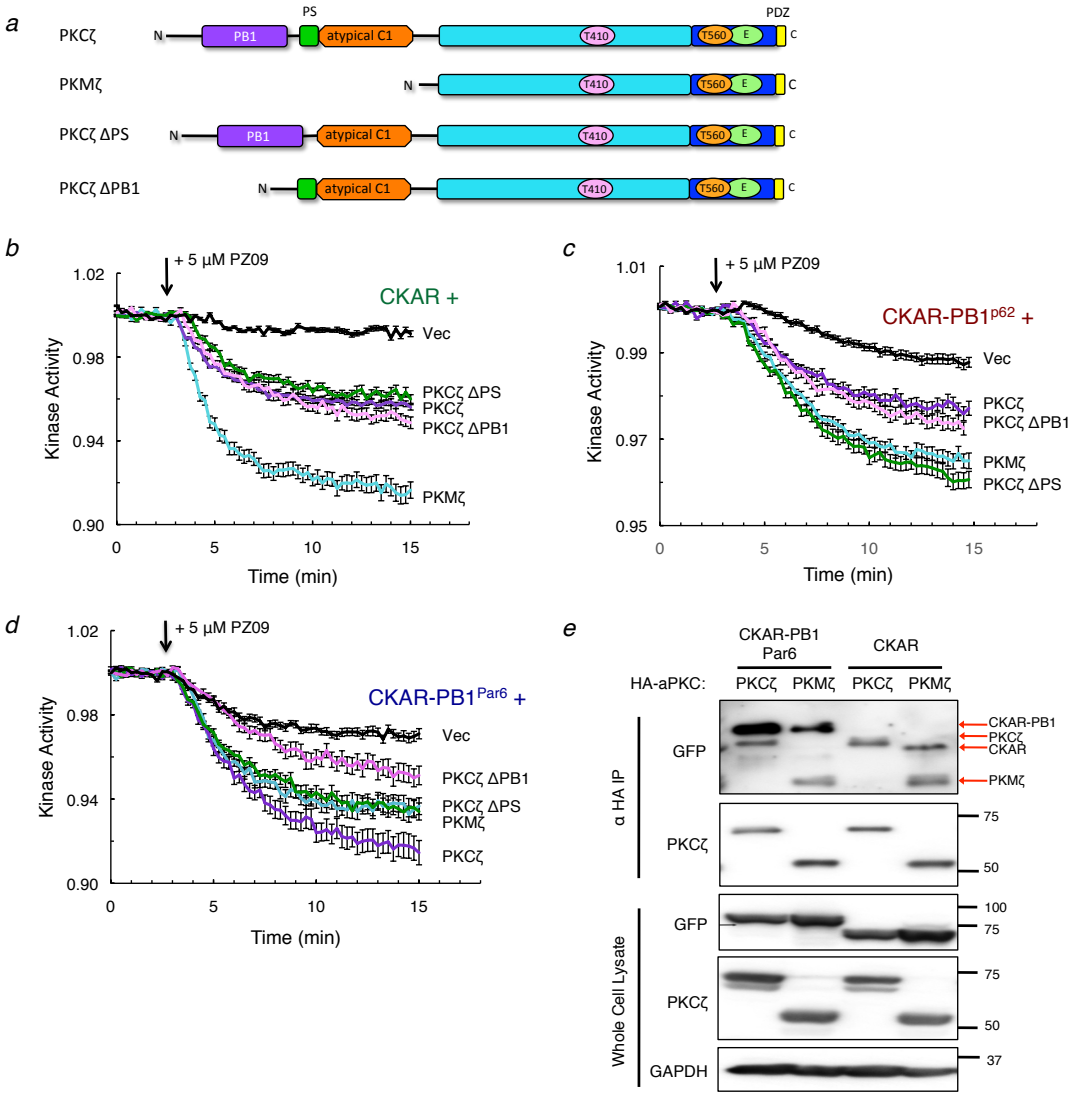

Figure 3.4: The basal activity of PKCζ is regulated by a combination of autoinhibtion and scaffold-regulated localization or sequestration. **(a)** Domain schematic of PKCζ, PKMζ and deletion constructs ΔPS (deleted pseudosubstrate) and ΔPB1 (deleted PB1 domain) used in basal activity assays. **(b,c,d)** Basal kinase activity of mCherry-PKCζ vs mCherry-tagged deletion constructs and mCherry-Vec control on CKAR **(b)**, CKAR-PB1^{p62} **(c)** and CKAR-PB1^{Par6} **(d)** in COS-7 cells treated with 5 μM PZ09. The trace for each cell imaged was normalized to its t=0 min baseline value, and normalized FRET ratios were combined from 3-5 independent experiments and plotted as mean ± S.E. **(e)** HA-PKCζ or HA-PKMζ were co-expressed with CKAR-PB1^{Par6} or CKAR in COS-7. aPKC was immunoprecipitated from soluble lysates using anti-HA antibody and blotted for co-IP of CKAR using anti-GFP antibody, whole cell lysate loaded at 10% input. The band sizes of CKAR-PB1, HA-PKCζ, CKAR and HA-PKMζ detected in the overexposed anti-GFP blot are indicated with red arrows, as the αGFP antibody detected overexpressed aPKC as well as the fluorophores.

PKMζ is more sensitive to dephosphorylation at the activation loop, T410 than PKCζ

We have previously used the general kinase inhibitor staurosporine to inhibit the basal activity of PKMζ on CKAR (112). The inhibitory action of staurosporine on PKMζ is mostly indirect through its potent active site inhibition of PDK1 thus reducing basal phosphorylation on the PDK1 site of PKMζ, the activation loop T410 (112). Inhibition of PDK1 permits conquest of PKMζ by opposing phosphatases acting basally on T410, a phosphorylation site necessary for aPKC catalytic activity (19, 106). To investigate the role of N-terminally-interacting aPKC scaffolds in regulating dephosphorylation of PKCζ at T410, we transfected COS-7 cells with either mCherry-PKMζ or mCherry-PKCζ and treated them with 1 μM staurosporine for 2 hours prior to lysis (**Fig 3.5a**). Phosphorylation of T410 was significantly reduced by 2-fold for PKMζ (lane 2 vs lane 1, p410 PKCζ vs total PKCζ blots) whereas staurosporine treatment of PKCζ had no effect on p410 levels (lane 4 vs lane 3). Thus p410 on full length PKCζ is less sensitive to PDK1 inhibition than PKMζ, indicating a protective mechanism against dephosphorylation provided by the N-terminal regulatory domains of PKCζ.

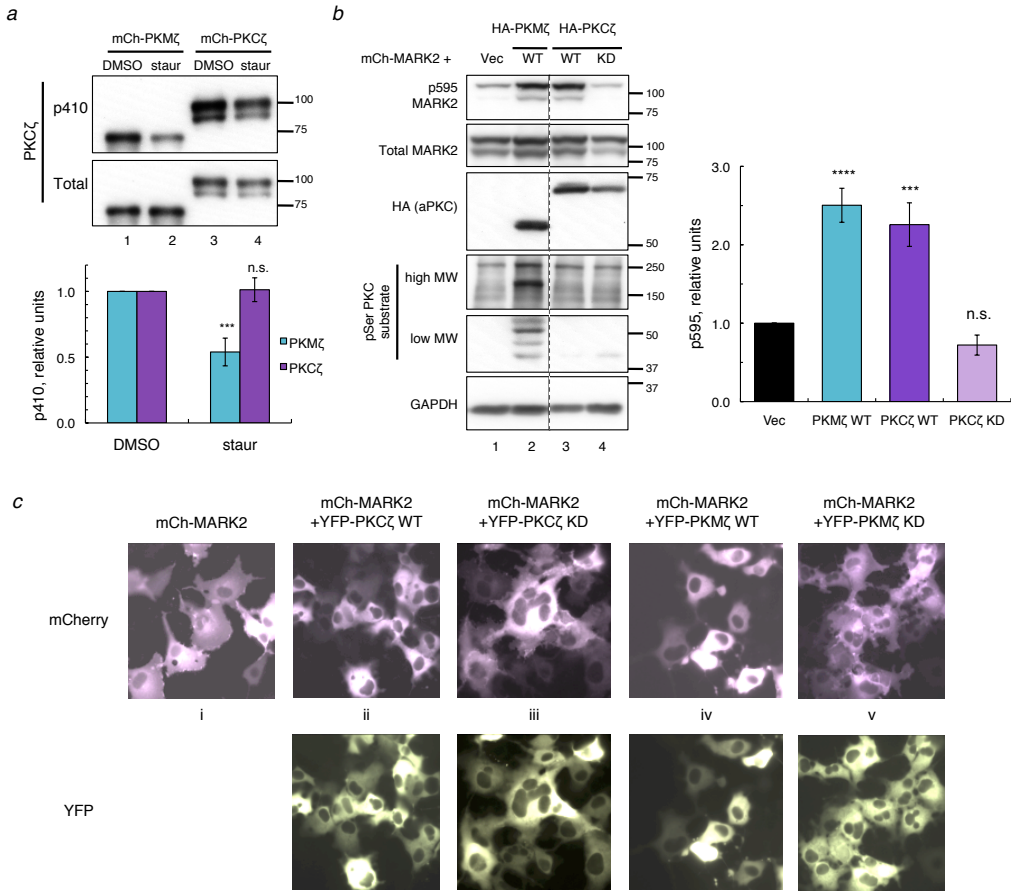

Figure 3.5: PKMζ is more sensitive to dephosphorylation than PKCζ and active on global substrates while both are basally active on MARK2 substrate. (a) Immunoblots showing activation loop phosphorylation (p410 PKCζ) of mCherry-PKMζ vs mCherry-PKCζ expressed in COS-7 cells treated with either DMSO vehicle or 1 μM staurosporine (staur) for 2 hours prior to lysis. The p410/total PKCζ ratios were quantified from 4-5 independent experiments, normalized to DMSO controls and plotted as mean ± S.E. Statistical analysis was performed using 2 separate t-tests comparing staurosporine treatment vs DMSO control for each protein. Significance notated as *** ($p < 0.001$) or n.s. (not significant). **(b)** Immunoblots of COS-7 co-expressing mCherry-MARK2 and either vector, HA-tagged wild-type (WT) PKMζ or PKCζ or kinase-dead (KD) PKCζ. The p595/total MARK2 ratios were quantified from 4-6 independent experiments, normalized to Vec-transfected control and plotted as mean ± S.E. Statistical analysis was performed using ordinary two-way ANOVA followed by Dunnett's multiple comparison test with Vec as control. Significance notated as **** ($p < 0.0001$), *** ($p < 0.001$) or n.s. (not significant). **(c)** Images of live COS-7 expressing mCherry-MARK2 alone or co-expressed with YFP-tagged WT or KD versions of PKMζ or PKCζ.

PKMζ but not PKCζ is active on global substrates while both are basally active on MARK2 substrate

PKCζ is known to phosphorylate and interact with microtubule-affinity regulating kinase 2 (MARK2) (66, 67), a phosphorylation event at the T595 site of MARK2 which results in the translocation of phosphorylated, inactive MARK2 away from the plasma membrane and into the cytosol (66, 67). However, the activity of aPKC on other non-interacting substrates that contain a PKC phosphorylation site is unclear. Using p595 MARK2 as a read-out for aPKC activity in cells, we compared the catalytic activities of over-expressed PKMζ vs full length PKCζ on global PKC substrates, using an antibody for PKC serine substrate (**Fig 3.5b**). Expression of PKMζ (lane 2) revealed an ensemble of induced serine substrate bands (including a higher molecular weight band previously seen with PKMζ, (112)) that were not present in lysates transfected with PKCζ (lane 3), indicating catalytic activity of PKMζ on multiple substrates inaccessible to PKCζ. Both kinase constructs were fully active basally to the same extent on co-expressed mCherry-MARK2 as quantified in **Fig 3.5b**, while the kinase-dead (KD) form of PKCζ showed no effect on p595 MARK2 (lane 4). Additionally, both YFP-tagged aPKC constructs revealed the same ability to induce translocation of MARK2 from the plasma membrane to the cytosol (panels ii and iv, **Fig 3.5c**), a feature that was absent when co-expressed with KD versions of PKCζ and PKMζ (panels iii and v, **Fig 3.5c**).

Scaffold proteins differentially regulate the phosphorylation and localization of the aPKC substrate MARK2

Using the MARK2 co-expression system validated for PKCζ catalytic activity and MARK2 cellular localization from **Fig 3.5**, we set out to examine the effects of PKCζ-regulating scaffolds on MARK2 phosphorylation and localization. In addition to the PB1 domains of p62 and Par6 that directly interact with PKCζ (35, 36), we also examined the effects on MARK2 localization of insulin receptor substrate 1 (IRS-1), a large scaffold protein known to interact with PKCζ through its agonist-induced interaction with p62 (60, 61). Intriguingly, co-expression of IRS-1 with MARK2 resulted in a decrease of p595 MARK2 levels (**Fig 3.6a**, compare lanes 1 and 3), contrasting with the increased p595 levels produced with PKCζ co-expression (**Fig 3.6a**, compare lanes 1 and 2). Additionally, co-expression of the PB1 domain of p62 had no effect on p595 MARK2 (lane 4) while the PB1 domain of Par6 increased p595 levels (lane 5), similar to PKCζ effects (quantification in **Fig 3.6a**). We also examined the concordant effects on MARK2 cellular localization for each of the scaffolds used in **Fig 3.6a**. In agreement with phosphorylation results, co-expression of PKCζ resulted in localization of MARK2 into the cytosol (panel ii). Expression of the PB1 domain of p62 did not change MARK2 localization (panel iv), whereas co-expression of IRS-1 resulted in even more MARK2 at the plasma membrane (as evidenced by the enhanced staining at membrane and absence of visible nuclei for mCherry-MARK2 stained cells when expressed with CFP-IRS-1, **Fig 3.6b** (panel iii) compared with membrane/cytosolic staining for mCherry-MARK2 expressed alone (panel i)).

Curiously, co-expression of the Par6 PB1 domain did not change MARK2 localization relative to the plasma membrane (panel v) even though elevated p595 levels were observed. Similar results were also seen when conducted in polarized epithelial MDCK cells (data not shown).

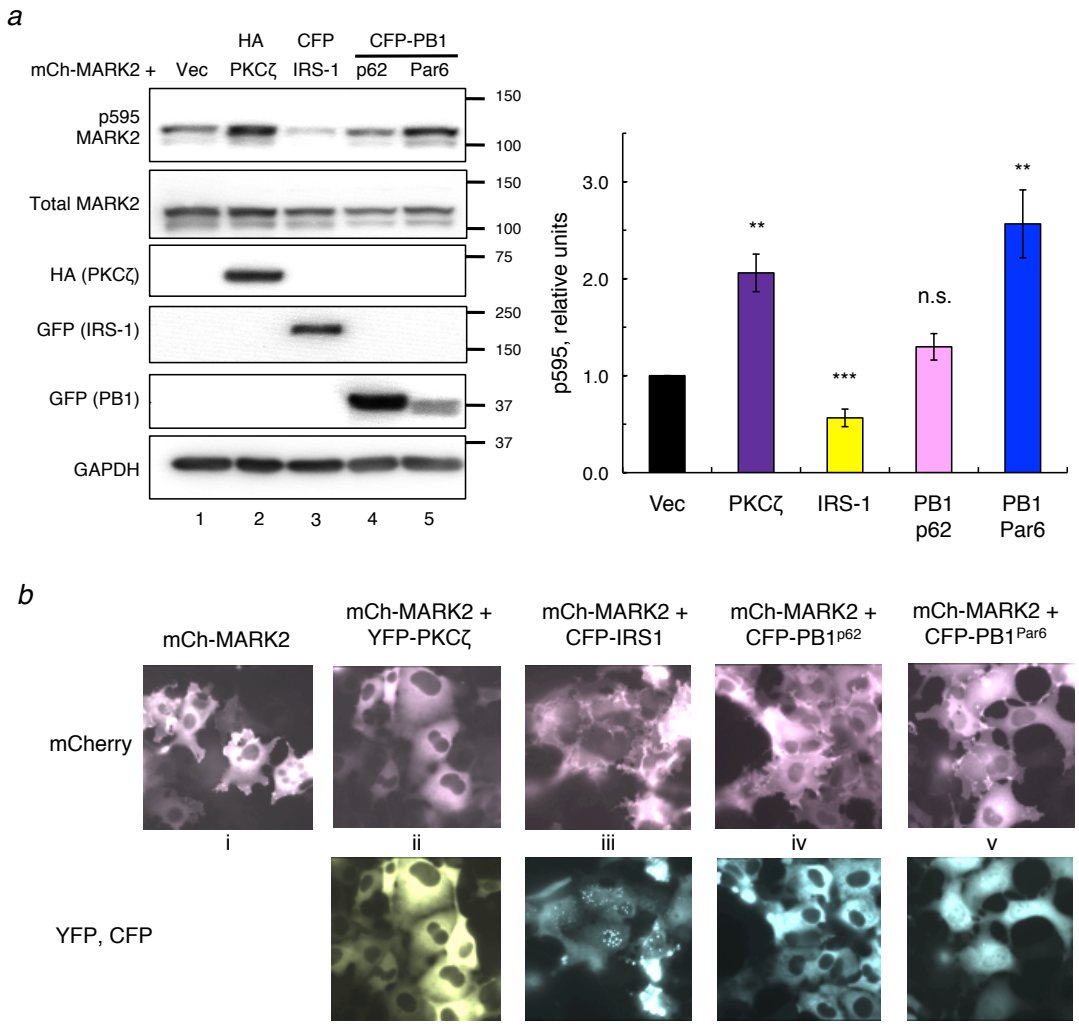

Figure 3.6: Scaffold proteins differentially regulate the phosphorylation and localization of the aPKC substrate MARK2. (a) Immunoblots of COS-7 co-expressing mCherry-MARK2 and either vector, HA-PKCζ, CFP-IRS-1, CFP-PB1^{p62} or CFP-PB1^{Par6}. The p595/total MARK2 ratios were quantified from 4-6 independent experiments, normalized to Vec-transfected control and plotted as mean ± S.E. Statistical analysis was performed using separate t-tests between each co-expression (PKCζ, IRS-1, PB1^{p62}, PB1^{Par6}) and Vec control. Significance notated as *** ($p < 0.001$), ** ($p < 0.01$) or n.s. (not significant). **(b)** Images of live COS-7 expressing mCherry-MARK2 alone or co-expressed with YFP-tagged PKCζ, CFP-IRS-1, CFP-PB1^{p62} or CFP-PB1^{Par6}.

Insulin regulates the localization of scaffolded PKCζ

Recent studies have demonstrated through co-IP experiments that insulin promotes the binding of p62 to IRS-1 via an interaction between the PB1 domain of

p62 and an insulin-induced YXXM phosphorylation motif on IRS-1 (60). Additionally, insulin stimulates increased binding of PKCζ to p62 (61) and subsequent PKCζ engagement to IRS-1 through p62, also shown through co-IP (155). To investigate these interactions in real-time translocation assays, we examined combinations of various YFP, CFP and mCherry-tagged versions of p62, PKCζ, and IRS-1 in CHO-IR cells serum-starved overnight. The YFP tag was placed on the translocating protein (p62 or PKCζ), the CFP tag was placed on the destination protein (IRS-1 or p62), and the mCherry tag was placed on the third protein to confirm expression (cartoon diagram shown in **Fig 3.7a**). Analysis of FRET as a measure of translocation (described previously (43)) revealed that insulin stimulation caused translocation of both YFP-p62 and YFP-PKCζ to CFP-IRS-1, in addition to translocation of YFP-PKCζ to CFP-p62 (**Fig 3.7b**). We note that the increase in FRET upon insulin stimulation was only observed in a sub-fraction of the CHO-IR cells imaged in each time; an increase was observed for 26% (n=94 cells), 40% (n=50 cells), and 52% (n=31 cells) of cells imaged for the FRET from PKCζ to IRS-1, PKCζ to p62, and p62-IRS-1, respectively.

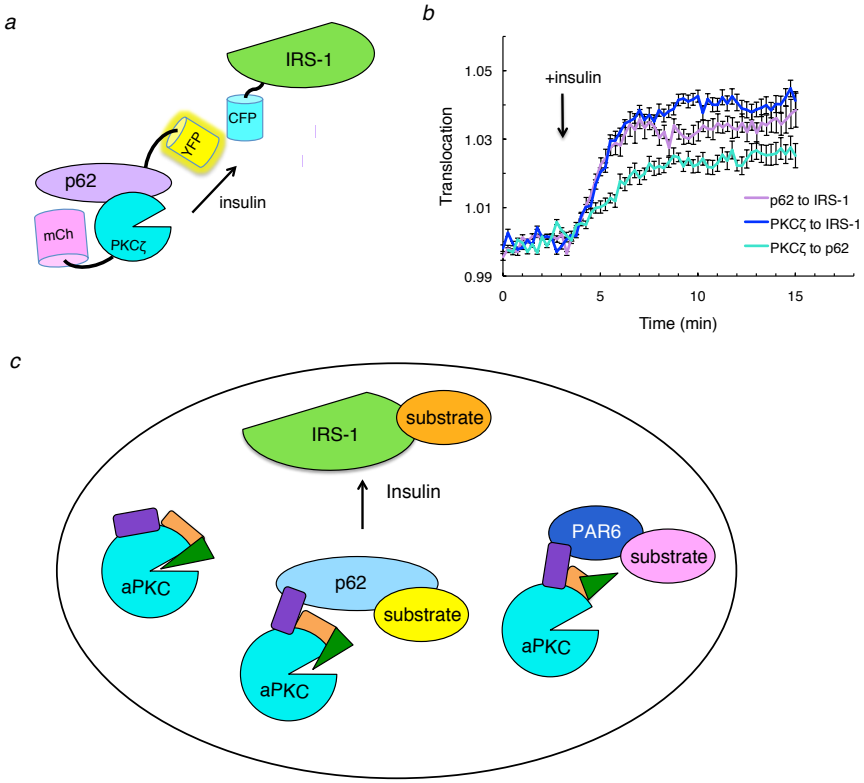

Figure 3.7: Insulin regulates the localization of scaffolded PKCζ. (a) Schematic showing of FRET-based translocation assay. CFP is tagged to the destination protein (IRS-1 or p62), YFP is tagged to the translocating protein (p62 or PKCζ), and mCherry is tagged to the third protein to confirm cellular expression. **(b)** CHO-IR cells expressing the indicated proteins were serum-starved overnight and FRET over CFP was measured before and after treatment with 100 nM insulin: 1) YFP-p62 with CFP-IRS-1 and mCherry- PKCζ (p62 to PKCζ), 2) YFP- PKCζ with CFP-IRS-1 and mCherry-p62 (PKCζ to IRS-1) and 3) YFP- PKCζ with CFP-p62 and mCherry-IRS-1 (PKCζ to p62). The trace for each responding cell imaged was normalized to its t=0 min baseline value, and normalized FRET ratios were combined from 3-4 independent experiments and plotted as mean ± S.E. **(c)** Model showing regulation of the localization and activity of aPKC by protein scaffolds. Non-scaffolded aPKC is effectively autoinhibited by intramolecular interactions that mask the active site of the kinase domain (cyan circle). Binding through the PB1 domain (purple) of scaffolds such as p62 (light blue) or Par6 (dark blue) results in partial or complete removal of the pseudosubstrate (green triangle) from the substrate binding cavity, resulting in low (p62) to maximal (Par6) activity at the scaffold. Agonists such as insulin relocalize these scaffolds, for example recruiting the aPKC:p62 complex to IRS-1 where it can phosphorylate proximal substrates to affect downstream signaling.

3.4 Discussion

The lack of regulation by either phosphorylation or second messengers (2, 93, 156)), including the Akt activator, PIP_3 (38, 106, 157)), has confounded the understanding of how aPKCs signal in cells. Here we show that protein scaffolds relocalize aPKC in response to insulin, and that the binding to specific scaffolds differentially tunes the activity of aPKCs. Using FRET-based technologies to study the real time dynamics of aPKC activity and location in live cells, we show that p62 and Par6 tether PKCζ in a partially active or completely active, respectively, conformation to enhance signaling on these PB1 domain scaffolds. Translocation experiments reveal that insulin enhances the interaction of aPKC to p62, in turn recruiting the complex to IRS-1. Additionally, we show that IRS-1 can sequester aPKC away from phosphorylating the membrane substrate MARK2. As part of this study, we validate the use of a suitable, newly available aPKC-specific active site inhibitor, PZ09, for study of aPKC regulation in live cells with PKC-specific substrates, noting that its inhibition of other non-PKC kinases such as PDK1 may cloud its utility for studying aPKC-specific function *in vivo*. These findings underscore the importance of scaffold interactions in controlling the cellular function of aPKCs and are particularly relevant as the exceptionally low catalytic activity (5 mol phosphate per min per mol PKC, (106) compared to 200 mol phosphate per min per mol PKC for cPKCs (128)), would require localization of substrates in the vicinity of aPKC for effective phosphorylation.

The PB1 domain mediates multiple protein interactions primarily through electrostatic interactions between acidic and basic residues of heterodimerizing PB1 domains (37). p62 and Par6 are the two most characterized PB1 binding partners of aPKC and are thought to regulate separate downstream pathways of aPKC signaling (120). Here we demonstrate that the basal activity of PKCζ is differentially regulated by these two scaffolds, with maximal signaling when scaffolded to Par6α compared to p62, which tethers a conformation that relieves significant autoinhibition. In addition, we show that the PB1 domain of Par6α binds more tightly to PKCζ than the PB1 domain of p62, indicating that the increased population of PKCζ localized to CKAR-$PB1^{Par6}$ contributes to the considerably high basal activity on this scaffold. However, the attenuated activity response of PKCζ on bound CKAR-$PB1^{p62}$ compared to unbound CKAR may also reflect greater PKCζ resistance to active site inhibitors when scaffolded to p62 but not to Par6, a feature known to impede the efficacy of other active site inhibitors on scaffolded PKC (39).

Investigation of the enhanced binding of PKCζ to Par6 compared to p62 led us to identify another key regulatory residue on the PB1 domain: Ser vs Ala at the position corresponding to Ser24 and Ala30 on p62 vs Par6, respectively, tunes the affinity for the aPKC PB1 domain. This residue is within a consensus region present only in the PB1 domains of p62 and the Par6 isoforms and not other human PB1 domain proteins (37). Previous work by Christian et al demonstrated that Ser24 on p62 is phosphorylated by PKA, a modification that disrupts the interaction of p62 with aPKC (154). Consistent with phosphorylation at this site controlling protein

interactions, we show that introduction of a negative charge at the comparable position on Par6α (A30D mutation) disrupts the binding of PKCζ to this PB1 domain and significantly reduces the basal activity of PKCζ on CKAR-PB1^{Par6}. The Ala residue is only present on the Par6α isoform and is Ser at the corresponding site on Par6β and Par6γ. While previous work has shown that aPKC binds to all three Par6 isoforms, yeast two-hybrid screens demonstrated the most significant interaction of aPKC to Par6α (also known as Par6C) (36), in agreement with the Ala favoring aPKC binding. Curiously, mutation of Ser24 to either Asp or Ala on the p62 PB1 domain did not affect PKCζ activity. One possibility is that Asp is a poor phosphomimetic for this site on p62. However, mutation to Asp has been shown to inhibit aPKC binding (154), thus any drop in activity may be below the detection limit of our cellular activity assays. Importantly, extended forskolin stimulation to promote PKA phosphorylation at this site decreased the binding of PKCζ to PB1 p62. Taken together, these data support a model wherein the unique Ser at position 24 on p62 provides a consensus phosphorylation site that regulates the binding and activity of aPKC.

The deletion of the PB1 domain (ΔPB1), the pseudosubstrate (ΔPS) or both (PKMζ) allows dissection of how scaffold interactions relieve the autoinhibition of aPKC to tune its the level of localized basal activity. For the non-scaffolded CKAR, PKMζ demonstrates the highest basal activity of all the constructs as it is neither autoinhibited (no PS) nor sequestered on an endogenous scaffold (no PB1), therefore unrestricted to phosphorylate a globally expressed substrate such as CKAR.

Supporting the model of PKMζ's unrestricted access to CKAR, co-IP results reveal that PKMζ interacts with CKAR whereas PKCζ does not, suggesting sequestration of the full-length kinase on a scaffold thus restricting its interaction with CKAR. Similarly, analysis with an antibody to PKC phosphorylation sites reveals that PKMζ exerts highly enhanced phosphorylation of global endogenous PKC substrates compared with PKCζ. However, PKCζ still has the ability to phosphorylate interactive specific substrates such as MARK2 with equal capacity as PKMζ and to regulate its localization from the plasma membrane into the cytosol. Deletion of either the PS or the PB1 domain did not significantly affect the basal activity of PKCζ on non-scaffolded CKAR. In contrast, activity at the protein scaffolds was sensitive to deletion of the PB1 domain and, depending on the scaffold, the pseudosubstrate. On CKAR-PB1^{p62}, deletion of the pseudosubstrate significantly enhanced basal activity, revealing some autoinhibition by the pseudosubstrate when PKCζ is bound to p62. This is consistent with our previous study showing that full length PKCζ displays ~25% of its maximal, unrestrained activity on p62 as assessed with a p62-scaffolded CKAR (43). Deletion of the pseudosubtrate had no significant effect on the activity on the Par6 scaffold, revealing that the majority of the PKCζ bound to Par6 is in the open conformation, as reported previously (44), with the pseudosubstrate tethered away from the substrate-binding cavity. Activity on both scaffolds was sensitive to deletion of the PB1 domain, consistent with release of the enzymes from the scaffolds. These results reveal that interaction with regulatory determinants autoinhibit PKCζ, and that these inhibitory constraints are differentially relieved by binding to protein scaffolds.

Further supporting autoinhibitory constraints of PKCζ, we show that PKMζ is more sensitive to dephosphorylation at its activation loop phosphorylation site, T410 (19, 106), compared to PKCζ (19, 106). Thus, similar to conventional PKCs (15), intramolecular autoinhibitory interactions with regulatory domains mask this phosphorylation site not only *in vitro* (106), but also in cells. Additionally, binding to scaffolds may sequester aPKCs from phosphatases, although localization of phosphatases to protein scaffolds also serves as mechanism to control signaling output of kinases (41).

Lastly, we show that scaffold interactions can regulate the sequestration or localization of PKCζ to restrict its phosphorylation of physiological substrates. Specifically, overexpression of IRS-1 inhibited the aPKC-dependent phosphorylation of MARK2, thus preventing the release of this substrate from the plasma membrane. In contrast, overexpression of the PB1 domain of Par6 enhanced the phosphorylation on the aPKC-regulated site of MARK2, suggesting that this scaffold may localize aPKC near MARK2. Note that this Par6-induced MARK2 phosphorylation did not displace the substrate from the plasma membrane, likely because shuttling phosphorylated MARK2 away from the apical surface of polarized cells depends on a second step, binding to the polarity regulator Par5 (also known as 14-3-3) (51, 67). Overexpression of Par6 may indeed localize more endogenous aPKC to phosphorylate MARK2 yet interfere with the Par5 ability to bind MARK2.

How insulin controls aPKC function has been difficult to reconcile with the inability of this agonist to alter the phosphorylation state or activity of aPKC (106).

Live cell imaging studies reveal that insulin promotes the association of PKCζ to both p62 and PKCζ, with a half-time on the order of 5 min under the conditions of our assays. This time frame agrees with aPKC-dependent changes in functions such as glucose transport, observed within 5-15 minutes of insulin stimulation (81, 83, 87). The insulin-dependent association of aPKC with these scaffolds supports previous co-IP results (60, 61). IRS-1 is a large docking hub for downstream insulin signaling events to occur (153), and possesses Ser/Thr phosphorylation sites previously shown to be regulated by aPKC (62-65). Taken together, these results suggest that the major effect of insulin on controlling aPKC function is by re-localizing the kinase to cellular signaling hubs such as IRS-1, poising it next to relevant downstream substrates.

In summary, our data support a model in which aPKC is regulated by binding to specific protein scaffolds that differentially control its activity. When unscaffolded, aPKC has low basal activity because of efficient autoinhibition by its regulatory domains, such as the pseudosubstrate (green triangle, **Fig 3.7c**) masking the kinase domain (cyan circle). Binding to Par6 tethers the kinase in an open conformation, with the pseudosubstrate removed from the substrate-binding cavity in the kinase domain to allow maximal activity. Lower affinity binding to p62 results in less effective tethering of the pseudosubstrate, so that the scaffolded enzyme has approximately 25% maximal activity (43). This sequestration on protein scaffolds can either enhance phosphorylation of co-localized substrates or suppress phosphorylation of other substrates (e.g. the inhibition of MARK2 phosphorylation upon sequestration of aPKC by IRS-1 overexpression). The particularly low catalytic activity of aPKCs

ensures that signaling is kept at a minimum in the absence of regulated scaffold interactions, which poise the enzyme for stoichiometric phosphorylation of substrates recruited to the same signaling platform.

Chapter 3 in its entirety is published online as “Protein scaffolds control localized Protein Kinase Cζ activity,” Tobias IS and Newton AC in *J Biol Chem* with expected print publication in July 2016. The dissertation author was the primary investigator and author of this work.

Chapter 4:

Conclusions and Future Work

4.1 Conclusions

In this dissertation work, we show how aPKC relies on scaffolding interactions to regulate its localized activity towards specific substrates rather than the previously thought mechanism of agonist-induced phosphorylation for activation. It shares important mechanisms and functions with related AGC kinases such as constitutive phosphorylation at its activation loop and turn motif exhibited by cPKC and regulation of insulin-induced glucose transport executed by Akt. However, its unique composition of N-terminal domains, particularly its protein-interacting PB1 domain, causes aPKC to be principally regulated by localized interactions with scaffold proteins rather than the lipid second messengers that control cPKC and Akt activity. aPKC can indeed respond to the agonist insulin, but in a mechanism that changes its subcellular localization and scaffold-regulated conformation rather than a change in phosphorylation state to transduce the signal and functional output.

In Chapter 2, we demonstrate how PKCζ is constitutively phosphorylated at both its activation loop and turn motif, sites previously thought to be agonist-induced and autophosphorylated, respectively. Phosphorylation at the turn motif occurs first during the process of translation and is mediated by mTORC2 while secondary post-translational phosphorylation occurs at the activation loop by PDK1 (**Fig 4.1**). Additionally, we show that PKCζ has a relatively low rate of basal activity, nearly 50-fold less than PKCα. Our data also show that PKCζ activity is not insulin-stimulated through the PIP_3-activated pathway that induces plasma membrane translocation and activation loop phosphorylation of Akt, as previously thought in the literature. Our conclusion that the

accepted literature model of aPKC insulin-induced activation was incorrect led us to pursue a more thorough investigation into the molecular mechanisms of aPKC regulation presented in Chapter 3. Our hypothesis was that aPKC is principally regulated by scaffolding interactions that induce conformational changes and promote substrate localization given the composition of its regulatory N-terminal domain structure.

The data presented in Chapter 3 dissect the differences in the molecular regulation of PKCζ by the PB1 domain scaffolds p62 and Par6, both which bind the PB1 domain of aPKCs. The PB1 domain of Par6α is shown to bind PKCζ with higher affinity than the PB1 domain of p62, to induce displacement of the pseudosubstrate more effectively than p62, and to promote phosphorylation of the aPKC substrate MARK2, an effect shown to be lacking by the PB1 domain of p62. The full length PKCζ is also shown to lack activity on global substrates exhibited by its short transcript PKMζ that lacks the N-terminal regulatory domains, indicating its sequestration on scaffolds as a mechanism of regulating its activity towards specific substrates. The ability of the insulin-regulated scaffold IRS-1 to sequester PKCζ away from phosphorylating MARK2 and regulating its subcellular localization is also demonstrated. Finally, we show that insulin stimulates translocation of PKCζ to p62 and IRS-1, indicating a shuttle mechanism for p62 transport of aPKCs to IRS-1 (**Fig 4.1**). This translocation to an alternate signaling platform may allow aPKC to phosphorylate substrates localized to IRS-1 and potentially relieve any remaining autoinhibition. This complex forms in an intracellular location, as PKCζ was not found to translocate to the plasma membrane in response to insulin. Additionally, the insulin receptor is known to be rapidly internalized following insulin stimulation and

binds to IRS-1 in endosomal compartments (158), thus will no longer be present at the plasma membrane at the time which IRS-1 binds to the p62/PKCζ complex (**Fig 4.1**). Our conclusions from Chapter 3 support a model for aPKC regulation by insulin in which scaffolds mediate insulin-induced translocation and localization of aPKC towards specific substrates and sequestration away from other substrates. Thus, downstream signaling of aPKC in response to insulin depends on more subtle effects of substrate localization and kinase conformation rather than the dramatic changes in the catalytic activity of Akt induced by insulin-stimulated phosphorylation.

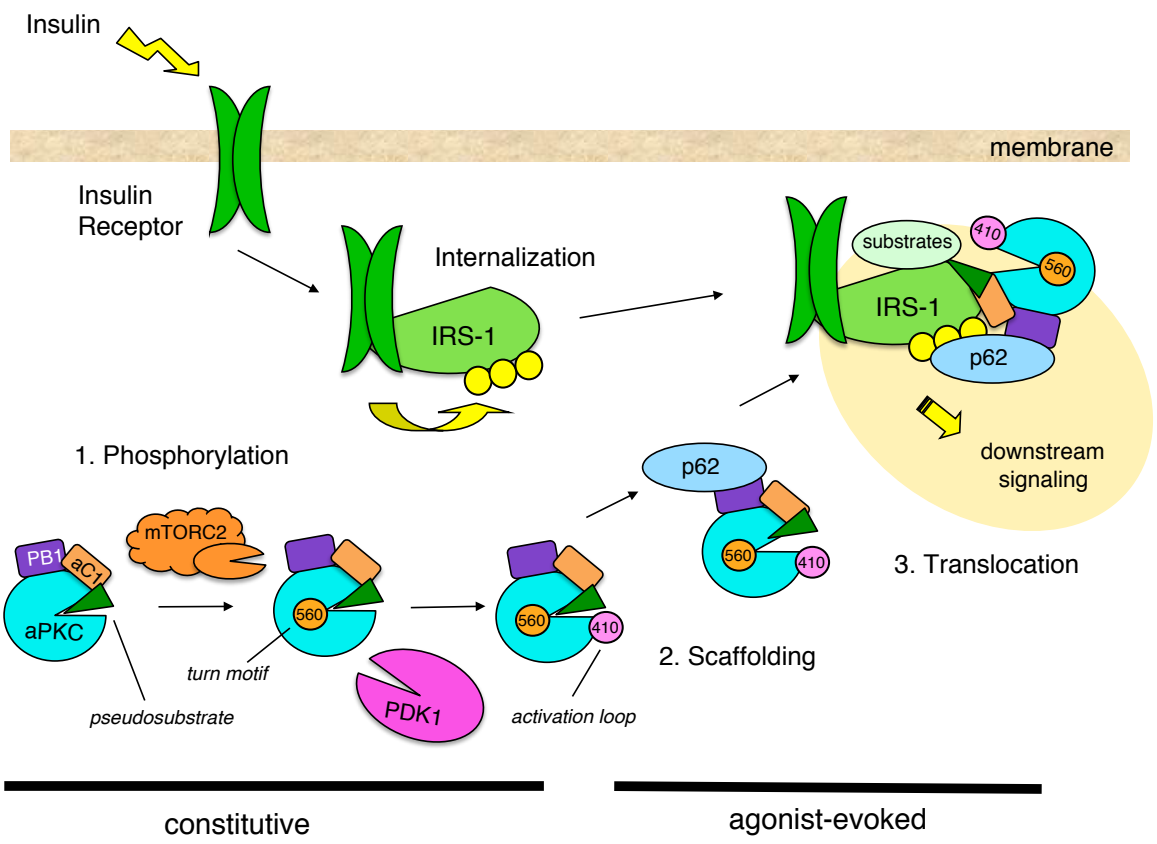

Figure 4.1: Model of Atypical PKC Signaling. Phosphorylation of the aPKC turn motif occurs first, as a constitutive process during translation mediated by mTORC2 with subsequent constitutive phosphorylation at the activation loop by PDK1. Insulin signaling induces internalization of the insulin receptor where it recruits binding of IRS-1 to be phosphorylated at tyrosine residues. Insulin stimulation also induces the binding of aPKC to p62 and partially relieves autoinhibition. p62 then shuttles aPKC to IRS-1 where it binds the phosphorylated tyrosine residues on IRS-1 and provides a potential platform for aPKC to experience further relief from autoinhibition and access to localized substrates.

4.2 Future Work

An important question to direct future work of this project centers on the downstream mechanisms of aPKC-regulated glucose transport, which remain poorly understood. More specifically, which substrates become localized towards aPKC direct phosphorylation when stimulated by insulin, and how do they connect the signal towards translocation of GLUT4 to the plasma membrane for glucose transport? IRS-1 has

several Ser/Thr phosphorylation sites, some which have been identified as substrates of PKCζ (Ser323, Ser503, Ser574 and Ser616 on human IRS-1 (63, 64) and can either have positive or negative feedback towards the insulin signal downstream of IRS-1 (153). Given the identified insulin-induced recruitment of PKCζ to IRS-1, these sites are attractive localized substrate candidates for further investigation. Does aPKC have differential selectivity for one IRS-1 site over another, and does this preference change over the temporal course of insulin stimulation? More specifically, does aPKC phosphorylate the positive feedback site first (Ser323) then later transition towards phosphorylating the negative feedback sites to shut off the signal at the appropriate time? Do scaffolding interactions also regulate the switch of aPKC from one substrate site to another?

Vesicle-associated membrane protein 2 (VAMP2), a component of the vesicle that transports GLUT4 has also been identified as a substrate of PKCζ in one study (89), although follow-up studies for this effect have not been as extensive as those validating MARK2 as an aPKC substrate. VAMP2 interacts with syntaxin-4 to fuse the vesicle with the plasma membrane and deliver GLUT4 to uptake glucose from the bloodstream (159-161). Thus, phosphorylation by aPKC to activate VAMP2 for GLUT4 translocation is a logical proposed mechanism for aPKC regulation of insulin-induced glucose transport. However, studies that further validate this substrate and how it may be regulated by scaffold localization towards aPKC are required.

aPKC may also regulate glucose transport not only through its catalytic activity on substrates but also through protein-binding interactions. An insulin-stimulated

interaction between PKCζ and the 80K-H protein was identified to form a complex with munc18c, a known component of the GLUT4 vesicle trafficking pathway (162). This interaction is thought to regulate GLUT4 vesicle fusion with the plasma membrane by unlocking the clamping interaction of munc18c with syntaxin-4, allowing VAMP2 to bind syntaxin-4 and fuse the vesicle to deliver GLUT4 for glucose uptake. Future investigation as to how insulin-induced scaffolding interactions may regulate the formation of the PKCζ-80K-H-munc18c is proposed, and whether aPKC-mediated phosphorylation of VAMP2 is also regulated by the formation of this complex.

Another attractive mechanism for continued investigation is aPKC's effects on MARK2 and how they may contribute to insulin-stimulated downstream signaling. Knockout of MARK2 has a metabolic phenotype in mice, yielding animals that are hypersensitive to insulin and resistant to weight gain (75). Phosphorylation of MARK2 by aPKC inactivates it and relocalizes it from the plasma membrane into the cytosol (66). One hypothesis for aPKC signaling to MARK2 is that the insulin-induced sequestration of aPKC by IRS-1 away from MARK2 may decrease phosphorylation of MARK2 and allow it to become active, thus transducing the signal. More active MARK2 localized at the plasma membrane may allow the kinase to phosphorylate other target proteins that could signal to induce glucose transport or other insulin-stimulated functional outputs.

As a well-validated substrate of aPKC that can show clear phosphorylation effects even when used in an overexpression system, the substrate recognition sequence of MARK2 might also be useful for constructing a novel reporter specific to aPKC activity. Specifically, the PKC peptide sequence present in the PKC-specific reporter CKAR could

be replaced with a peptide sequence from MARK2 containing the T595 site that is phosphorylated by aPKC. This reporter might be able to show even higher basal activity of aPKC and perhaps agonist-induced activity effects of aPKC when tethered to an appropriate scaffold while reducing background activity effects from the other PKCs.

The atypical C1 domain present on aPKCs is another topic for future investigation, as little is known about its effects on aPKC regulation, other than it binds phosphatidylserine and induces aPKC activity *in vitro* but does not bind to diacyglycerol, a function of the tandem C1 domains present in cPKC and nPKC. One study has shown that the atypical C1 domain has autoinhibitory effects by enhancing the binding of the pseudosubstrate into the active site of the kinase (44). Deletion of the C1 domain moderately enhanced the activity of aPKC *in vitro*, although deletion of only the pseudosubstrate caused aPKC to exhibit the same activity as the kinase domain alone, indicating that the autoinhibitory effects of the C1 domain work in conjunction with the pseudosubstrate and not through an alternate, independent mechanism. However, little is known regarding the regulatory effects of lipids on aPKC through the C1 domain occurring in live cells or whether inducible lipid second messengers can signal through the C1 domain to mediate aPKC signaling.

Further study of insulin-regulated effects on scaffolds other than p62 and IRS-1 should also be performed. Par6 has mainly been defined as a cell polarity regulator but the question of whether or not it functions in insulin signaling requires future examination. For example, the translocation assays performed in **Fig 3.7** could also be performed with replacement of full length p62 for Par6, thus examining whether or not

Par6 translocates to IRS-1 or if PKCζ translocates to Par6 or potentially away from Par6 in response to insulin. Results from such studies could help better define the divergence in aPKC signaling through the p62 vs the Par6 platforms and how they may perpetuate different cell function outputs. Another scaffold to investigate is Grb14, an adaptor protein that has identified scaffolding interactions with p62 (163) and is also known to exhibit binding to the insulin receptor when stimulated by insulin (164). Grb14 may provide an additional platform for localized aPKC substrates to become phosphorylated when stimulated by insulin.

The PKN (Protein Kinase N) family of AGC kinases may be another interesting and relevant group of enzymes to study with regards to their mechanism of activation and how it may relate to that of aPKCs. PKNs (consisting of 3 isozymes, PKN1, PKN2 and PKN3) are next to the aPKCs on the kinome tree and share the same feature of a negatively charged phosphomimetic residue present at the hydrophobic motif (**Fig 1.2**, (11)). This residue is a phosphorylatable Ser or Thr on the surrounding Akt, SGK, S6K, MSK, nPKC and cPKC kinases present on the same branch. PKN1 has also been noted to have functions in insulin-stimulated glucose transport (165, 166) and insulin-stimulated actin cytoskeletal reorganization (167). The kinase domain of PKN shares homology with PKC and Akt and is capable of phosphorylating similar substrate sequences *in vitro* (168). The activation loop of PKN is also phosphorylated by PDK1 and is required for enzyme activity (167, 169). However, like aPKC, the agonist-induced nature of the PDK1 site on PKN remains controversial (166). Regulation of the PKN turn motif remains largely unstudied: investigation into whether this site shares many of

the aPKC regulation traits (such as requirement for catalytic activity and phosphorylation during translation mediated by mTORC2) would be intriguing to investigate.

PKN also has proposed regulation by autoinhibition through the C-terminus of its Ca^{2+}-independent C2-like domain (which shares subtle homology with the novel C2 domain of the nPKCs, (166)) that may function akin to a pseudosubstrate (170). Indeed, conformational changes induced by agonists have also been proposed to be a mechanism of activation for PKN (171-173). The structure of PKN does not contain a PB1 domain, instead harboring the presence of 3 antiparallel coiled-coil fold (ACC) domains that bind the small GTPase RhoA (174-177), an event proposed to trigger the unmasking of the active site (178). Also akin to aPKCs, PKN has a relatively low rate of basal catalytic activity (170, 172, 179) that could indicate a similar reliance on scaffolding interactions to localize the kinase near specific substrates. Therefore, a better understanding of this non-canonically insulin-stimulated family of AGC kinases and how they specifically induce glucose transport would help to complete the understanding of non-Akt-like insulin-activated pathways, their similarities, and their divergences in downstream signaling.

References

1. Newton AC. Protein kinase C: structural and spatial regulation by phosphorylation, cofactors, and macromolecular interactions. Chemical reviews. 2001;101(8):2353-64. Epub 2001/12/26. PubMed PMID: 11749377.

2. Newton AC. Protein kinase C: poised to signal. American journal of physiology Endocrinology and metabolism. 2010;298(3):E395-402. Epub 2009/11/26. doi: 10.1152/ajpendo.00477.2009. PubMed PMID: 19934406; PubMed Central PMCID: PMC2838521.

3. Pu Y, Peach ML, Garfield SH, Wincovitch S, Marquez VE, Blumberg PM. Effects on ligand interaction and membrane translocation of the positively charged arginine residues situated along the C1 domain binding cleft in the atypical protein kinase C isoforms. The Journal of biological chemistry. 2006;281(44):33773-88. doi: 10.1074/jbc.M606560200. PubMed PMID: 16950780.

4. Kazanietz MG, Bustelo XR, Barbacid M, Kolch W, Mischak H, Wong G, et al. Zinc finger domains and phorbol ester pharmacophore. Analysis of binding to mutated form of protein kinase C zeta and the vav and c-raf proto-oncogene products. The Journal of biological chemistry. 1994;269(15):11590-4. PubMed PMID: 8157692.

5. Behn-Krappa A, Newton AC. The hydrophobic phosphorylation motif of conventional protein kinase C is regulated by autophosphorylation. Current biology : CB. 1999;9(14):728-37. PubMed PMID: 10421574.

6. Toker A, Newton AC. Akt/protein kinase B is regulated by autophosphorylation at the hypothetical PDK-2 site. The Journal of biological chemistry. 2000;275(12):8271-4. PubMed PMID: 10722653.

7. Gao T, Furnari F, Newton AC. PHLPP: a phosphatase that directly dephosphorylates Akt, promotes apoptosis, and suppresses tumor growth. Molecular cell. 2005;18(1):13-24. doi: 10.1016/j.molcel.2005.03.008. PubMed PMID: 15808505.

8. Gao T, Brognard J, Newton AC. The phosphatase PHLPP controls the cellular levels of protein kinase C. The Journal of biological chemistry. 2008;283(10):6300-11. doi: 10.1074/jbc.M707319200. PubMed PMID: 18162466.

9. Edwards AS, Newton AC. Phosphorylation at conserved carboxyl-terminal hydrophobic motif regulates the catalytic and regulatory domains of protein kinase C. The Journal of biological chemistry. 1997;272(29):18382-90. Epub 1997/07/18. PubMed PMID: 9218480.

10. Bornancin F, Parker PJ. Phosphorylation of protein kinase C-alpha on serine 657 controls the accumulation of active enzyme and contributes to its phosphatase-resistant state. The Journal of biological chemistry. 1997;272(6):3544-9. Epub 1997/02/07. PubMed PMID: 9013603.

11. Manning G, Whyte DB, Martinez R, Hunter T, Sudarsanam S. The protein kinase complement of the human genome. Science. 2002;298(5600):1912-34. doi: 10.1126/science.1075762. PubMed PMID: 12471243.

12. Dutil EM, Toker A, Newton AC. Regulation of conventional protein kinase C isozymes by phosphoinositide-dependent kinase 1 (PDK-1). Current biology : CB. 1998;8(25):1366-75. Epub 1999/01/16. PubMed PMID: 9889098.

13. Le Good JA, Ziegler WH, Parekh DB, Alessi DR, Cohen P, Parker PJ. Protein kinase C isotypes controlled by phosphoinositide 3-kinase through the protein kinase PDK1. Science. 1998;281(5385):2042-5. Epub 1998/09/25. PubMed PMID: 9748166.

14. Chou MM, Hou W, Johnson J, Graham LK, Lee MH, Chen CS, et al. Regulation of protein kinase C zeta by PI 3-kinase and PDK-1. Current biology : CB. 1998;8(19):1069-77. Epub 1998/10/13. PubMed PMID: 9768361.

15. Dutil EM, Keranen LM, DePaoli-Roach AA, Newton AC. In vivo regulation of protein kinase C by trans-phosphorylation followed by autophosphorylation. The Journal of biological chemistry. 1994;269(47):29359-62. Epub 1994/11/25. PubMed PMID: 7961910.

16. Alessi DR, Andjelkovic M, Caudwell B, Cron P, Morrice N, Cohen P, et al. Mechanism of activation of protein kinase B by insulin and IGF-1. The EMBO journal. 1996;15(23):6541-51. PubMed PMID: 8978681; PubMed Central PMCID: PMC452479.

17. Alessi DR, James SR, Downes CP, Holmes AB, Gaffney PR, Reese CB, et al. Characterization of a 3-phosphoinositide-dependent protein kinase which phosphorylates and activates protein kinase Balpha. Current biology : CB. 1997;7(4):261-9. PubMed PMID: 9094314.

18. Bandyopadhyay G, Standaert ML, Sajan MP, Karnitz LM, Cong L, Quon MJ, et al. Dependence of insulin-stimulated glucose transporter 4 translocation on 3-phosphoinositide-dependent protein kinase-1 and its target threonine-410 in the activation loop of protein kinase C-zeta. Mol Endocrinol. 1999;13(10):1766-72. Epub 1999/10/12. PubMed PMID: 10517677.

19. Standaert ML, Bandyopadhyay G, Kanoh Y, Sajan MP, Farese RV. Insulin and PIP3 activate PKC-zeta by mechanisms that are both dependent and independent of phosphorylation of activation loop (T410) and autophosphorylation (T560) sites. Biochemistry. 2001;40(1):249-55. Epub 2001/01/05. PubMed PMID: 11141077.

20. Hirai T, Chida K. Protein kinase Czeta (PKCzeta): activation mechanisms and cellular functions. Journal of biochemistry. 2003;133(1):1-7. PubMed PMID: 12761192.

21. Li X, Gao T. mTORC2 phosphorylates protein kinase Czeta to regulate its stability and activity. EMBO reports. 2014;15(2):191-8. doi: 10.1002/embr.201338119. PubMed PMID: 24375676; PubMed Central PMCID: PMC3989865.

22. Chen W, Goff MR, Kuang H, Chen G. Higher Protein Kinase C zeta in Fatty Rat Liver and Its Effect on Insulin Actions in Primary Hepatocytes. PloS one. 2015;10(3):e0121890. doi: 10.1371/journal.pone.0121890. PubMed PMID: 25822413; PubMed Central PMCID: PMC4379029.

23. Frosig C, Sajan MP, Maarbjerg SJ, Brandt N, Roepstorff C, Wojtaszewski JF, et al. Exercise improves phosphatidylinositol-3,4,5-trisphosphate responsiveness of atypical protein kinase C and interacts with insulin signalling to peptide elongation in human skeletal muscle. The Journal of physiology. 2007;582(Pt 3):1289-301. Epub 2007/06/02. doi: 10.1113/jphysiol.2007.136614. PubMed PMID: 17540697; PubMed Central PMCID: PMC2075270.

24. Hauge C, Antal TL, Hirschberg D, Doehn U, Thorup K, Idrissova L, et al. Mechanism for activation of the growth factor-activated AGC kinases by turn motif phosphorylation. The EMBO journal. 2007;26(9):2251-61. Epub 2007/04/21. doi: 10.1038/sj.emboj.7601682. PubMed PMID: 17446865; PubMed Central PMCID: PMC1864980.

25. Bornancin F, Parker PJ. Phosphorylation of threonine 638 critically controls the dephosphorylation and inactivation of protein kinase Calpha. Current biology : CB. 1996;6(9):1114-23. Epub 1996/09/01. PubMed PMID: 8805373.

26. Edwards AS, Faux MC, Scott JD, Newton AC. Carboxyl-terminal phosphorylation regulates the function and subcellular localization of protein kinase C betaII. The Journal of biological chemistry. 1999;274(10):6461-8. Epub 1999/02/26. PubMed PMID: 10037738.

27. Facchinetti V, Ouyang W, Wei H, Soto N, Lazorchak A, Gould C, et al. The mammalian target of rapamycin complex 2 controls folding and stability of Akt and protein kinase C. The EMBO journal. 2008;27(14):1932-43. Epub 2008/06/21. doi: 10.1038/emboj.2008.120. PubMed PMID: 18566586; PubMed Central PMCID: PMC2486276.

28. Ikenoue T, Inoki K, Yang Q, Zhou X, Guan KL. Essential function of TORC2 in PKC and Akt turn motif phosphorylation, maturation and signalling. The EMBO journal. 2008;27(14):1919-31. Epub 2008/06/21. doi: 10.1038/emboj.2008.119. PubMed PMID: 18566587; PubMed Central PMCID: PMC2486275.

29. Oh WJ, Wu CC, Kim SJ, Facchinetti V, Julien LA, Finlan M, et al. mTORC2 can associate with ribosomes to promote cotranslational phosphorylation and stability of nascent Akt polypeptide. The EMBO journal. 2010;29(23):3939-51. doi: 10.1038/emboj.2010.271. PubMed PMID: 21045808; PubMed Central PMCID: PMC3020639.

30. Zinzalla V, Stracka D, Oppliger W, Hall MN. Activation of mTORC2 by association with the ribosome. Cell. 2011;144(5):757-68. doi: 10.1016/j.cell.2011.02.014. PubMed PMID: 21376236.

31. Borner C, Filipuzzi I, Wartmann M, Eppenberger U, Fabbro D. Biosynthesis and posttranslational modifications of protein kinase C in human breast cancer cells. The Journal of biological chemistry. 1989;264(23):13902-9. PubMed PMID: 2474538.

32. Dutil EM, Newton AC. Dual role of pseudosubstrate in the coordinated regulation of protein kinase C by phosphorylation and diacylglycerol. The Journal of biological chemistry. 2000;275(14):10697-701. PubMed PMID: 10744767.

33. Guertin DA, Stevens DM, Thoreen CC, Burds AA, Kalaany NY, Moffat J, et al. Ablation in mice of the mTORC components raptor, rictor, or mLST8 reveals that mTORC2 is required for signaling to Akt-FOXO and PKCalpha, but not S6K1. Developmental cell. 2006;11(6):859-71. doi: 10.1016/j.devcel.2006.10.007. PubMed PMID: 17141160.

34. Standaert ML, Bandyopadhyay G, Perez L, Price D, Galloway L, Poklepovic A, et al. Insulin activates protein kinases C-zeta and C-lambda by an autophosphorylation-dependent mechanism and stimulates their translocation to GLUT4 vesicles and other membrane fractions in rat adipocytes. The Journal of biological chemistry. 1999;274(36):25308-16. PubMed PMID: 10464256.

35. Puls A, Schmidt S, Grawe F, Stabel S. Interaction of protein kinase C zeta with ZIP, a novel protein kinase C-binding protein. Proceedings of the National Academy of Sciences of the United States of America. 1997;94(12):6191-6. PubMed PMID: 9177193; PubMed Central PMCID: PMC21025.

36. Joberty G, Petersen C, Gao L, Macara IG. The cell-polarity protein Par6 links Par3 and atypical protein kinase C to Cdc42. Nature cell biology. 2000;2(8):531-9. doi: 10.1038/35019573. PubMed PMID: 10934474.

37. Sumimoto H, Kamakura S, Ito T. Structure and function of the PB1 domain, a protein interaction module conserved in animals, fungi, amoebas, and plants. Science's STKE : signal transduction knowledge environment. 2007;2007(401):re6. doi: 10.1126/stke.4012007re6. PubMed PMID: 17726178.

38. Terasawa H, Noda Y, Ito T, Hatanaka H, Ichikawa S, Ogura K, et al. Structure and ligand recognition of the PB1 domain: a novel protein module binding to the PC motif. The EMBO journal. 2001;20(15):3947-56. doi: 10.1093/emboj/20.15.3947. PubMed PMID: 11483498; PubMed Central PMCID: PMC149143.

39. Noda Y, Kohjima M, Izaki T, Ota K, Yoshinaga S, Inagaki F, et al. Molecular recognition in dimerization between PB1 domains. The Journal of biological chemistry. 2003;278(44):43516-24. doi: 10.1074/jbc.M306330200. PubMed PMID: 12920115.

40. Wilson MI, Gill DJ, Perisic O, Quinn MT, Williams RL. PB1 domain-mediated heterodimerization in NADPH oxidase and signaling complexes of atypical protein kinase C with Par6 and p62. Molecular cell. 2003;12(1):39-50. PubMed PMID: 12887891.

41. Lamark T, Perander M, Outzen H, Kristiansen K, Overvatn A, Michaelsen E, et al. Interaction codes within the family of mammalian Phox and Bem1p domain-containing proteins. The Journal of biological chemistry. 2003;278(36):34568-81. doi: 10.1074/jbc.M303221200. PubMed PMID: 12813044.

42. Yoshinaga S, Kohjima M, Ogura K, Yokochi M, Takeya R, Ito T, et al. The PB1 domain and the PC motif-containing region are structurally similar protein binding modules. The EMBO journal. 2003;22(19):4888-97. doi: 10.1093/emboj/cdg475. PubMed PMID: 14517229; PubMed Central PMCID: PMC204459.

43. Tsai LC, Xie L, Dore K, Xie L, Del Rio JC, King CC, et al. Zeta Inhibitory Peptide Disrupts Electrostatic Interactions That Maintain Atypical Protein Kinase C in Its Active Conformation on the Scaffold p62. The Journal of biological chemistry. 2015. doi: 10.1074/jbc.M115.676221. PubMed PMID: 26187466.

44. Graybill C, Wee B, Atwood SX, Prehoda KE. Partitioning-defective protein 6 (Par-6) activates atypical protein kinase C (aPKC) by pseudosubstrate displacement. The Journal of biological chemistry. 2012;287(25):21003-11. doi: 10.1074/jbc.M112.360495. PubMed PMID: 22544755; PubMed Central PMCID: PMC3375524.

45. Lin D, Edwards AS, Fawcett JP, Mbamalu G, Scott JD, Pawson T. A mammalian PAR-3-PAR-6 complex implicated in Cdc42/Rac1 and aPKC signalling and cell polarity. Nature cell biology. 2000;2(8):540-7. doi: 10.1038/35019582. PubMed PMID: 10934475.

46. Hirose T, Izumi Y, Nagashima Y, Tamai-Nagai Y, Kurihara H, Sakai T, et al. Involvement of ASIP/PAR-3 in the promotion of epithelial tight junction formation. Journal of cell science. 2002;115(Pt 12):2485-95. PubMed PMID: 12045219.

47. Nagai-Tamai Y, Mizuno K, Hirose T, Suzuki A, Ohno S. Regulated protein-protein interaction between aPKC and PAR-3 plays an essential role in the polarization of epithelial cells. Genes to cells : devoted to molecular & cellular mechanisms. 2002;7(11):1161-71. PubMed PMID: 12390250.

48. Yamanaka T, Horikoshi Y, Sugiyama Y, Ishiyama C, Suzuki A, Hirose T, et al. Mammalian Lgl forms a protein complex with PAR-6 and aPKC independently of PAR-3 to regulate epithelial cell polarity. Current biology : CB. 2003;13(9):734-43. PubMed PMID: 12725730.

49. Betschinger J, Mechtler K, Knoblich JA. The Par complex directs asymmetric cell division by phosphorylating the cytoskeletal protein Lgl. Nature. 2003;422(6929):326-30. doi: 10.1038/nature01486. PubMed PMID: 12629552.

50. Plant PJ, Fawcett JP, Lin DC, Holdorf AD, Binns K, Kulkarni S, et al. A polarity complex of mPar-6 and atypical PKC binds, phosphorylates and regulates mammalian Lgl. Nature cell biology. 2003;5(4):301-8. doi: 10.1038/ncb948. PubMed PMID: 12629547.

51. Macara IG. Parsing the polarity code. Nature reviews Molecular cell biology. 2004;5(3):220-31. doi: 10.1038/nrm1332. PubMed PMID: 14991002.

52. Izumi Y, Hirose T, Tamai Y, Hirai S, Nagashima Y, Fujimoto T, et al. An atypical PKC directly associates and colocalizes at the epithelial tight junction with ASIP, a mammalian homologue of Caenorhabditis elegans polarity protein PAR-3. The Journal of cell biology. 1998;143(1):95-106. PubMed PMID: 9763423; PubMed Central PMCID: PMC2132825.

53. Suzuki A, Ishiyama C, Hashiba K, Shimizu M, Ebnet K, Ohno S. aPKC kinase activity is required for the asymmetric differentiation of the premature junctional complex during epithelial cell polarization. Journal of cell science. 2002;115(Pt 18):3565-73. PubMed PMID: 12186943.

54. Yamanaka T, Horikoshi Y, Suzuki A, Sugiyama Y, Kitamura K, Maniwa R, et al. PAR-6 regulates aPKC activity in a novel way and mediates cell-cell contact-induced formation of the epithelial junctional complex. Genes to cells : devoted to molecular & cellular mechanisms. 2001;6(8):721-31. PubMed PMID: 11532031.

55. Gao L, Joberty G, Macara IG. Assembly of epithelial tight junctions is negatively regulated by Par6. Current biology : CB. 2002;12(3):221-5. PubMed PMID: 11839275.

56. Moscat J, Diaz-Meco MT. p62 at the crossroads of autophagy, apoptosis, and cancer. Cell. 2009;137(6):1001-4. doi: 10.1016/j.cell.2009.05.023. PubMed PMID: 19524504; PubMed Central PMCID: PMC3971861.

57. Komatsu M, Kageyama S, Ichimura Y. p62/SQSTM1/A170: physiology and pathology. Pharmacological research : the official journal of the Italian Pharmacological Society. 2012;66(6):457-62. doi: 10.1016/j.phrs.2012.07.004. PubMed PMID: 22841931.

58. Rodriguez A, Duran A, Selloum M, Champy MF, Diez-Guerra FJ, Flores JM, et al. Mature-onset obesity and insulin resistance in mice deficient in the signaling adapter p62. Cell metabolism. 2006;3(3):211-22. Epub 2006/03/07. doi: 10.1016/j.cmet.2006.01.011. PubMed PMID: 16517408.

59. Okada K, Yanagawa T, Warabi E, Yamastu K, Uwayama J, Takeda K, et al. The alpha-glucosidase inhibitor acarbose prevents obesity and simple steatosis in sequestosome 1/A170/p62 deficient mice. Hepatology research : the official journal of the Japan Society of Hepatology. 2009;39(5):490-500. doi: 10.1111/j.1872-034X.2008.00478.x. PubMed PMID: 19207582.

60. Geetha T, Zheng C, Vishwaprakash N, Broderick TL, Babu JR. Sequestosome 1/p62, a scaffolding protein, is a newly identified partner of IRS-1 protein. The Journal of biological chemistry. 2012;287(35):29672-8. doi: 10.1074/jbc.M111.322404. PubMed PMID: 22761437; PubMed Central PMCID: PMC3436154.

61. Xi G, Shen X, Rosen CJ, Clemmons DR. IRS-1 Functions as a Molecular Scaffold to Coordinate IGF-I/IGFBP-2 Signaling During Osteoblast Differentiation. Journal of bone and mineral research : the official journal of the American Society for Bone and Mineral Research. 2016. doi: 10.1002/jbmr.2791. PubMed PMID: 26773517.

62. Ravichandran LV, Esposito DL, Chen J, Quon MJ. Protein kinase C-zeta phosphorylates insulin receptor substrate-1 and impairs its ability to activate phosphatidylinositol 3-kinase in response to insulin. The Journal of biological chemistry. 2001;276(5):3543-9. doi: 10.1074/jbc.M007231200. PubMed PMID: 11063744.

63. Sommerfeld MR, Metzger S, Stosik M, Tennagels N, Eckel J. In vitro phosphorylation of insulin receptor substrate 1 by protein kinase C-zeta: functional analysis and identification of novel phosphorylation sites. Biochemistry. 2004;43(19):5888-901. doi: 10.1021/bi049640v. PubMed PMID: 15134463.

64. Moeschel K, Beck A, Weigert C, Lammers R, Kalbacher H, Voelter W, et al. Protein kinase C-zeta-induced phosphorylation of Ser318 in insulin receptor substrate-1 (IRS-1) attenuates the interaction with the insulin receptor and the tyrosine phosphorylation of IRS-1. The Journal of biological chemistry. 2004;279(24):25157-63. doi: 10.1074/jbc.M402477200. PubMed PMID: 15069075.

65. Lee S, Lynn EG, Kim JA, Quon MJ. Protein kinase C-zeta phosphorylates insulin receptor substrate-1, -3, and -4 but not -2: isoform specific determinants of specificity in insulin signaling. Endocrinology. 2008;149(5):2451-8. doi: 10.1210/en.2007-1595. PubMed PMID: 18202124; PubMed Central PMCID: PMC2329288.

66. Hurov JB, Watkins JL, Piwnica-Worms H. Atypical PKC phosphorylates PAR-1 kinases to regulate localization and activity. Current biology : CB. 2004;14(8):736-41. doi: 10.1016/j.cub.2004.04.007. PubMed PMID: 15084291.

67. Suzuki A, Hirata M, Kamimura K, Maniwa R, Yamanaka T, Mizuno K, et al. aPKC acts upstream of PAR-1b in both the establishment and maintenance of mammalian epithelial polarity. Current biology : CB. 2004;14(16):1425-35. doi: 10.1016/j.cub.2004.08.021. PubMed PMID: 15324659.

68. Moravcevic K, Mendrola JM, Schmitz KR, Wang YH, Slochower D, Janmey PA, et al. Kinase associated-1 domains drive MARK/PAR1 kinases to membrane targets by binding acidic phospholipids. Cell. 2010;143(6):966-77. doi: 10.1016/j.cell.2010.11.028. PubMed PMID: 21145462; PubMed Central PMCID: PMC3031122.

69. Drewes G, Ebneth A, Preuss U, Mandelkow EM, Mandelkow E. MARK, a novel family of protein kinases that phosphorylate microtubule-associated proteins and trigger microtubule disruption. Cell. 1997;89(2):297-308. PubMed PMID: 9108484.

70. Cohen D, Brennwald PJ, Rodriguez-Boulan E, Musch A. Mammalian PAR-1 determines epithelial lumen polarity by organizing the microtubule cytoskeleton. The Journal of cell biology. 2004;164(5):717-27. doi: 10.1083/jcb.200308104. PubMed PMID: 14981097; PubMed Central PMCID: PMC2172160.

71. Guo S, Kemphues KJ. par-1, a gene required for establishing polarity in C. elegans embryos, encodes a putative Ser/Thr kinase that is asymmetrically distributed. Cell. 1995;81(4):611-20. PubMed PMID: 7758115.

72. Bayraktar J, Zygmunt D, Carthew RW. Par-1 kinase establishes cell polarity and functions in Notch signaling in the Drosophila embryo. Journal of cell science. 2006;119(Pt 4):711-21. doi: 10.1242/jcs.02789. PubMed PMID: 16449319.

73. Bohm H, Brinkmann V, Drab M, Henske A, Kurzchalia TV. Mammalian homologues of C. elegans PAR-1 are asymmetrically localized in epithelial cells and may influence their polarity. Current biology : CB. 1997;7(8):603-6. PubMed PMID: 9259552.

74. Hurov J, Piwnica-Worms H. The Par-1/MARK family of protein kinases: from polarity to metabolism. Cell cycle. 2007;6(16):1966-9. PubMed PMID: 17721078.

75. Hurov JB, Huang M, White LS, Lennerz J, Choi CS, Cho YR, et al. Loss of the Par-1b/MARK2 polarity kinase leads to increased metabolic rate, decreased adiposity, and insulin hypersensitivity in vivo. Proceedings of the National Academy of Sciences of the United States of America. 2007;104(13):5680-5. doi: 10.1073/pnas.0701179104. PubMed PMID: 17372192; PubMed Central PMCID: PMC1838456.

76. Smyth S, Heron A. Diabetes and obesity: the twin epidemics. Nature medicine. 2006;12(1):75-80. doi: 10.1038/nm0106-75. PubMed PMID: 16397575.

77. Farese RV, Sajan MP, Standaert ML. Insulin-sensitive protein kinases (atypical protein kinase C and protein kinase B/Akt): actions and defects in obesity and type II diabetes. Experimental biology and medicine. 2005;230(9):593-605. PubMed PMID: 16179727.

78. Farese RV, Sajan MP. Atypical protein kinase C in cardiometabolic abnormalities. Current opinion in lipidology. 2012;23(3):175-81. doi: 10.1097/MOL.0b013e328352c4c7. PubMed PMID: 22449812; PubMed Central PMCID: PMC3519242.

79. Farese RV. Function and dysfunction of aPKC isoforms for glucose transport in insulin-sensitive and insulin-resistant states. American journal of physiology Endocrinology and metabolism. 2002;283(1):E1-11. doi: 10.1152/ajpendo.00045.2002. PubMed PMID: 12067836.

80. Bandyopadhyay G, Standaert ML, Zhao L, Yu B, Avignon A, Galloway L, et al. Activation of protein kinase C (alpha, beta, and zeta) by insulin in 3T3/L1 cells. Transfection studies suggest a role for PKC-zeta in glucose transport. The Journal of biological chemistry. 1997;272(4):2551-8. Epub 1997/01/24. PubMed PMID: 8999972.

81. Kotani K, Ogawa W, Matsumoto M, Kitamura T, Sakaue H, Hino Y, et al. Requirement of atypical protein kinase clambda for insulin stimulation of glucose uptake but not for Akt activation in 3T3-L1 adipocytes. Molecular and cellular biology. 1998;18(12):6971-82. PubMed PMID: 9819385; PubMed Central PMCID: PMC109280.

82. Kotani K, Ogawa W, Hashiramoto M, Onishi T, Ohno S, Kasuga M. Inhibition of insulin-induced glucose uptake by atypical protein kinase C isotype-specific interacting protein in 3T3-L1 adipocytes. The Journal of biological chemistry. 2000;275(34):26390-5. doi: 10.1074/jbc.M002537200. PubMed PMID: 10869347.

83. Bandyopadhyay G, Kanoh Y, Sajan MP, Standaert ML, Farese RV. Effects of adenoviral gene transfer of wild-type, constitutively active, and kinase-defective protein kinase C-lambda on insulin-stimulated glucose transport in L6 myotubes. Endocrinology. 2000;141(11):4120-7. PubMed PMID: 11089544.

84. Bandyopadhyay G, Standaert ML, Galloway L, Moscat J, Farese RV. Evidence for involvement of protein kinase C (PKC)-zeta and noninvolvement of diacylglycerol-sensitive PKCs in insulin-stimulated glucose transport in L6 myotubes. Endocrinology. 1997;138(11):4721-31. PubMed PMID: 9348199.

85. Bandyopadhyay G, Sajan MP, Kanoh Y, Standaert ML, Quon MJ, Lea-Currie R, et al. PKC-zeta mediates insulin effects on glucose transport in cultured preadipocyte-derived human adipocytes. The Journal of clinical endocrinology and metabolism. 2002;87(2):716-23. PubMed PMID: 11836310.

86. Sajan MP, Rivas J, Li P, Standaert ML, Farese RV. Repletion of atypical protein kinase C following RNA interference-mediated depletion restores insulin-stimulated glucose transport. The Journal of biological chemistry. 2006;281(25):17466-73. doi: 10.1074/jbc.M510803200. PubMed PMID: 16644736.

87. Farese RV, Sajan MP, Yang H, Li P, Mastorides S, Gower WR, Jr., et al. Muscle-specific knockout of PKC-lambda impairs glucose transport and induces metabolic and diabetic syndromes. The Journal of clinical investigation. 2007;117(8):2289-301. doi: 10.1172/JCI31408. PubMed PMID: 17641777; PubMed Central PMCID: PMC1913489.

88. Bandyopadhyay G, Standaert ML, Kikkawa U, Ono Y, Moscat J, Farese RV. Effects of transiently expressed atypical (zeta, lambda), conventional (alpha, beta) and novel (delta, epsilon) protein kinase C isoforms on insulin-stimulated translocation of epitope-tagged GLUT4 glucose transporters in rat adipocytes: specific interchangeable effects of protein kinases C-zeta and C-lambda. The Biochemical journal. 1999;337 (Pt 3):461-70. PubMed PMID: 9895289; PubMed Central PMCID: PMC1219997.

89. Braiman L, Alt A, Kuroki T, Ohba M, Bak A, Tennenbaum T, et al. Activation of protein kinase C zeta induces serine phosphorylation of VAMP2 in the GLUT4 compartment and increases glucose transport in skeletal muscle. Molecular and cellular biology. 2001;21(22):7852-61. doi: 10.1128/MCB.21.22.7852-7861.2001. PubMed PMID: 11604519; PubMed Central PMCID: PMC99955.

90. Imamura T, Huang J, Usui I, Satoh H, Bever J, Olefsky JM. Insulin-induced GLUT4 translocation involves protein kinase C-lambda-mediated functional coupling between Rab4 and the motor protein kinesin. Molecular and cellular biology. 2003;23(14):4892-900. PubMed PMID: 12832475; PubMed Central PMCID: PMC162221.

91. Imamura T, Ishibashi K, Dalle S, Ugi S, Olefsky JM. Endothelin-1-induced GLUT4 translocation is mediated via Galpha(q/11) protein and phosphatidylinositol 3-kinase in 3T3-L1 adipocytes. The Journal of biological chemistry. 1999;274(47):33691-5. PubMed PMID: 10559259.

92. Farese RV, Sajan MP. Metabolic functions of atypical protein kinase C: "good" and "bad" as defined by nutritional status. American journal of physiology Endocrinology and metabolism. 2010;298(3):E385-94. doi: 10.1152/ajpendo.00608.2009. PubMed PMID: 19996389; PubMed Central PMCID: PMC3774273.

93. Matsumoto M, Ogawa W, Akimoto K, Inoue H, Miyake K, Furukawa K, et al. PKClambda in liver mediates insulin-induced SREBP-1c expression and determines both hepatic lipid content and overall insulin sensitivity. The Journal of clinical investigation. 2003;112(6):935-44. doi: 10.1172/JCI18816. PubMed PMID: 12975478; PubMed Central PMCID: PMC193669.

94. Sajan MP, Standaert ML, Nimal S, Varanasi U, Pastoor T, Mastorides S, et al. The critical role of atypical protein kinase C in activating hepatic SREBP-1c and NFkappaB in obesity. Journal of lipid research. 2009;50(6):1133-45. doi: 10.1194/jlr.M800520-JLR200. PubMed PMID: 19202134; PubMed Central PMCID: PMC2681395.

95. Sajan MP, Jurzak MJ, Samuels VT, Shulman GI, Braun U, Leitges M, et al. Impairment of insulin-stimulated glucose transport and ERK activation by adipocyte-specific knockout of PKC-lambda produces a phenotype characterized by diminished adiposity and enhanced insulin suppression of hepatic gluconeogenesis. Adipocyte. 2014;3(1):19-29. doi: 10.4161/adip.26305. PubMed PMID: 24575365; PubMed Central PMCID: PMC3917928.

96. Sajan MP, Standaert ML, Rivas J, Miura A, Kanoh Y, Soto J, et al. Role of atypical protein kinase C in activation of sterol regulatory element binding protein-1c and nuclear factor kappa B (NFkappaB) in liver of rodents used as a model of diabetes, and relationships to hyperlipidaemia and insulin resistance. Diabetologia. 2009;52(6):1197-207. doi: 10.1007/s00125-009-1336-5. PubMed PMID: 19357831.

97. Taniguchi CM, Kondo T, Sajan M, Luo J, Bronson R, Asano T, et al. Divergent regulation of hepatic glucose and lipid metabolism by phosphoinositide 3-kinase via Akt and PKClambda/zeta. Cell metabolism. 2006;3(5):343-53. doi: 10.1016/j.cmet.2006.04.005. PubMed PMID: 16679292.

98. Bandyopadhyay GK, Yu JG, Ofrecio J, Olefsky JM. Increased p85/55/50 expression and decreased phosphotidylinositol 3-kinase activity in insulin-resistant human skeletal muscle. Diabetes. 2005;54(8):2351-9. PubMed PMID: 16046301.

99. Beeson M, Sajan MP, Dizon M, Grebenev D, Gomez-Daspet J, Miura A, et al. Activation of protein kinase C-zeta by insulin and phosphatidylinositol-3,4,5-(PO4)3 is defective in muscle in type 2 diabetes and impaired glucose tolerance: amelioration by rosiglitazone and exercise. Diabetes. 2003;52(8):1926-34. PubMed PMID: 12882907.

100. Kim YB, Kotani K, Ciaraldi TP, Henry RR, Kahn BB. Insulin-stimulated protein kinase C lambda/zeta activity is reduced in skeletal muscle of humans with obesity and type 2 diabetes: reversal with weight reduction. Diabetes. 2003;52(8):1935-42. PubMed PMID: 12882908.

101. Beeson M, Sajan MP, Daspet JG, Luna V, Dizon M, Grebenev D, et al. Defective Activation of Protein Kinase C-z in Muscle by Insulin and Phosphatidylinositol-3,4,5,-(PO(4))(3) in Obesity and Polycystic Ovary Syndrome. Metabolic syndrome and related disorders. 2004;2(1):49-56. doi: 10.1089/met.2004.2.49. PubMed PMID: 18370676.

102. Sajan MP, Farese RV. Insulin signalling in hepatocytes of humans with type 2 diabetes: excessive production and activity of protein kinase C-iota (PKC-iota) and dependent processes and reversal by PKC-iota inhibitors. Diabetologia. 2012;55(5):1446-57. doi: 10.1007/s00125-012-2477-5. PubMed PMID: 22349071; PubMed Central PMCID: PMC3543149.

103. Nakanishi H, Exton JH. Purification and characterization of the zeta isoform of protein kinase C from bovine kidney. The Journal of biological chemistry. 1992;267(23):16347-54. PubMed PMID: 1322899.

104. Nakanishi H, Brewer KA, Exton JH. Activation of the zeta isozyme of protein kinase C by phosphatidylinositol 3,4,5-trisphosphate. The Journal of biological chemistry. 1993;268(1):13-6. PubMed PMID: 8380153.

105. Ting AY, Kain KH, Klemke RL, Tsien RY. Genetically encoded fluorescent reporters of protein tyrosine kinase activities in living cells. Proceedings of the National Academy of Sciences of the United States of America. 2001;98(26):15003-8. doi: 10.1073/pnas.211564598. PubMed PMID: 11752449; PubMed Central PMCID: PMC64973.

106. Zhang J, Ma Y, Taylor SS, Tsien RY. Genetically encoded reporters of protein kinase A activity reveal impact of substrate tethering. Proceedings of the National Academy of Sciences of the United States of America. 2001;98(26):14997-5002. doi: 10.1073/pnas.211566798. PubMed PMID: 11752448; PubMed Central PMCID: PMC64972.

107. Kunkel MT, Ni Q, Tsien RY, Zhang J, Newton AC. Spatio-temporal dynamics of protein kinase B/Akt signaling revealed by a genetically encoded fluorescent reporter. The Journal of biological chemistry. 2005;280(7):5581-7. doi: 10.1074/jbc.M411534200. PubMed PMID: 15583002; PubMed Central PMCID: PMC2913970.

108. Kunkel MT, Toker A, Tsien RY, Newton AC. Calcium-dependent regulation of protein kinase D revealed by a genetically encoded kinase activity reporter. The Journal of biological chemistry. 2007;282(9):6733-42. doi: 10.1074/jbc.M608086200. PubMed PMID: 17189263; PubMed Central PMCID: PMC2921767.

109. Violin JD, Zhang J, Tsien RY, Newton AC. A genetically encoded fluorescent reporter reveals oscillatory phosphorylation by protein kinase C. The Journal of cell biology. 2003;161(5):899-909. doi: 10.1083/jcb.200302125. PubMed PMID: 12782683; PubMed Central PMCID: PMC2172956.

110. Kunkel MT, Newton AC. Spatiotemporal Dynamics of Kinase Signaling Visualized by Targeted Reporters. Current protocols in chemical biology. 2009;1(1):17-8. doi: 10.1002/9780470559277.ch090106. PubMed PMID: 21804950; PubMed Central PMCID: PMC3146362.

111. Wu-Zhang AX, Newton AC. Protein kinase C pharmacology: refining the toolbox. The Biochemical journal. 2013;452(2):195-209. doi: 10.1042/BJ20130220. PubMed PMID: 23662807.

112. Wu-Zhang AX, Schramm CL, Nabavi S, Malinow R, Newton AC. Cellular pharmacology of protein kinase Mzeta (PKMzeta) contrasts with its in vitro profile: implications for PKMzeta as a mediator of memory. The Journal of biological chemistry. 2012;287(16):12879-85. Epub 2012/03/02. doi: 10.1074/jbc.M112.357244. PubMed PMID: 22378786; PubMed Central PMCID: PMC3339930.

113. Price TJ, Ghosh S. ZIPping to pain relief: the role (or not) of PKMzeta in chronic pain. Molecular pain. 2013;9:6. doi: 10.1186/1744-8069-9-6. PubMed PMID: 23433248; PubMed Central PMCID: PMC3621284.

114. Shema R, Sacktor TC, Dudai Y. Rapid erasure of long-term memory associations in the cortex by an inhibitor of PKM zeta. Science. 2007;317(5840):951-3. doi: 10.1126/science.1144334. PubMed PMID: 17702943.

115. Pastalkova E, Serrano P, Pinkhasova D, Wallace E, Fenton AA, Sacktor TC. Storage of spatial information by the maintenance mechanism of LTP. Science. 2006;313(5790):1141-4. doi: 10.1126/science.1128657. PubMed PMID: 16931766.

116. Serrano P, Friedman EL, Kenney J, Taubenfeld SM, Zimmerman JM, Hanna J, et al. PKMzeta maintains spatial, instrumental, and classically conditioned long-term memories. PLoS biology. 2008;6(12):2698-706. doi: 10.1371/journal.pbio.0060318. PubMed PMID: 19108606; PubMed Central PMCID: PMC2605920.

117. Yamamoto S, Seta K, Morisco C, Vatner SF, Sadoshima J. Chelerythrine rapidly induces apoptosis through generation of reactive oxygen species in cardiac myocytes. Journal of molecular and cellular cardiology. 2001;33(10):1829-48. doi: 10.1006/jmcc.2001.1446. PubMed PMID: 11603925.

118. Bain J, Plater L, Elliott M, Shpiro N, Hastie CJ, McLauchlan H, et al. The selectivity of protein kinase inhibitors: a further update. The Biochemical journal. 2007;408(3):297-315. doi: 10.1042/BJ20070797. PubMed PMID: 17850214; PubMed Central PMCID: PMC2267365.

119. Trujillo JI, Kiefer JR, Huang W, Thorarensen A, Xing L, Caspers NL, et al. 2-(6-Phenyl-1H-indazol-3-yl)-1H-benzo[d]imidazoles: design and synthesis of a potent and isoform selective PKC-zeta inhibitor. Bioorganic & medicinal chemistry letters. 2009;19(3):908-11. doi: 10.1016/j.bmcl.2008.11.105. PubMed PMID: 19097791.

120. Kusne Y, Carrera-Silva EA, Perry AS, Rushing EJ, Mandell EK, Dietrich JD, et al. Targeting aPKC disables oncogenic signaling by both the EGFR and the proinflammatory cytokine TNFalpha in glioblastoma. Science signaling. 2014;7(338):ra75. doi: 10.1126/scisignal.2005196. PubMed PMID: 25118327; PubMed Central PMCID: PMC4486020.

121. Shao QC, Zhang CJ, Li J. Structure-based lead discovery for protein kinase C zeta inhibitor design by exploiting kinase-inhibitor complex crystal structure data and potential therapeutics for preterm labour. Archives of pharmacal research. 2014. doi: 10.1007/s12272-014-0495-1. PubMed PMID: 25311663.

122. Zhang H, Neimanis S, Lopez-Garcia LA, Arencibia JM, Amon S, Stroba A, et al. Molecular mechanism of regulation of the atypical protein kinase C by N-terminal domains and an allosteric small compound. Chemistry & biology. 2014;21(6):754-65. doi: 10.1016/j.chembiol.2014.04.007. PubMed PMID: 24836908.

123. Bandyopadhyay G, Standaert ML, Sajan MP, Kanoh Y, Miura A, Braun U, et al. Protein kinase C-lambda knockout in embryonic stem cells and adipocytes impairs insulin-stimulated glucose transport. Mol Endocrinol. 2004;18(2):373-83. doi: 10.1210/me.2003-0087. PubMed PMID: 14615604.

124. Sajan MP, Standaert ML, Miura A, Bandyopadhyay G, Vollenweider P, Franklin DM, et al. Impaired activation of protein kinase C-zeta by insulin and phosphatidylinositol-3,4,5-(PO4)3 in cultured preadipocyte-derived adipocytes and myotubes of obese subjects. The Journal of clinical endocrinology and metabolism. 2004;89(8):3994-8. doi: 10.1210/jc.2004-0106. PubMed PMID: 15292339.

125. Standaert ML, Sajan MP, Miura A, Kanoh Y, Chen HC, Farese RV, Jr., et al. Insulin-induced activation of atypical protein kinase C, but not protein kinase B, is maintained in diabetic (ob/ob and Goto-Kakazaki) liver. Contrasting insulin signaling patterns in liver versus muscle define phenotypes of type 2 diabetic and high fat-induced insulin-resistant states. The Journal of biological chemistry. 2004;279(24):24929-34. doi: 10.1074/jbc.M402440200. PubMed PMID: 15069067.

126. Ezhevsky SA, Ho A, Becker-Hapak M, Davis PK, Dowdy SF. Differential regulation of retinoblastoma tumor suppressor protein by G(1) cyclin-dependent kinase complexes in vivo. Molecular and cellular biology. 2001;21(14):4773-84. doi: 10.1128/MCB.21.14.4773-4784.2001. PubMed PMID: 11416152; PubMed Central PMCID: PMC87164.

127. Wu-Zhang AX, Murphy AN, Bachman M, Newton AC. Isozyme-specific interaction of protein kinase Cdelta with mitochondria dissected using live cell fluorescence imaging. The Journal of biological chemistry. 2012;287(45):37891-906. doi: 10.1074/jbc.M112.412635. PubMed PMID: 22988234; PubMed Central PMCID: PMC3488061.

128. Johnson JE, Edwards AS, Newton AC. A putative phosphatidylserine binding motif is not involved in the lipid regulation of protein kinase C. The Journal of biological chemistry. 1997;272(49):30787-92. Epub 1998/01/10. PubMed PMID: 9388219.

129. Taylor SS, Shaw A, Hu J, Meharena HS, Kornev A. Pseudokinases from a structural perspective. Biochemical Society transactions. 2013;41(4):981-6. doi: 10.1042/BST20130120. PubMed PMID: 23863167.

130. Johnson JE, Giorgione J, Newton AC. The C1 and C2 domains of protein kinase C are independent membrane targeting modules, with specificity for phosphatidylserine conferred by the C1 domain. Biochemistry. 2000;39(37):11360-9. PubMed PMID: 10985781.

131. Orr JW, Newton AC. Interaction of protein kinase C with phosphatidylserine. 2. Specificity and regulation. Biochemistry. 1992;31(19):4667-73. PubMed PMID: 1581317.

132. Orr JW, Newton AC. Interaction of protein kinase C with phosphatidylserine. 1. Cooperativity in lipid binding. Biochemistry. 1992;31(19):4661-7. PubMed PMID: 1581316.

133. Bell RM, Hannun Y, Loomis C. Mixed micelle assay of protein kinase C. Methods in enzymology. 1986;124:353-9. PubMed PMID: 3520216.

134. Hannun YA, Loomis CR, Bell RM. Protein kinase C activation in mixed micelles. Mechanistic implications of phospholipid, diacylglycerol, and calcium interdependencies. The Journal of biological chemistry. 1986;261(16):7184-90. PubMed PMID: 3711083.

135. Newton AC, Koshland DE, Jr. Phosphatidylserine affects specificity of protein kinase C substrate phosphorylation and autophosphorylation. Biochemistry. 1990;29(28):6656-61. PubMed PMID: 2397206.

136. Sabatini DM. mTOR and cancer: insights into a complex relationship. Nature reviews Cancer. 2006;6(9):729-34. doi: 10.1038/nrc1974. PubMed PMID: 16915295.

137. Pearson RB, Dennis PB, Han JW, Williamson NA, Kozma SC, Wettenhall RE, et al. The principal target of rapamycin-induced p70s6k inactivation is a novel phosphorylation site within a conserved hydrophobic domain. The EMBO journal. 1995;14(21):5279-87. PubMed PMID: 7489717; PubMed Central PMCID: PMC394637.

138. Standaert ML, Galloway L, Karnam P, Bandyopadhyay G, Moscat J, Farese RV. Protein kinase C-zeta as a downstream effector of phosphatidylinositol 3-kinase during insulin stimulation in rat adipocytes. Potential role in glucose transport. The Journal of biological chemistry. 1997;272(48):30075-82. PubMed PMID: 9374484.

139. Akimoto K, Takahashi R, Moriya S, Nishioka N, Takayanagi J, Kimura K, et al. EGF or PDGF receptors activate atypical PKClambda through phosphatidylinositol 3-kinase. The EMBO journal. 1996;15(4):788-98. PubMed PMID: 8631300; PubMed Central PMCID: PMC450277.

140. Antal CE, Violin JD, Kunkel MT, Skovso S, Newton AC. Intramolecular conformational changes optimize protein kinase C signaling. Chemistry & biology. 2014;21(4):459-69. doi: 10.1016/j.chembiol.2014.02.008. PubMed PMID: 24631122; PubMed Central PMCID: PMC4020788.

141. Andjelkovic M, Alessi DR, Meier R, Fernandez A, Lamb NJ, Frech M, et al. Role of translocation in the activation and function of protein kinase B. The Journal of biological chemistry. 1997;272(50):31515-24. PubMed PMID: 9395488.

142. Bellacosa A, Chan TO, Ahmed NN, Datta K, Malstrom S, Stokoe D, et al. Akt activation by growth factors is a multiple-step process: the role of the PH domain. Oncogene. 1998;17(3):313-25. doi: 10.1038/sj.onc.1201947. PubMed PMID: 9690513.

143. Kelly MT, Crary JF, Sacktor TC. Regulation of protein kinase Mzeta synthesis by multiple kinases in long-term potentiation. The Journal of neuroscience : the official journal of the Society for Neuroscience. 2007;27(13):3439-44. doi: 10.1523/JNEUROSCI.5612-06.2007. PubMed PMID: 17392460.

144. Smith L, Wang Z, Smith JB. Caspase processing activates atypical protein kinase C zeta by relieving autoinhibition and destabilizes the protein. The Biochemical journal. 2003;375(Pt 3):663-71. doi: 10.1042/BJ20030926. PubMed PMID: 12887331; PubMed Central PMCID: PMC1223714.

145. Ivey RA, Sajan MP, Farese RV. Requirements for Pseudosubstrate Arginine Residues During Auto-inhibition and Phosphatidylinositol-3,4,5-(PO4)3-dependent Activation of Atypical PKC. The Journal of biological chemistry. 2014. doi: 10.1074/jbc.M114.565671. PubMed PMID: 25035426.

146. Lopez-Garcia LA, Schulze JO, Frohner W, Zhang H, Suss E, Weber N, et al. Allosteric regulation of protein kinase PKCzeta by the N-terminal C1 domain and small compounds to the PIF-pocket. Chemistry & biology. 2011;18(11):1463-73. doi: 10.1016/j.chembiol.2011.08.010. PubMed PMID: 22118680.

147. Limatola C, Schaap D, Moolenaar WH, van Blitterswijk WJ. Phosphatidic acid activation of protein kinase C-zeta overexpressed in COS cells: comparison with other protein kinase C isotypes and other acidic lipids. The Biochemical journal. 1994;304 (Pt 3):1001-8. PubMed PMID: 7818462; PubMed Central PMCID: PMC1137431.

148. Cho H, Mu J, Kim JK, Thorvaldsen JL, Chu Q, Crenshaw EB, 3rd, et al. Insulin resistance and a diabetes mellitus-like syndrome in mice lacking the protein kinase Akt2 (PKB beta). Science. 2001;292(5522):1728-31. doi: 10.1126/science.292.5522.1728. PubMed PMID: 11387480.

149. Tsuru M, Katagiri H, Asano T, Yamada T, Ohno S, Ogihara T, et al. Role of PKC isoforms in glucose transport in 3T3-L1 adipocytes: insignificance of atypical PKC. American journal of physiology Endocrinology and metabolism. 2002;283(2):E338-45. doi: 10.1152/ajpendo.00457.2001. PubMed PMID: 12110540.

150. Hung TJ, Kemphues KJ. PAR-6 is a conserved PDZ domain-containing protein that colocalizes with PAR-3 in Caenorhabditis elegans embryos. Development. 1999;126(1):127-35. PubMed PMID: 9834192.

151. Toker A, Newton AC. Cellular signaling: pivoting around PDK-1. Cell. 2000;103(2):185-8. PubMed PMID: 11057891.

152. Sajan MP, Ivey RA, 3rd, Lee M, Mastorides S, Jurczak MJ, Samuels VT, et al. PKClambda haploinsufficiency prevents diabetes by a mechanism involving alterations in hepatic enzymes. Mol Endocrinol. 2014;28(7):1097-107. doi: 10.1210/me.2014-1025. PubMed PMID: 24877563; PubMed Central PMCID: PMC4075159.

153. Copps KD, White MF. Regulation of insulin sensitivity by serine/threonine phosphorylation of insulin receptor substrate proteins IRS1 and IRS2. Diabetologia. 2012;55(10):2565-82. doi: 10.1007/s00125-012-2644-8. PubMed PMID: 22869320.

154. Christian F, Krause E, Houslay MD, Baillie GS. PKA phosphorylation of p62/SQSTM1 regulates PB1 domain interaction partner binding. Biochimica et biophysica acta. 2014;1843(11):2765-74. doi: 10.1016/j.bbamcr.2014.07.021. PubMed PMID: 25110345.

155. Xi G, Shen X, Wai C, Vilas CK, Clemmons DR. Hyperglycemia stimulates p62/PKCzeta interaction, which mediates NF-kappaB activation, increased Nox4 expression, and inflammatory cytokine activation in vascular smooth muscle. FASEB journal : official publication of the Federation of American Societies for Experimental Biology. 2015;29(12):4772-82. doi: 10.1096/fj.15-275453. PubMed PMID: 26231202; PubMed Central PMCID: PMC4653052.

156. Herbert JM, Augereau JM, Gleye J, Maffrand JP. Chelerythrine is a potent and specific inhibitor of protein kinase C. Biochemical and biophysical research communications. 1990;172(3):993-9. PubMed PMID: 2244923.

157. Hirano Y, Yoshinaga S, Takeya R, Suzuki NN, Horiuchi M, Kohjima M, et al. Structure of a cell polarity regulator, a complex between atypical PKC and Par6 PB1 domains. The Journal of biological chemistry. 2005;280(10):9653-61. doi: 10.1074/jbc.M409823200. PubMed PMID: 15590654.

158. Di Guglielmo GM, Drake PG, Baass PC, Authier F, Posner BI, Bergeron JJ. Insulin receptor internalization and signalling. Molecular and cellular biochemistry. 1998;182(1-2):59-63. PubMed PMID: 9609114.

159. Elmendorf JS. Signals that regulate GLUT4 translocation. The Journal of membrane biology. 2002;190(3):167-74. doi: 10.1007/s00232-002-1035-3. PubMed PMID: 12533782.

160. Foster LJ, Klip A. Mechanism and regulation of GLUT-4 vesicle fusion in muscle and fat cells. American journal of physiology Cell physiology. 2000;279(4):C877-90. PubMed PMID: 11003568.

161. Watson RT, Kanzaki M, Pessin JE. Regulated membrane trafficking of the insulin-responsive glucose transporter 4 in adipocytes. Endocrine reviews. 2004;25(2):177-204. doi: 10.1210/er.2003-0011. PubMed PMID: 15082519.

162. Hodgkinson CP, Mander A, Sale GJ. Identification of 80K-H as a protein involved in GLUT4 vesicle trafficking. The Biochemical journal. 2005;388(Pt 3):785-93. doi: 10.1042/BJ20041845. PubMed PMID: 15707389; PubMed Central PMCID: PMC1183457.

163. Cariou B, Perdereau D, Cailliau K, Browaeys-Poly E, Bereziat V, Vasseur-Cognet M, et al. The adapter protein ZIP binds Grb14 and regulates its inhibitory action on insulin signaling by recruiting protein kinase Czeta. Molecular and cellular biology. 2002;22(20):6959-70. Epub 2002/09/21. PubMed PMID: 12242277; PubMed Central PMCID: PMC139806.

164. Nouaille S, Blanquart C, Zilberfarb V, Boute N, Perdereau D, Roix J, et al. Interaction with Grb14 results in site-specific regulation of tyrosine phosphorylation of the insulin receptor. EMBO reports. 2006;7(5):512-8. doi: 10.1038/sj.embor.7400668. PubMed PMID: 16582879; PubMed Central PMCID: PMC1479551.

165. Standaert M, Bandyopadhyay G, Galloway L, Ono Y, Mukai H, Farese R. Comparative effects of GTPgammaS and insulin on the activation of Rho, phosphatidylinositol 3-kinase, and protein kinase N in rat adipocytes. Relationship to glucose transport. The Journal of biological chemistry. 1998;273(13):7470-7. PubMed PMID: 9516446.

166. Mukai H. The structure and function of PKN, a protein kinase having a catalytic domain homologous to that of PKC. Journal of biochemistry. 2003;133(1):17-27. PubMed PMID: 12761194.

167. Dong LQ, Landa LR, Wick MJ, Zhu L, Mukai H, Ono Y, et al. Phosphorylation of protein kinase N by phosphoinositide-dependent protein kinase-1 mediates insulin signals to the actin cytoskeleton. Proceedings of the National Academy of Sciences of the United States of America. 2000;97(10):5089-94. doi: 10.1073/pnas.090491897. PubMed PMID: 10792047; PubMed Central PMCID: PMC25786.

168. Matsuzawa K, Kosako H, Azuma I, Inagaki N, Inagaki M. Possible regulation of intermediate filament proteins by Rho-binding kinases. Sub-cellular biochemistry. 1998;31:423-35. PubMed PMID: 9932501.

169. Flynn P, Mellor H, Casamassima A, Parker PJ. Rho GTPase control of protein kinase C-related protein kinase activation by 3-phosphoinositide-dependent protein kinase. The Journal of biological chemistry. 2000;275(15):11064-70. PubMed PMID: 10753910.

170. Yoshinaga C, Mukai H, Toshimori M, Miyamoto M, Ono Y. Mutational analysis of the regulatory mechanism of PKN: the regulatory region of PKN contains an arachidonic acid-sensitive autoinhibitory domain. Journal of biochemistry. 1999;126(3):475-84. PubMed PMID: 10467162.

171. Mukai H, Kitagawa M, Shibata H, Takanaga H, Mori K, Shimakawa M, et al. Activation of PKN, a novel 120-kDa protein kinase with leucine zipper-like sequences, by unsaturated fatty acids and by limited proteolysis. Biochemical and biophysical research communications. 1994;204(1):348-56. doi: 10.1006/bbrc.1994.2466. PubMed PMID: 7945381.

172. Kitagawa M, Shibata H, Toshimori M, Mukai H, Ono Y. The role of the unique motifs in the amino-terminal region of PKN on its enzymatic activity. Biochemical and biophysical research communications. 1996;220(3):963-8. doi: 10.1006/bbrc.1996.0515. PubMed PMID: 8607876.

173. Takahashi M, Mukai H, Toshimori M, Miyamoto M, Ono Y. Proteolytic activation of PKN by caspase-3 or related protease during apoptosis. Proceedings of the National Academy of Sciences of the United States of America. 1998;95(20):11566-71. PubMed PMID: 9751706; PubMed Central PMCID: PMC21681.

174. Amano M, Mukai H, Ono Y, Chihara K, Matsui T, Hamajima Y, et al. Identification of a putative target for Rho as the serine-threonine kinase protein kinase N. Science. 1996;271(5249):648-50. PubMed PMID: 8571127.

175. Watanabe G, Saito Y, Madaule P, Ishizaki T, Fujisawa K, Morii N, et al. Protein kinase N (PKN) and PKN-related protein rhophilin as targets of small GTPase Rho. Science. 1996;271(5249):645-8. PubMed PMID: 8571126.

176. Shibata H, Mukai H, Inagaki Y, Homma Y, Kimura K, Kaibuchi K, et al. Characterization of the interaction between RhoA and the amino-terminal region of PKN. FEBS letters. 1996;385(3):221-4. PubMed PMID: 8647255.

177. Flynn P, Mellor H, Palmer R, Panayotou G, Parker PJ. Multiple interactions of PRK1 with RhoA. Functional assignment of the Hr1 repeat motif. The Journal of biological chemistry. 1998;273(5):2698-705. PubMed PMID: 9446575.

178. Maesaki R, Ihara K, Shimizu T, Kuroda S, Kaibuchi K, Hakoshima T. The structural basis of Rho effector recognition revealed by the crystal structure of human RhoA complexed with the effector domain of PKN/PRK1. Molecular cell. 1999;4(5):793-803. PubMed PMID: 10619026.

179. Kitagawa M, Mukai H, Shibata H, Ono Y. Purification and characterization of a fatty acid-activated protein kinase (PKN) from rat testis. The Biochemical journal. 1995;310 (Pt 2):657-64. PubMed PMID: 7654208; PubMed Central PMCID: PMC1135946.